

DOE JPL 954376-78/1
Distribution Category UC-63

LASER-ZONE GROWTH IN A RIBBON-TO-RIBBON (RTR) PROCESS
SILICON SHEET GROWTH DEVELOPMENT FOR THE LARGE AREA
SILICON SHEET TASK OF THE LOW COST SILICON SOLAR
ARRAY PROJECT

Motorola Report No. 2256/8

TECHNICAL QUARTERLY REPORT NO. 6

10 October 1977 - 31 December 1977

JPL CONTRACT NO. 954376

BY

R. W. GURTLER, A. BAGHDADI, R. LEGGE, B. SOPORI, R. J. ELLIS

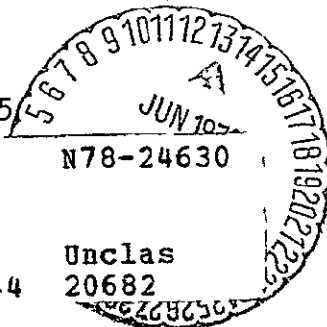
PREPARED BY

MOTOROLA INC. SEMICONDUCTOR GROUP
5005 E. McDowell Road
Phoenix, Arizona 85008

This work was performed for the Jet Propulsion Laboratory, California Institute of Technology, under NASA Contract NAS7-100 for the Department of Energy, Division of Solar Energy.

The JPL Low-Cost Silicon Solar Array Project is funded by DOE and forms part of the DOE Photovoltaic Conversion Program to initiate a major effort toward the development of low-cost solar arrays.

Motorola Project No's 2319 - 25



(DOE/JPL-954376-78/1) LASER-ZONE GROWTH IN
A RIBBON-TO-RIBBON (RTR) PROCESS. SILICON
SHEET GROWTH DEVELOPMENT FOR THE LARGE AREA
SILICON SHEET TASK OF THE LOW COST SILICON
SOLAR ARRAY PROJECT Technical (Motorola,

N78-24630

G3/44

Unclass
20682

LASER-ZONE GROWTH IN A RIBBON-TO-RIBBON (RTR) PROCESS
SILICON SHEET GROWTH DEVELOPMENT FOR THE LARGE AREA
SILICON SHEET TASK OF THE LOW COST SILICON SOLAR
ARRAY PROJECT

Motorola Report No. 2256/8

TECHNICAL QUARTERLY REPORT NO. 6

10 October 1977 - 31 December 1977

JPL CONTRACT NO. 954376

BY

R. W. GURTLER, A. BAGHDADI, R. LEGGE, B. SOPORI, R. J. ELLIS

PREPARED BY

MOTOROLA INC. SEMICONDUCTOR GROUP
5005 E. McDowell Road
Phoenix, Arizona 85008

This work was performed for the Jet Propulsion Laboratory, California Institute of Technology, under NASA Contract NAS7-100 for the Department of Energy, Division of Solar Energy.

The JPL Low-Cost Silicon Solar Array Project is funded by DOE and forms part of the DOE Photovoltaic Conversion Program to initiate a major effort toward the development of low-cost solar arrays.

Motorola Project No's 2319 - 25

ABSTRACT

The objective of this research is to fully investigate the Ribbon-to-Ribbon (RTR) approach to silicon ribbon growth. An existing RTR apparatus is to be upgraded to its full capabilities and operated routinely to investigate and optimize the effects of various growth parameters on growth results. A new RTR apparatus is to be constructed to incorporate increased capabilities and improvements over the first apparatus and to be capable of continuous growth. Material analyses and solar cell fabrication process optimization are to be performed with a goal of 12% cell efficiency.

During this quarter the laser lab was relocated and operation resumed. New high power lasers have been implemented and this has led to major improvements in growth velocity -- 4"/min. growth has been demonstrated. This high growth capability has been accompanied, however, with the appearance of dendritic growth. A major step in demonstration of the full feasibility of the RTR process is reported in the demonstration of RTR growth from CVD polyribbon rather than sliced polyribbon ingots.

Cell and material evaluations have continued. Average solar cell efficiencies of >9% and a best cell efficiency of 11.7% are reported. Processing has been shown to provide a substantial improvement in material minority carrier diffusion length.

An economic analysis is reported which treats both the polyribbon fabrication and RTR processes. Indications are that the long term DOE goals may be met.

SUMMARY

During this quarter, significant progress has been realized on various aspects of the RTR program:

Relocation of the laser lab and installation of the new higher power laser systems have been completed. RTR#1 has been modified and is now fully operational although a water accident caused considerable damage and delay. The new growth station, RTR#2, is nearing completion.

With increased capabilities of laser power, RTR ribbons have been grown at the highest rate ever -- 2cm wide at 10cm/min. Accompanying this increase in growth velocity capability has been the emergence of a new growth phenomenon in the form of dendritic growth. This results in a non-planar surface. The onset of dendritic growth is related to attainment of a critical velocity which is a function of the thermal environment. With modifications to the thermal profile, non-dendritic growth has been achieved at velocities up to 7.5cm/min. Numerous growth runs have been completed with growth velocities ranging from 2.5 - 9cm/min. Many of these samples are being processed into solar cells, others are being used for material analysis.

Another major achievement this quarter has been the demonstration of RTR growth with true polyribbon feedstock; i.e., doped polysilicon ribbon obtained from a unique CVD process capable of ultimately supplying low cost, high purity, polyribbon for the RTR process. Initial SPV evaluations of this regrown material indicates equivalent performance to material regrown from single crystal feedstock.

Solar cell evaluations have continued. Recent lots of cells have been disappointing in performance. Two lots have been evaluated with a total of

41 and 20 ribbon cells. Average and best efficiencies for these lots were 7.5%, 9.4% and 7.7%, 9.5% respectively. However, for all of these cells, a metallization degradation effect has been observed; measurement of V_{OC} before and after metallization for one lot of cells showed an average loss of 40mV. This is also accompanied by a degradation of fill factor. Had these degradation effects not been in effect, average efficiencies of greater than 9.5% would have been realized. Experiments with alternative metallizations are now in progress.

A processed ribbon with numerous solar cells has been studied in some detail by correlating OCPV measurements of diffusion length on finished cells, SPV measurements on the same cells after etch removal of the junction, and Wright-delineated dislocation densities. These studies demonstrate the following; 1) large diffusion lengths ($>100\mu\text{m}$) are obtained on RTR solar cells; 2) the substrates indeed exhibit these large diffusion lengths; 3) positive correlation of diffusion lengths and dislocation density are found; 4) diffusion lengths on grain boundaries show a variety of values.

The large diffusion lengths observed on processed substrates are in contrast to the relatively low values measured on as-grown ribbons. Examination of processing steps has shown that the lifetime improvement occurs during the junction diffusion and AR coating steps.

Material and device analysis have been proceeding. EBIC mode SEM photos are reported which show that -- as reported by others in ribbon and non-perfect crystal technology -- not all visible structure is electrically active. Moreover, it is demonstrated that a one-to-one correlation of EBIC exhibited activity with device performance cannot be made.

Beam size effects have been characterized for the SPV technique. When the beam size is comparable to the diffusion length, anomalous effects are

present which can lead to erroneous or uninterpretable results. Experimental results illustrating these effects are presented.

Economic analysis of the RTR process has been performed with the inclusion of proposed processes for feedstock polysilicon ribbon. In addition, the SAMICS procedure has been applied to our proposed systems and an established polysilicon factory to compare projections made by this technique with our projections and established data respectively.

TABLE OF CONTENTS

<u>SECTION</u>	<u>TITLE</u>	<u>PAGE</u>
1.0	Laser Lab	1
1.1	Lab Status	1
1.2	"Flood"	1
2.0	Beam Shaping Systems	12
2.1	Polygon Scanner	12
2.2	Cylindrical Lens Beam Shaping System	12
3.0	Crystal Growth	14
3.1	Appearance of Dendritic Structure and Relation to Critical Growth Velocity	14
3.2	Routine Growth of Ribbon Samples	22
3.3	Stress Measurements and Buckling Observations	23
3.4	Growth of RTR Ribbons from CVD Polyribbon	24
4.0	Solar Cell Processing/Evaluation	24
4.1	Evaluation Results	26
4.2	Discussion of Solar Cell Evaluations	27
5.0	Material Evaluation	28
6.0	Device and Processing Studies	34
6.1	Dislocation Length and Dislocation Density Mapping on Ribbon Solar Cells	34
6.2	Discussion	41
6.3	Gettering Studies	44
7.0	Measurement Technology	44
7.1	High Resolution Diffusion Length Mapping	45
8.0	Economic Analysis	45
8.1	Evaluation of SAMICS Model	48

TABLE OF CONTENTS

<u>SECTION</u>	<u>TITLE</u>	<u>PAGE</u>
8.2	Polycrystalline Feedstock	48
8.3	RTR Crystal Growth	51
9.0	Problems	55
10.0	Plans	55
11.0	New Technology	55
12.0	Program Plan/Milestones	55
13.0	Engineering Drawings	55

LIST OF FIGURES

<u>FIGURE NUMBER</u>	<u>TITLE</u>	<u>PAGE</u>
1	GTE 1.2kW Laser and Control Station.	2
2	GTE 1.2kW Laser. Note Active Region Discharge in Central Region of Laser.	3
3	Nd:YAG Laser System and Power Supplies.	4
4	Nd:YAG Laser Systems (2) on Rails.	5
5	Original 375W CO ₂ laser. Note Beam Table which Directs Beam to Experimental Tables.	6
6	RTR#1 Experimental Table and Control/Monitor Electronics (in background).	7
7	RTR#1. Note Beam Ports (4) to Right of Table. Shown are two Polygon Scanners, a Ribbon Transport, and Beam Directing Mirrors.	8
8	Cover Installed	9
9	Polygon Scanner Operation	10
10	High Scan Frequency Polygon Scanner	11
11	Cylindrical Lens Beam Shaping System	13
12	Melt Zone Shapes for Growth Velocities Below and Above the Critical Velocity, V_C .	15
13	RTR Ribbon Exhibiting Dendritic Structure. Sample Width is ~2.5cm, Maximum Growth Velocity ~5cm/min.	17
14	RTR Ribbon Grown at a Maximum Velocity of 10cm/min. Dendritic Structure Occurs Around 5.7cm/min.	18
15	Close-up View of Sample of Figure 3 Showing Onset of Dendritic Growth.	19
16	Effects of Ambient Temperature on Critical Growth Velocity.	21

LIST OF FIGURES

<u>FIGURE NUMBER</u>	<u>TITLE</u>	<u>PAGE</u>
17	Large Area Samples of CVD Polyribbon	25
18	Doped CVD Polyribbon Regrown by the RTR Process.	25
19a	EBIC Mode Photo of Diode 7-3	29
19b	Optical Micrograph of Diode 7-3	29
20a	EBIC Mode Photo of Diode 5-6	30
20b	Optical Micrograph of Diode 5-6	30
21a	EBIC Mode Photo of Diode 11-2	31
21b	Optical Micrograph of Diode 11-2	31
22a	EBIC Mode Photo of Diode 5-5	32
22b	Optical Micrograph of Diode 5-5	32
23	Ribbon Solar Cells Utilized for OCPV/SPV/ Dislocation Density Correlations.	35
24	OCPV Diffusion Lengths (Numbers in Figure), SPV Diffusion Lengths (O) and Dislocation Densities (\square) Measured on Ribbon Solar Cells. Dislocation Densities are Times 10^4 cm^{-2} .	37
25	OCPV Diffusion Lengths (Numbers on Figure), SPV Diffusion Lengths (O) and Dislocation Densities (\square) measured on Ribbon Solar Cells. Dislocation Densities are Times 10^4 cm^{-2} .	38
26	OCPV Diffusion Lengths (Numbers on Figure), SPV Diffusion Lengths (O) and Dislocation Densities (\square) Measured on Ribbon Solar Cells. Dislocation Densities are Times 10^4 cm^{-2} .	39
27	OCPV Diffusion Lengths (Numbers on Figure), SPV Diffusion Lengths (O) and Dislocation Densities (\square) Measured on Ribbon Solar Cells. Dislocation Densities are Times 10^4 cm^{-2} .	40
28	Diffusion Length -- Dislocation Density Correlations.	42

**ORIGINAL PAGE IS
OF POOR QUALITY**

LIST OF FIGURES

<u>FIGURE NUMBER</u>	<u>TITLE</u>	<u>PAGE</u>
29	Position Relative to Final Melt Interface (mm).	43
30	SPV Behavior as a Function of Beam Size for a Sample with a Fixed Diffusion Length.	46
31	Measured SPV Diffusion Length as a Function of Beam Size/Diffusion Length Ratios.	47
32	Chemical Vapor Deposition Price Projection.	50
33	Plasma Deposition Price Projection.	52
34	RTR Add-On Price Projection.	53
35	RTR Price Projection.	54

1.0 LASER LAB

1.1 LAB STATUS

The RTR growth lab has now been completely relocated and all major items have been installed. This relocation effort has caused a great deal of effort to be expended in setting up the new stations. Figures 1 - 5 are photos of the new lab showing the various lasers, beam tables, and experimental tables.

RTR#1 was completely reconstructed on a new table. Figures 6 and 7 are photos of RTR#1 with cover removed while figure 8 shows the protection/environmental control cover in place. By use of beam directing mirrors, any, or all, of the three laser systems may be brought to one experimental table.

One major new item has been added to RTR#1 which is visible in figures 6 and 7. This is the polygon scanner system which allows scans of over 3" in width at rates of up to 5kHz. Figure 9 is a schematic illustration of the operation of the scanner while Figure 10 is a photo of an actual scanner. Further discussion of the polygon scanner operation will occur in later reports.

1.2 "FLOOD"

Just as RTR#1 was being completed and initial tests were beginning, and just after the photos of the previous figures were taken, a water hose fitting burst and the entire RTR#1 experimental table was totally flooded with water. Considerable damage was incurred by expensive lenses and the polygon scanner system. The water was removed quickly enough to prevent corrosion damage to most mechanical parts, but numerous lens surfaces were ruined, and the polygons were damaged. These components have now been repaired, but a considerable amount of lost time resulted.

ORIGINAL PAGE IS
OF POOR QUALITY

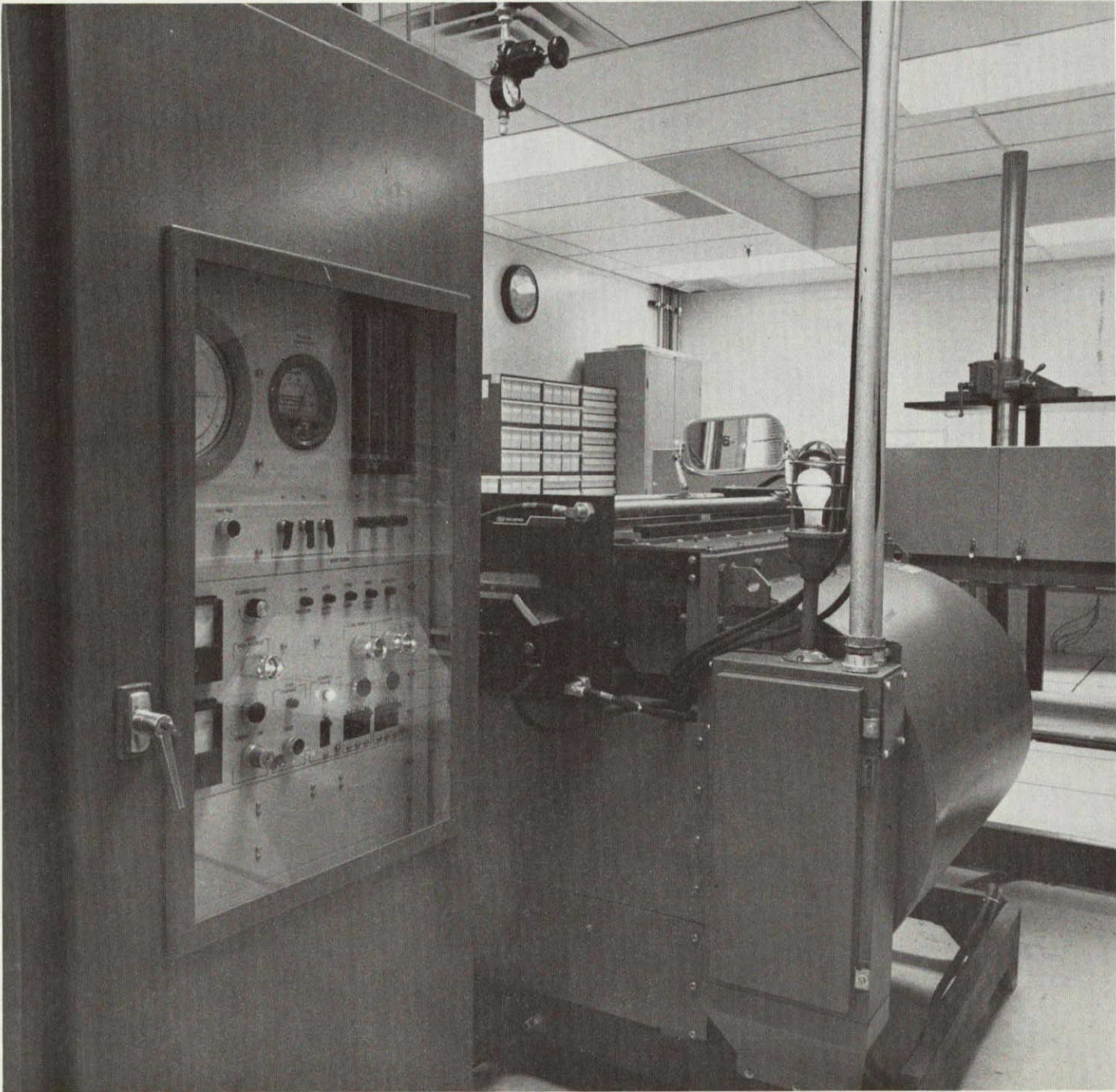


FIGURE 1: GTE 1.2kW LASER AND CONTROL STATION

ORIGINAL PAGE IS
OF POOR QUALITY

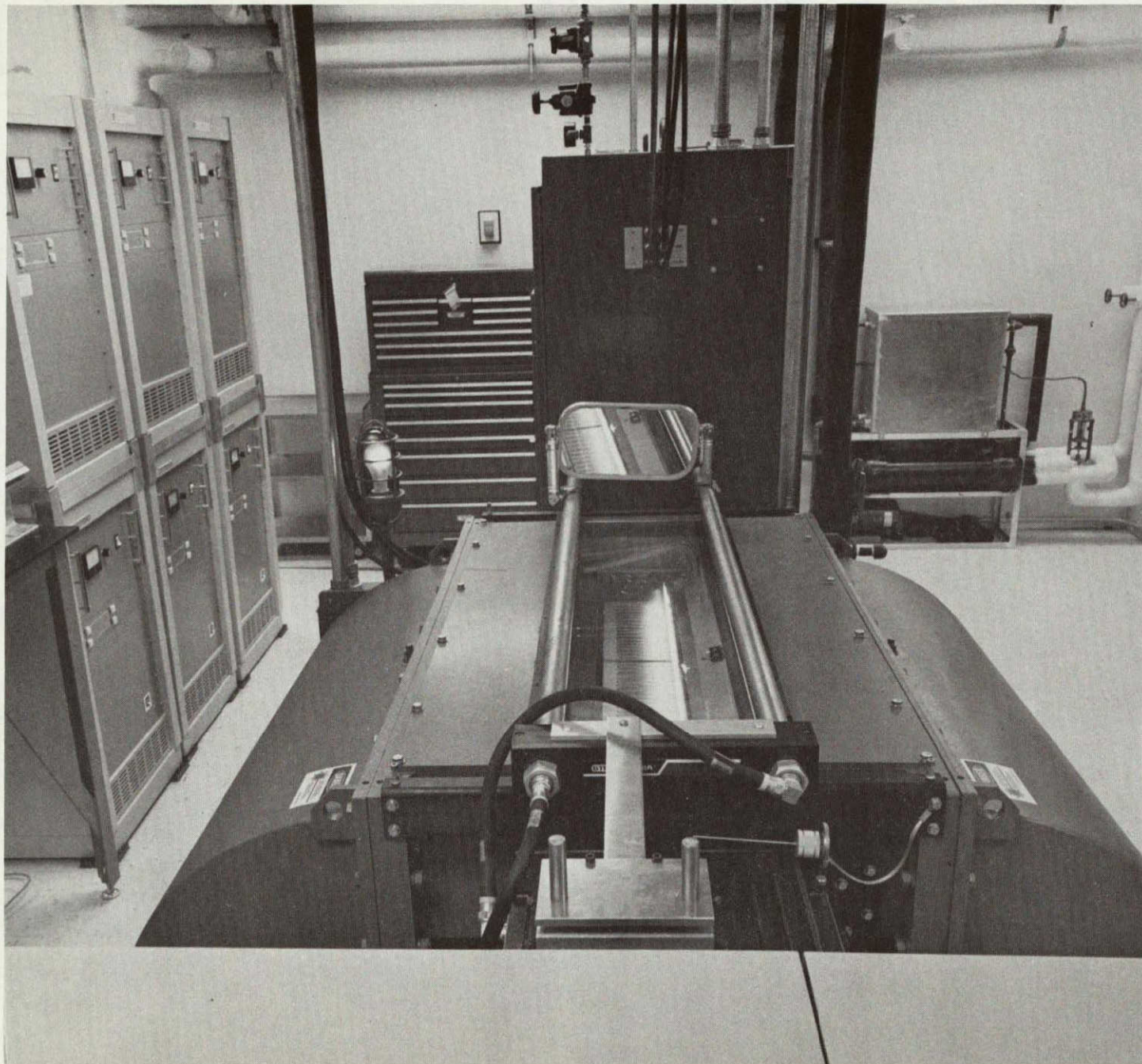


FIGURE 2: GTE 1.2kW LASER. NOTE ACTIVE REGION DISCHARGE IN CENTRAL REGION OF LASER.

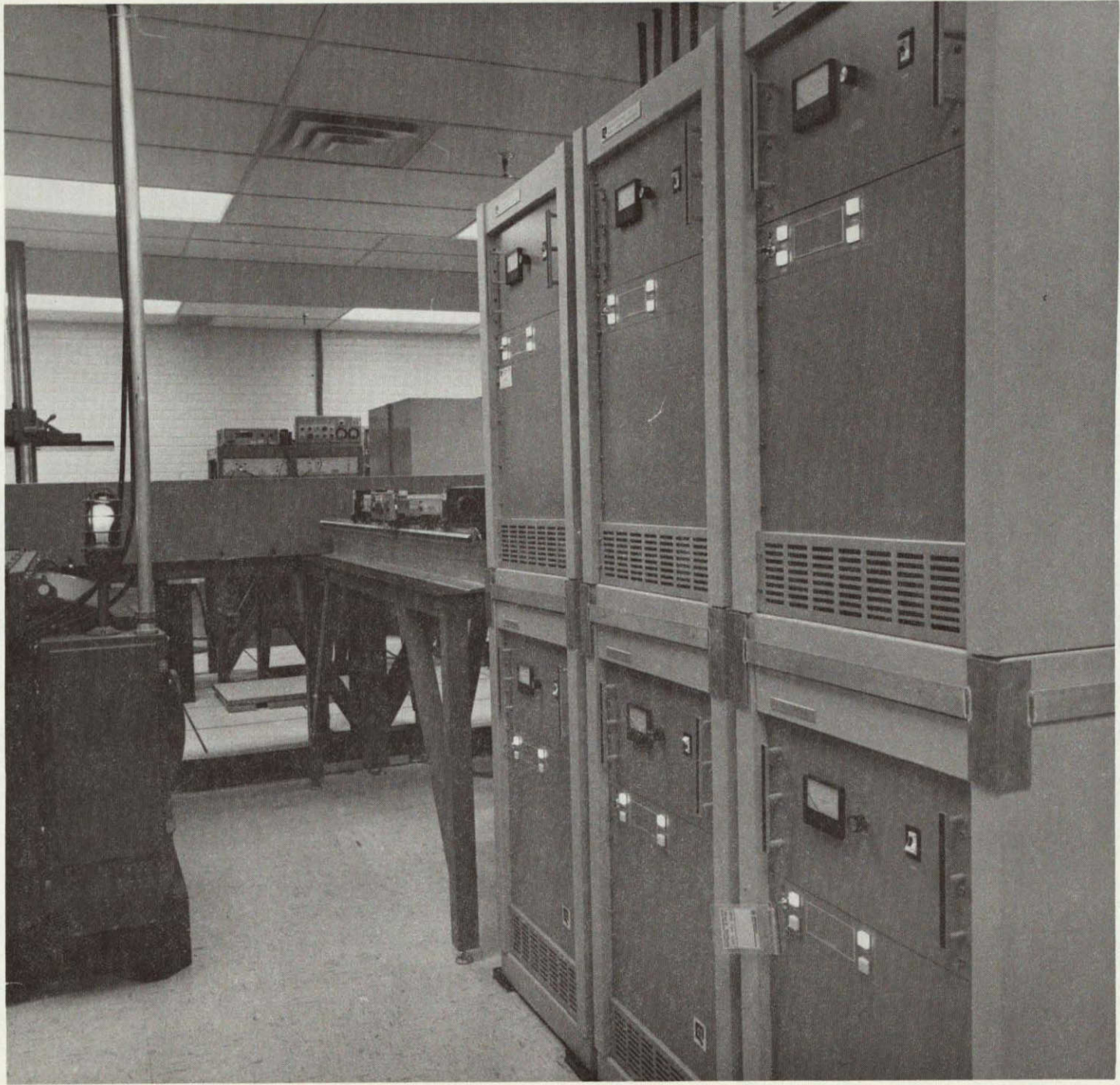


FIGURE 3: Nd:YAG LASER SYSTEM AND POWER SUPPLIES



FIGURE 4: Nd:YAG LASER SYSTEMS (2) ON RAILS

ORIGINAL PAGE IS
OF POOR QUALITY

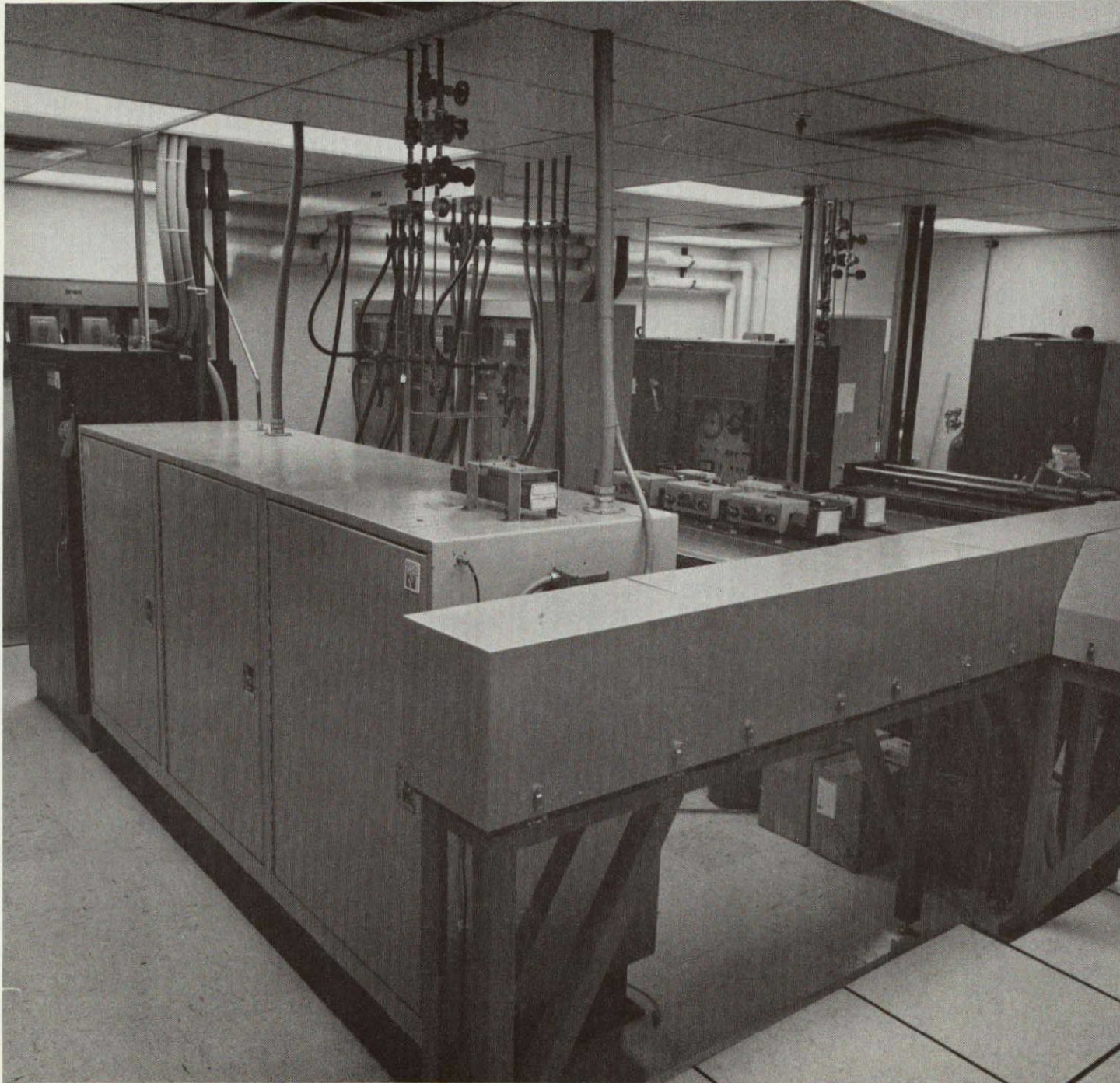


FIGURE 5: ORIGINAL 375W CO₂ LASER. NOTE BEAM TABLE WHICH DIRECTS BEAM TO EXPERIMENTAL TABLES.

ORIGINAL PAGE IS
OF POOR QUALITY

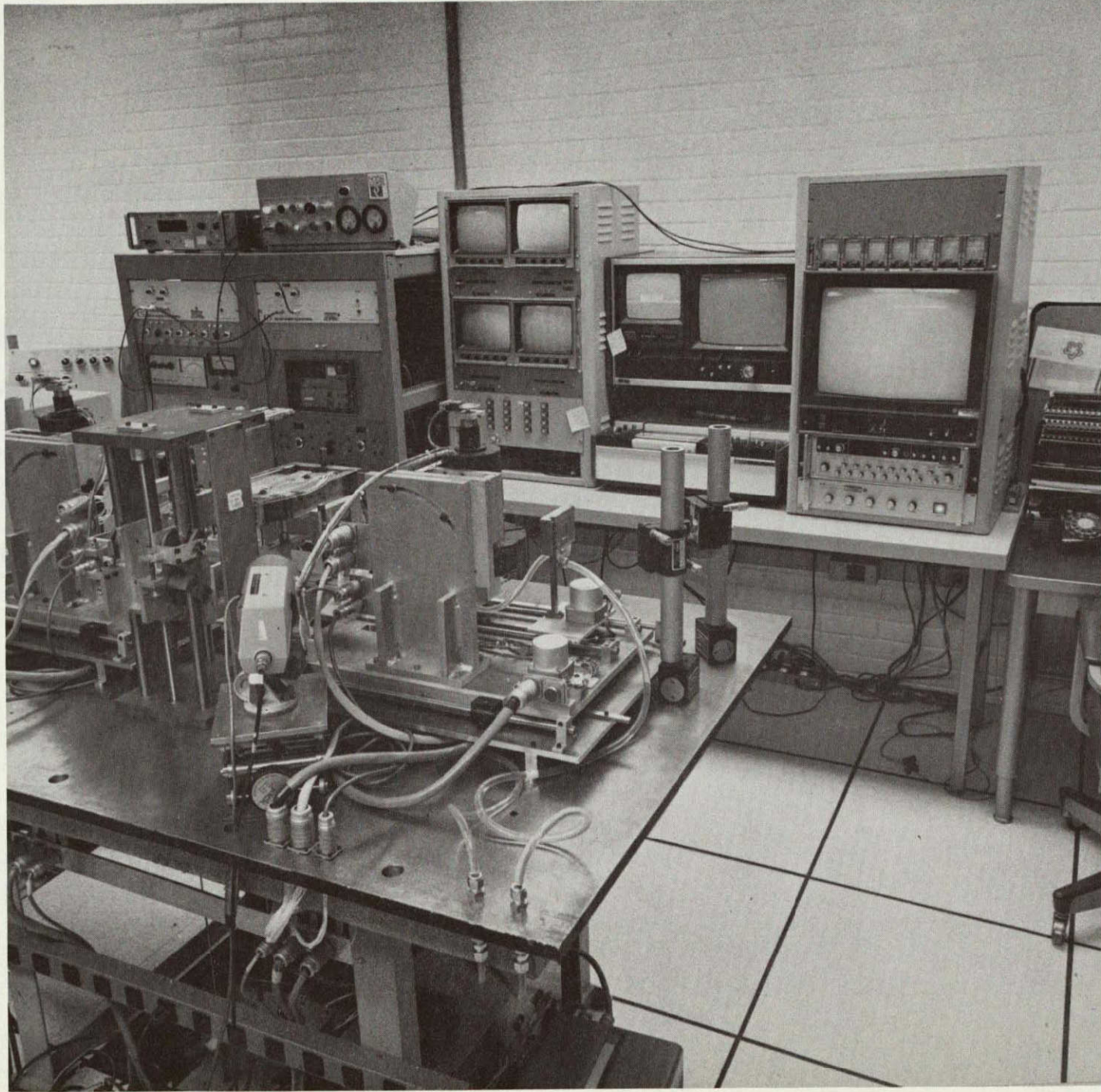


FIGURE 6: RTR#1 EXPERIMENTAL TABLE AND CONTROL/MONITOR ELECTRONICS (IN BACKGROUND).

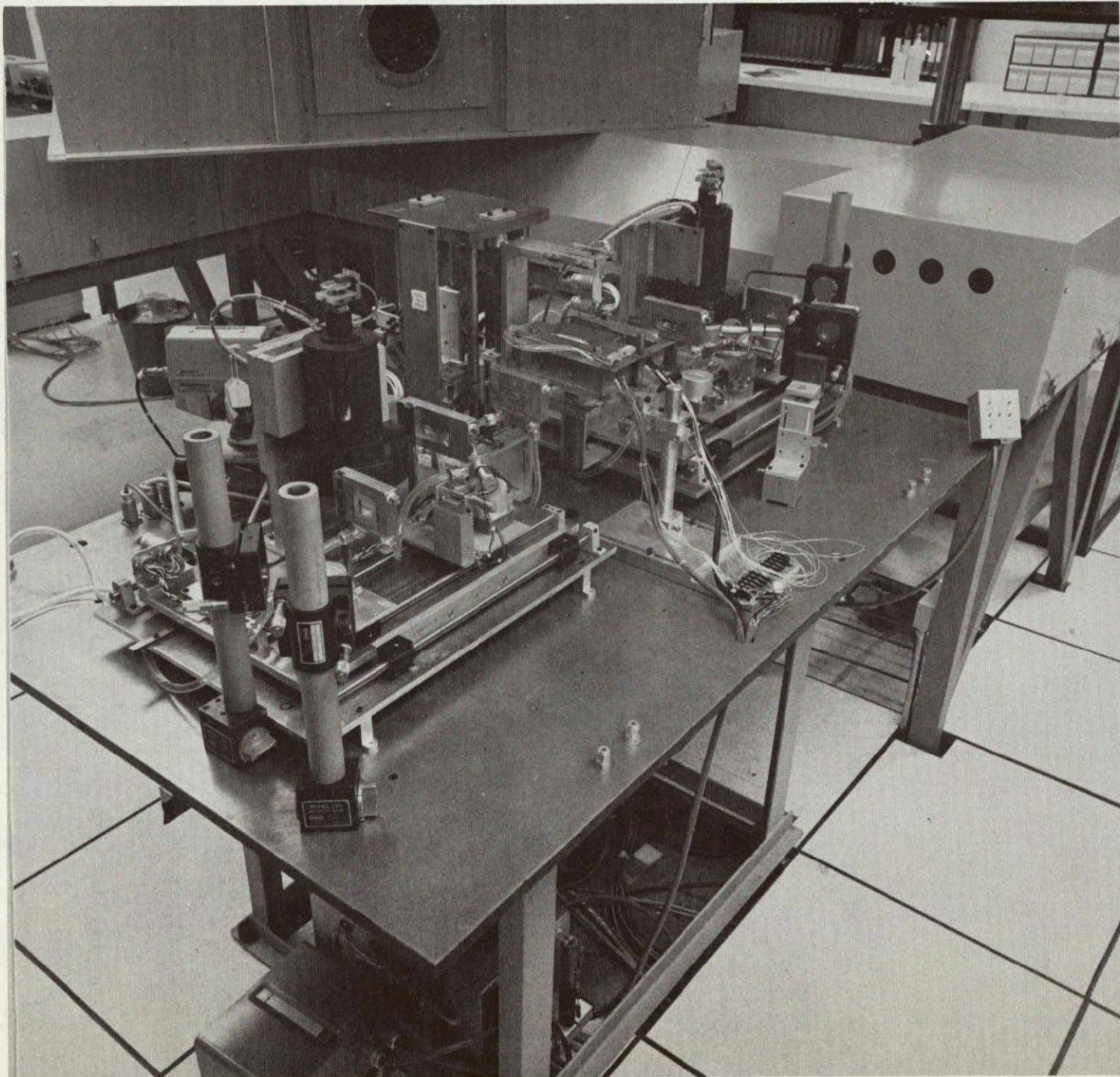


FIGURE 7: RTR#1 NOTE BEAM PORTS (4) TO RIGHT OF TABLE. SHOWN ARE TWO POLYGON SCANNERS, A RIBBON TRANSPORT, AND BEAM DIRECTING MIRRORS.

ORIGINAL PAGE IS
OF POOR QUALITY

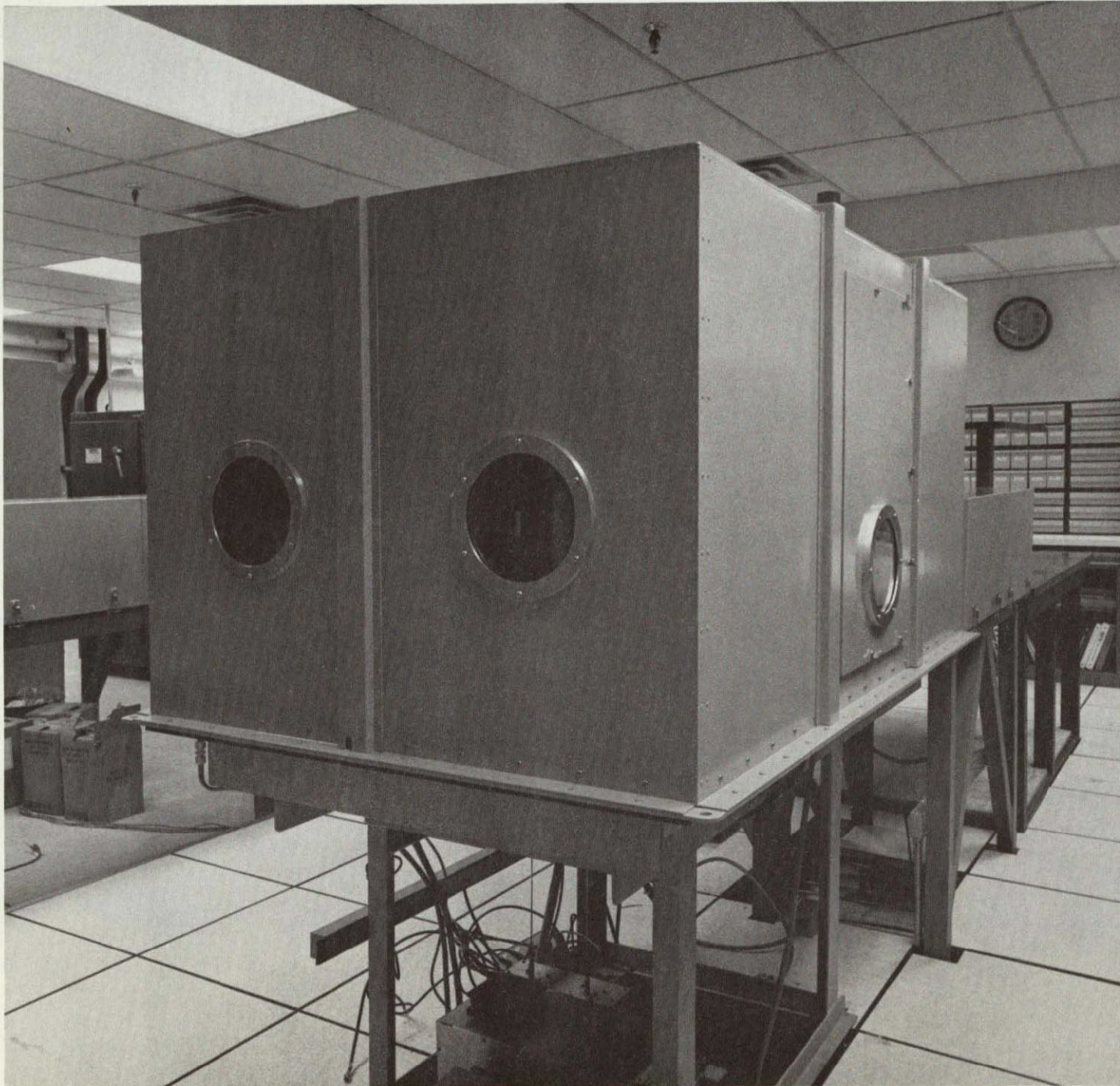


FIGURE 8: COVER INSTALLED

POLYGON SCANNING SYSTEM

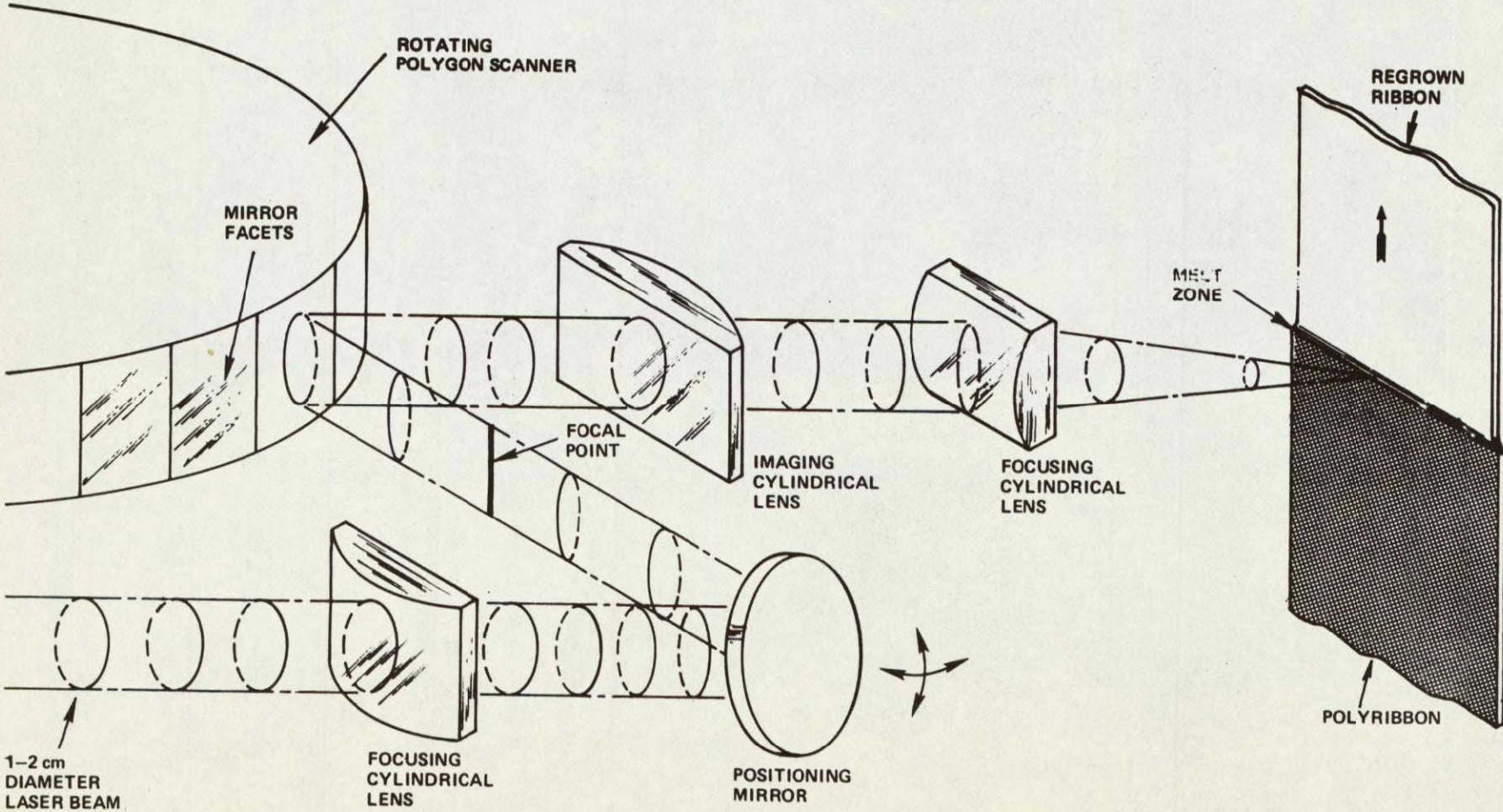


FIGURE 9: POLYGON SCANNER OPERATION

ORIGINAL PAGE IS
OF POOR QUALITY

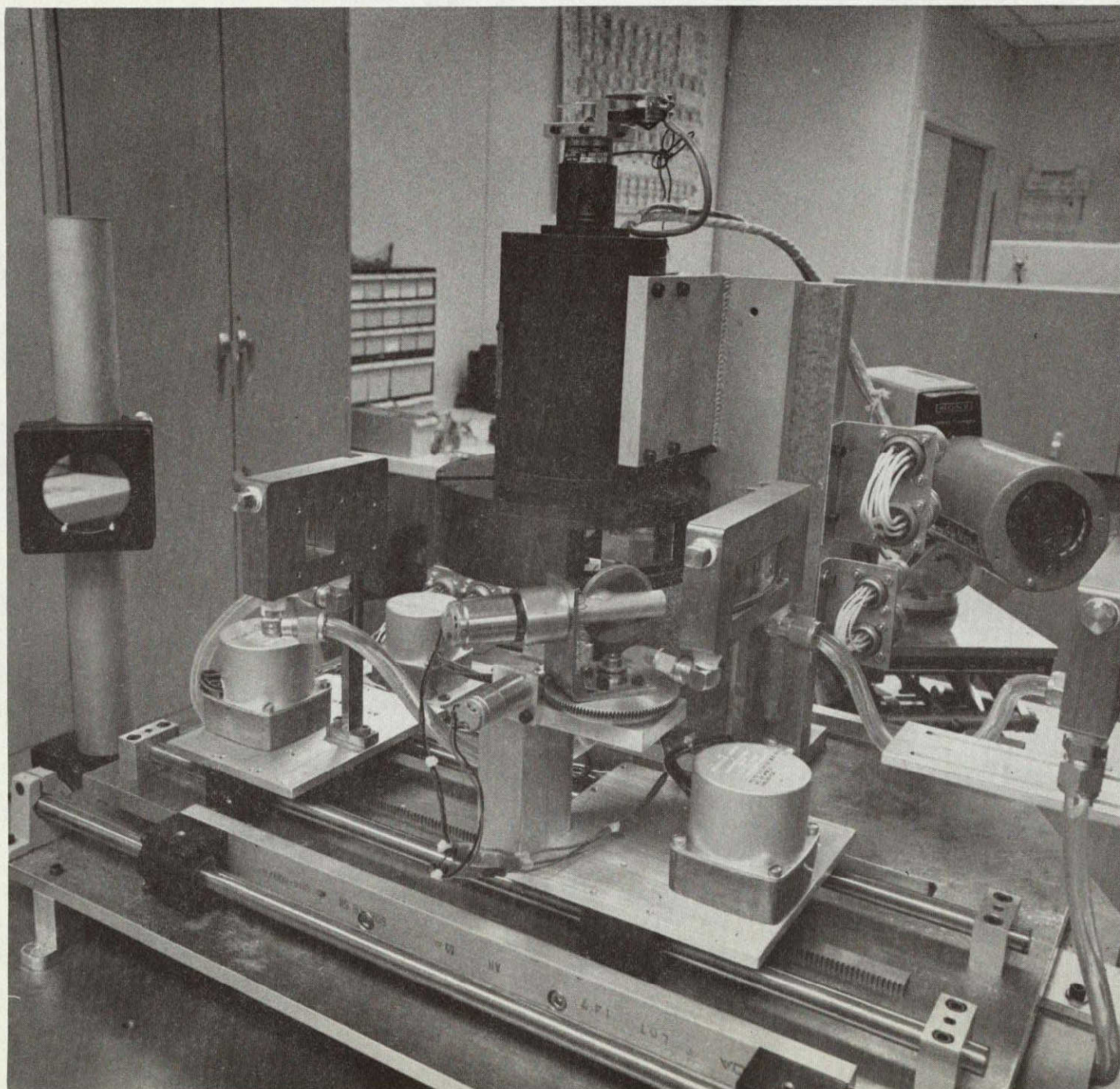


FIGURE 10: HIGH SCAN FREQUENCY POLYGON SCANNER

In the interim, while the various components were being resurfaced, repaired, etc., RTR#1 was rebuilt using the oscillating mirror scan system and/or a cylindrical beam shaping system. This system is now operational.

2.0 BEAM SHAPING SYSTEMS

2.1 POLYGON SCANNER

During the period of relocation and rebuilding after the "flood", few growth runs have been achieved and those have been primarily test runs. Just prior to the "flood", a few test runs were made with the polygon system to determine its performance. These tests were disappointing in that the power distribution is non-uniform -- tending to be much higher at the extremities of the scan. This is contrary to initial assumptions of operation since at the extremities of the scan, the beam will start to divide with one portion being at the end of a scan and the remaining portion at the beginning of the next scan. Consequently one would have expected a power drop-off at the extremities. What appears to be the problem is that aberrations of the imaging cylindrical lens cause smaller amounts of deflection near the edges of the scan than in the middle with the result that more time is spent near the extremities than in the middle. Further testing and analysis will be performed when the polygon scanner is again operational.

2.2 CYLINDRICAL LENS BEAM SHAPING SYSTEM

Without the polygon scanner, a cylindrical lens beam shaping technique has been investigated. This technique is shown in Figure 11. A beam which is nominally a 1 - 2cm diameter cylindrical beam is first diverged in one

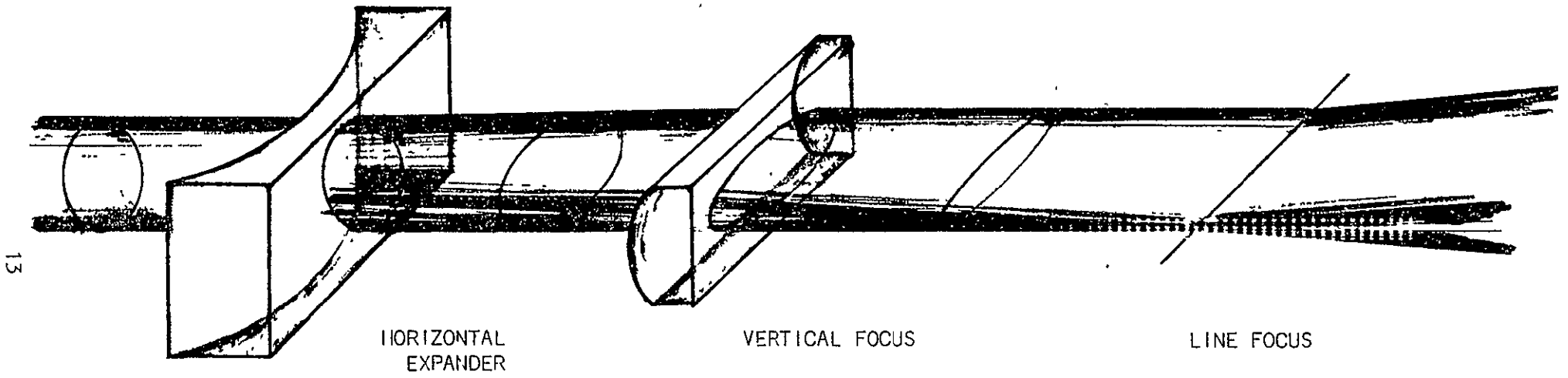


FIGURE 11: CYLINDRICAL LENS BEAM SHAPING SYSTEM

ORIGINAL PAGE IS
OF POOR QUALITY

dimension and then focussed in the other dimension. This gives a wide, but vertically thin, beam incident on the ribbon.

A drawback of this system is that a uniform power distribution cannot result since the initial beam has complex structure. The great advantage of this system is simplicity and the fact that no moving parts are required. Combinations of two or more cylindrical lens systems may offer the possibility for obtaining a more uniform melt.

3.0 CRYSTAL GROWTH

3.1 APPEARANCE OF DENDRITIC STRUCTURE AND RELATION TO CRITICAL GROWTH VELOCITY

One of the most significant achievements during this period has been the demonstration of ribbon growth at 10cm/min., the highest rate reported for ribbon growth as far as is known by the authors. It is also of interest to note (see below) that the attained velocity is in fact greater than the theoretical "maximum" velocity predicted by some authors. In fact, this predicted "maximum" velocity is in reality simply a critical velocity, marking a transition in growth behavior. This growth was achieved with 2.5cm wide feedstock while operating in the ratio growth mode. The resulting ribbon is about .15mm thick and 2cm wide.

Of particular interest is the occurrence of dendritic growth in these high growth velocity ribbons. Observation of the melt zone during growth shows that above a certain critical velocity, the molten zone length increases dramatically. This effect is first noticed in the central portion of the ribbon. Figure 12 illustrates typical behavior of the melt zone as the velocity becomes larger than the critical velocity. It is after the occurrence of this lengthening of the melt zone that the dendritic structure

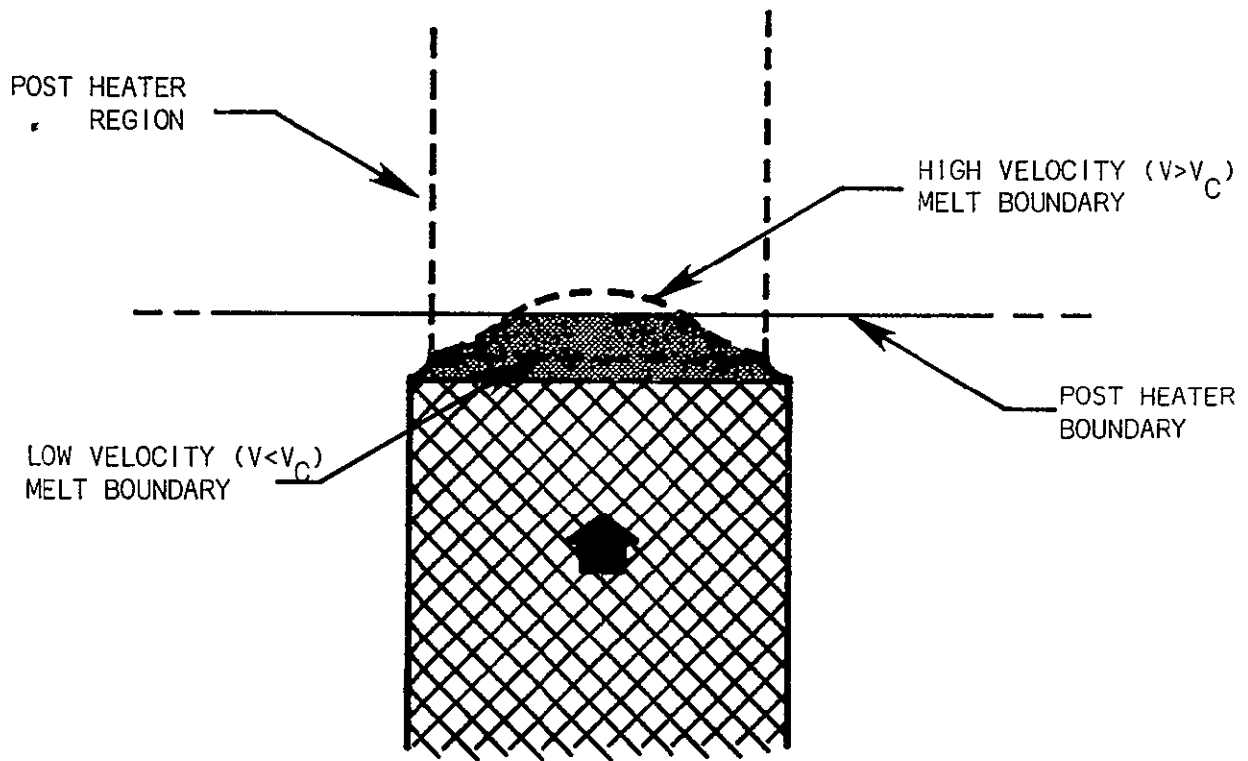


FIGURE 12: MELT ZONE SHAPES FOR GROWTH VELOCITIES BELOW AND ABOVE THE CRITICAL VELOCITY, v_c .

appears on the ribbons. Figure 13 - 15 show photographs of the dendritic structure. Figure 13 is a sample grown in the non-ratio mode with a grown sample thickness of about .33mm. The onset of the non-planar, dendritic structure occurred for this sample at around 3.8cm/min. Figure 14 shows a sample grown in the ratio mode with a grown thickness of about .15mm. Figure 15 is a close-up of the region near the onset of the dendritic structure. The velocity was steadily increased during growth until a maximum growth velocity of 10cm/min. was attained; then the velocity was held constant until growth was terminated. The onset of melt elongation occurred at about 5.7cm/min.

The lengthening of the melt zone is evidence of the critical velocity expected on the basis of thermal modeling of ribbon growth processes. Most authors have simply stated that there exists a limiting growth velocity determined by the condition that the convective transport of the latent heat of fusion match the heat removal rate due to conduction in the solidified ribbon; viz.,

$$V_c = \frac{-K_s \left. \frac{\partial T}{\partial x} \right|_{x=0 \text{ solid}}}{H}$$

where K_s is the thermal conductivity of the solid, and H is the latent heat of fusion per unit volume. This author, however, has considered this velocity as a critical velocity, in exactly the sense as we have observed; i.e., above this velocity the melt length will rapidly increase with increased input power or growth velocity. Attempting growth for velocities above this critical velocity simply increases the possibility of growth instabilities due to an increased melt length.

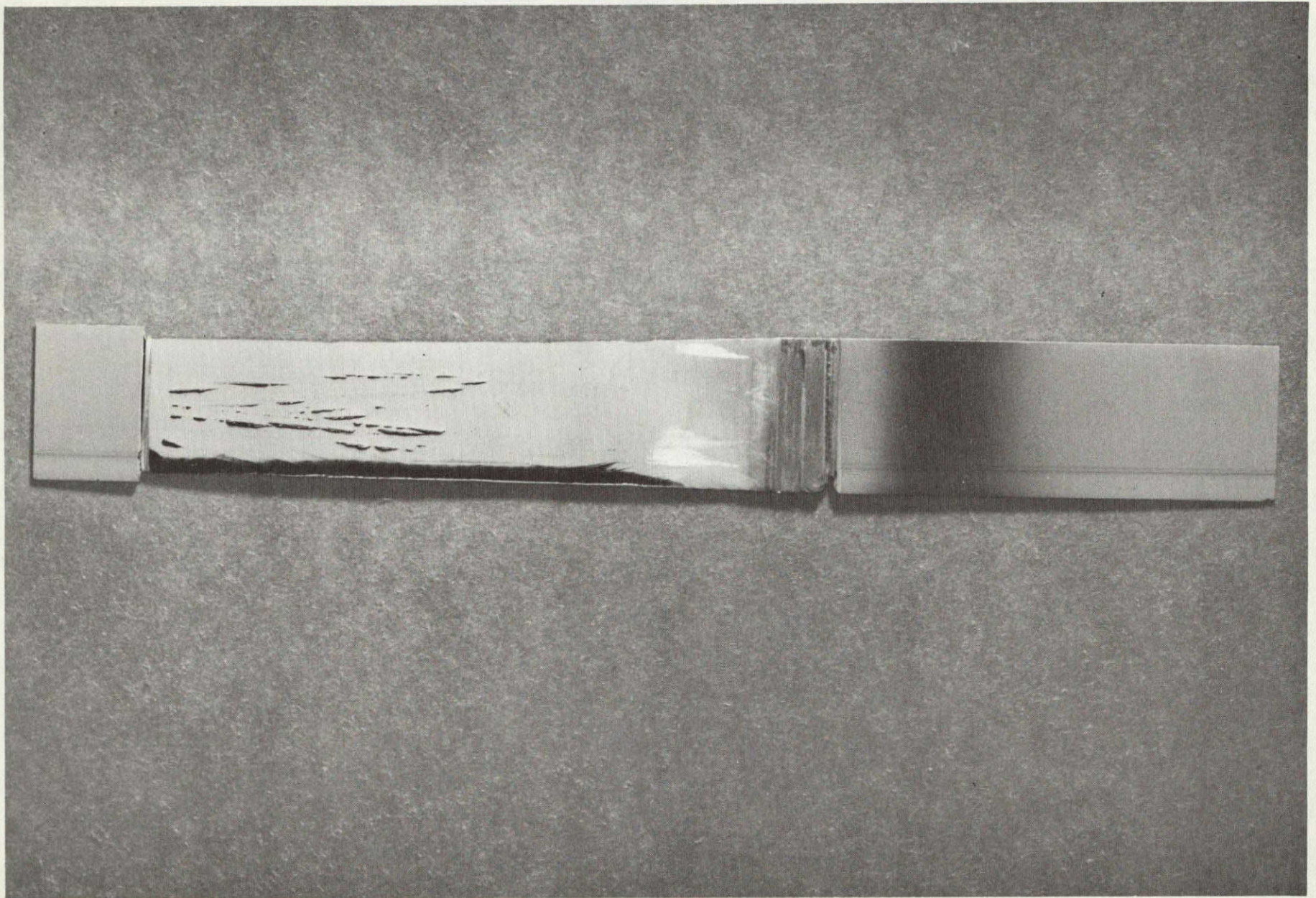


FIGURE 13: RTR RIBBON EXHIBITING DENDRITIC STRUCTURE. SAMPLE WIDTH IS ~ 2.5 cm, MAXIMUM GROWTH VELOCITY ~ 5 cm/min.

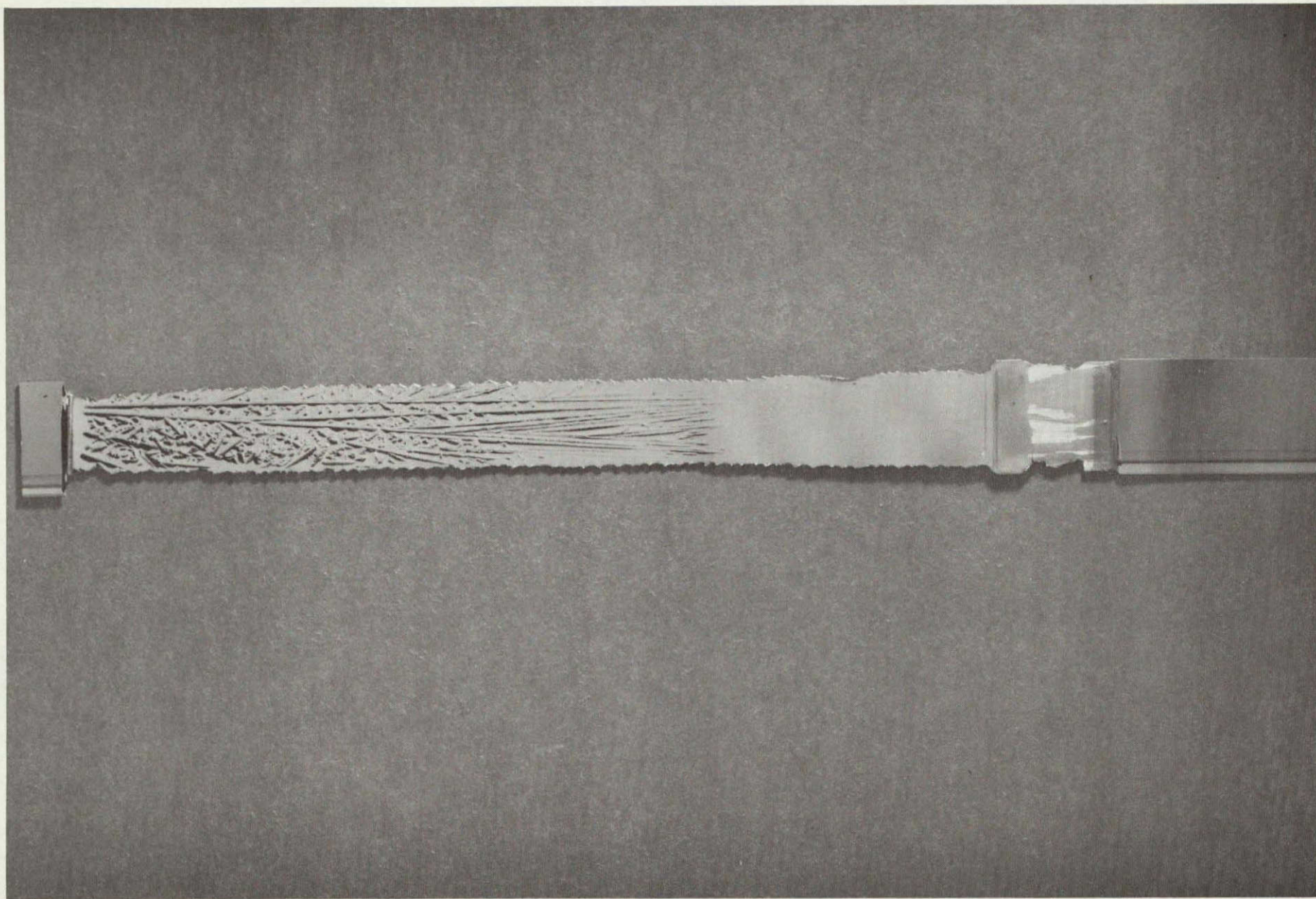


FIGURE 14: RTR RIBBON GROWN AT A MAXIMUM VELOCITY OF 10cm/min. DENDRITIC STRUCTURE OCCURS AROUND 5.7cm/min.

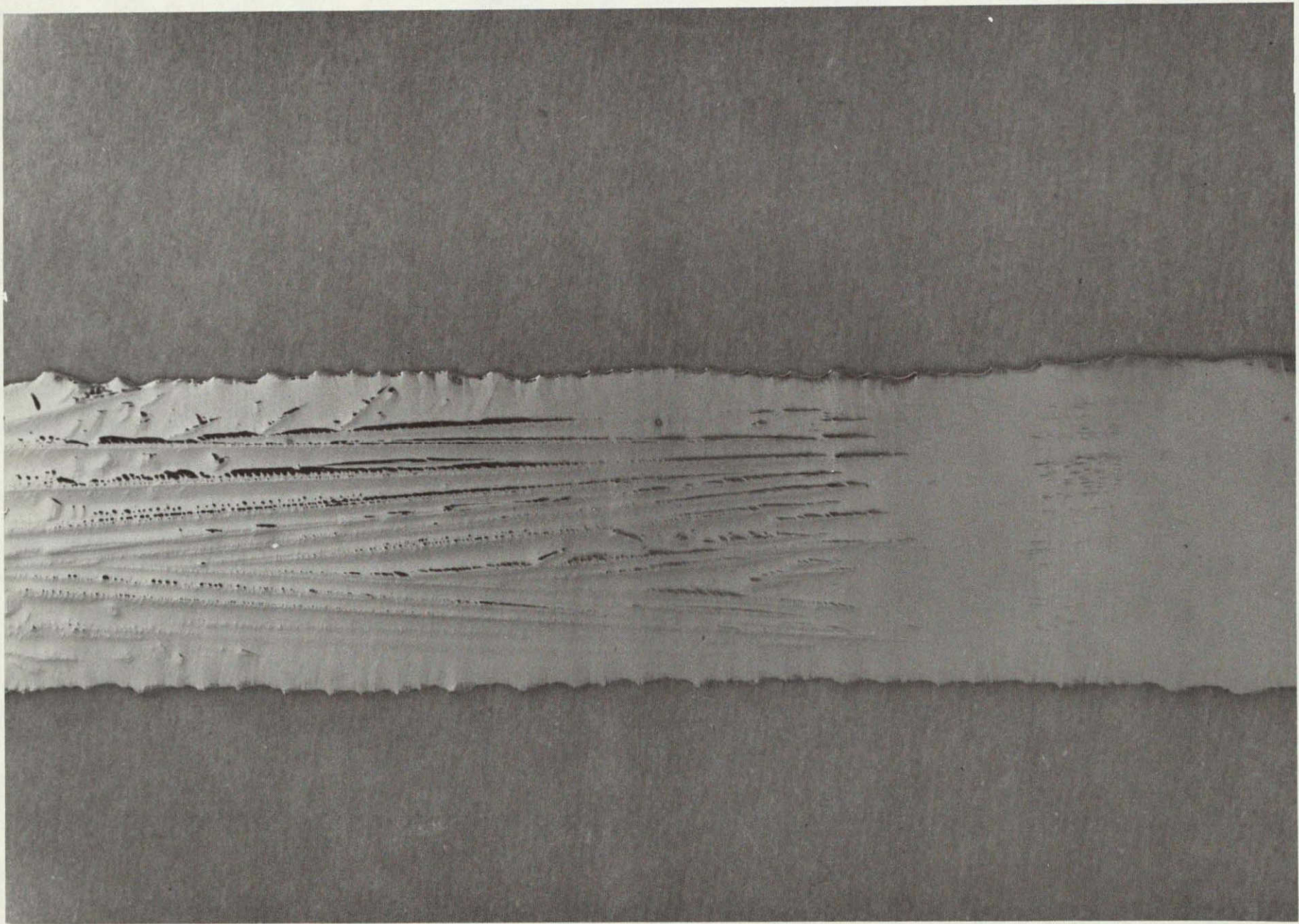


FIGURE 15: CLOSE-UP VIEW OF SAMPLE OF FIGURE 3 SHOWING ONSET OF DENDRITIC GROWTH.

Of the three parameters involved in V_C , K_S and H are supposedly known, and fixed parameters, only $-\partial_x T|_{x=0_+}$ is under experimental control. Affecting this parameter are numerous experimental and environmental parameters: radiation environment, ribbon thickness, location of temperature sources and sinks, convective heat loss properties, and growth velocity. In the June 1976 Quarterly Report (ERDA/JPL 954376-76/2), there was presented a thermal model which allowed calculation of the required thermal gradient parameter and also allowed calculation of the length of the excess molten region. These calculations assumed radiation losses to an isothermal ambient, conduction along the ribbon, and atmospheric convection losses from the surface.

The modeling reported differs in detail from our actual experimental growth environment because it did not treat the influence of a post heater on the interface gradient (modeling now in progress will include such effects). The presence of the post heater will reduce the interface gradient and thereby reduce the predicted critical velocity. An estimate of the impact of the post heater on critical velocity may be obtained by assuming an ambient temperature commensurate with the experimentally measured temperature at the interface region due to the post heater alone. Experimentally this has been determined to be $\sim 1000^\circ\text{C}$. Figure 16 shows calculated critical velocities for various thickness ribbons as a function of an assumed ambient temperature. As can be seen, the addition of a post heater markedly reduces the critical velocity from that of a room temperature environment. The estimated conditions due to the post-heater, and the experimentally observed critical velocities for the samples of Figures 13 - 15 are also indicated. The agreement is rather good, but possibly fortuitous.

The observed melt elongation behavior of Figure 12 may be explained on two counts; first, there is a slight additional heat loss mechanism at the edges due to edge radiation; second, and more important, the central

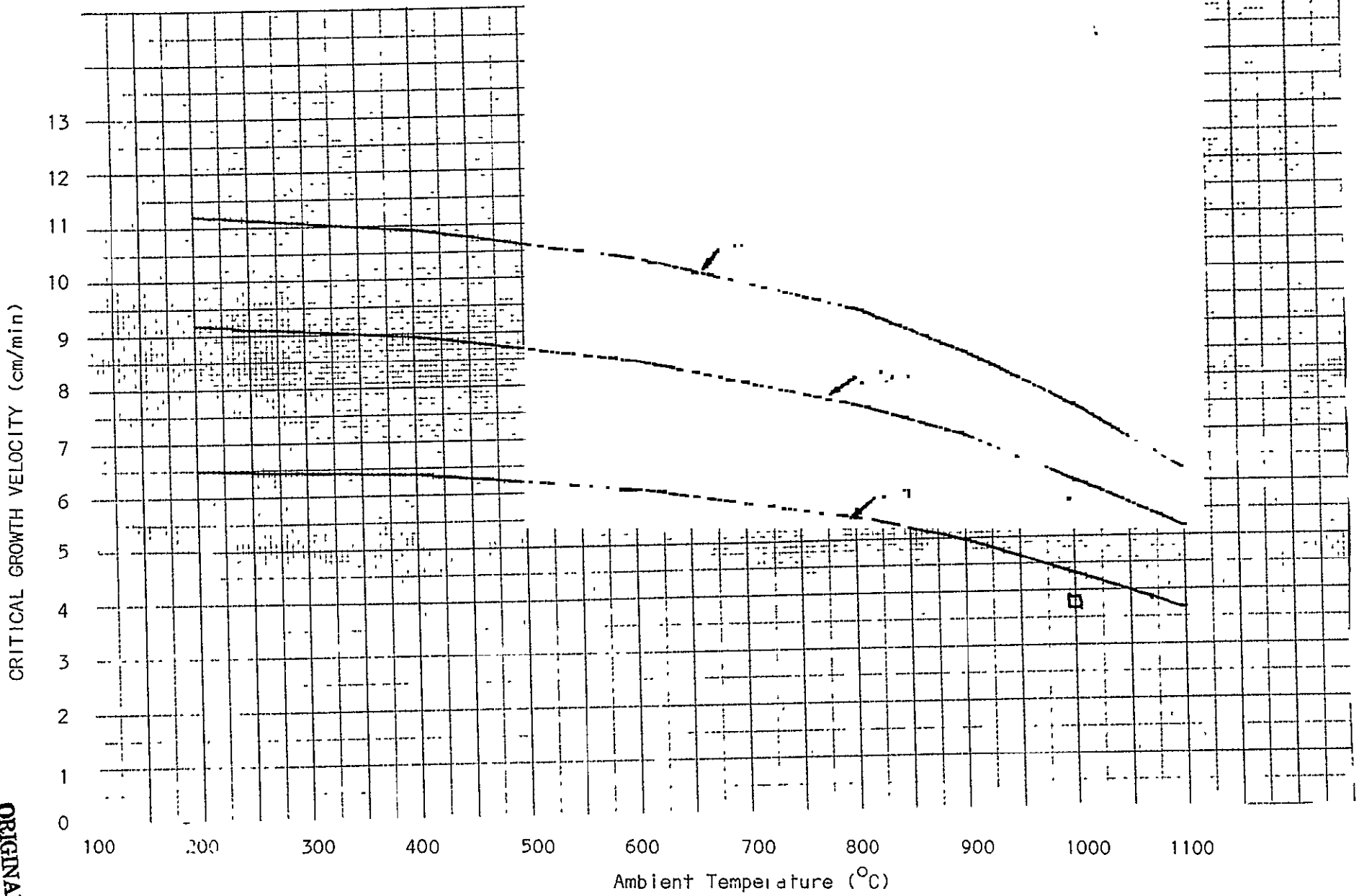


FIGURE 16: EFFECTS OF AMBIENT TEMPERATURE ON CRITICAL GROWTH VELOCITY.

region is thicker than the edges and this means a lower critical velocity in the central region than at the edges. This latter fact is advantageous to high speed growth since an increased melt width at the edge is much more troublesome to growth stability.

Dendritic growth requires that a certain amount of supercooling exist in the melt in order that the latent heat given off during solidification may be rejected to the melt. The driving force for all crystal growth processes in a pure crystal is the degree of supercooling. It is possible that the velocities now being achieved are requiring such a degree of supercooling that dendritic growth is a feasible process. Another possibility, however, is the assumption that as the melt elongates due to growth velocities exceeding the critical velocity, surface radiation losses cause a high degree of supercooling at the surface. The surface is highly conducive to dendritic growth, which first propagates along the surface, then through the bulk.

The influence of the dendritic structure on material characteristics and device performance remains to be seen. One noticeable effect, which may or may not be related to the appearance of the dendrites, is the elimination of buckling in the samples. This may be, as suggested by M. Leibold, a mechanical stiffening effect due to the thickness of the dendrites. Another possibility is a straightening of the thermal profile (tending to remove the "dip") and a consequential reduction in stresses. Dislocation etching and SPV characterization of these samples are in progress.

3.2 ROUTINE GROWTH OF RIBBON SAMPLES

RTR#1 has been used for routine growth from 2.5cm wide feedstock. Various conditions of growth were used to supply a variety of ribbon types

for characterization and for processing into solar cells. The parameters which were varied were ratio or non-ratio growth, and planar or non-planar growth. That is, both ratio and non-ratio samples were grown under conditions 1) which resulted primarily in planar, non-dendritic surfaces, and 2) which had a large amount of dendritic structure.

These samples were all grown with a constant temperature profile similar to that used for the samples of Figures 13 - 15. Another group of samples has also been processed with a new, higher gradient thermal profile. This had the effect of shifting our operating point to the left in Figure 16. With this new profile we have been able to achieve 7.5cm/min. growth velocities of .15mm thick ribbon without the appearance of dendrites.

3.3 STRESS MEASUREMENTS AND BUCKLING OBSERVATIONS

Stress-birefringence evaluations were performed on several ribbon samples. In evaluating the samples it was found that maximum stresses measured on samples fell into two groups. One group had typical maximum stress levels of 700 - 2000 PSI ($4.8 \cdot 10^7$ - $13.8 \cdot 10^7$ dynes/cm²) while the second group had stress levels of less than 350 PSI ($2.4 \cdot 10^7$ dynes/cm²). Review of growth conditions showed that an adjustment was made for the melt-furnace distance coincident with an improvement in residual stresses. The 350 PSI levels of stress are probably typical of the maximum stress levels occurring in properly grown samples. These samples represented non-ratio and ratio growth runs at growth velocities of 2.5 - 4cm/min. and 5 - 5.7cm/min. respectively.

Most of our thin samples have shown significant buckling if no dendritic structure is present. A substantial improvement in ribbon flatness is observed when the critical velocity is approached and dendritic structure occurs.

3.4 GROWTH OF RTR RIBBONS FROM CVD POLYRIBBON

All previously reported RTR growth runs have utilized feedstock (either single crystal or polycrystalline) which was sawn (under considerable hazard of breakage) from large ingots -- hardly an economical process for obtaining polyribbon feedstock. However such feedstock has been perfectly adequate for investigation of growth processes and material quality since, once the feedstock is melted, it loses all "memory" of its origin, except for purity (impurity contributions).

Of course, for the ultimate viability of the RTR process, an economical, high purity, polyribbon process must be available. Such a process has been under development at Motorola, and its basic feasibility demonstrated. Economic viability has also been considered, and is reported in section 8.1. Basically, this process uses CVD techniques to deposit doped polysilicon onto a substrate from which a uniform polyribbon may be detached. The substrate is reusable, the deposition process is efficient, and the throughput can match the RTR growth process.

Figure 17 is a photograph of two large CVD polyribbon samples. Figure 18 shows a 2cm wide sample after RTR growth. Visual examination of such samples reveals substantially the same crystallographic structure as is obtained from single crystal feedstock.

RTR-grown CVD polyribbons will soon be processed into solar cells. SPV measurements have been made on one RTR-grown CVD polyribbon. This particular sample was doped to approximately $.7 - 1.0\Omega\text{cm}$ and exhibited a diffusion length of about $6\mu\text{m}$ -- typical of as-grown RTR ribbons although heavier doped.

4.0 SOLAR CELL PROCESSING/EVALUATION

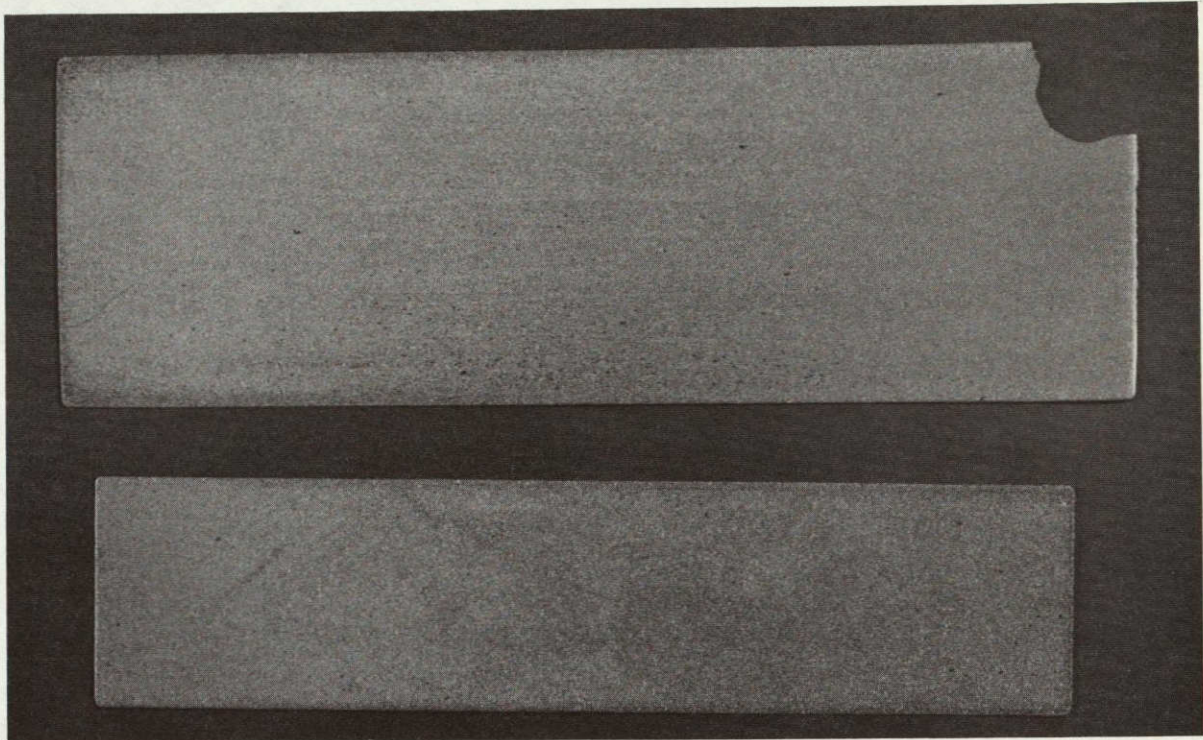


FIGURE 17: LARGE AREA SAMPLES OF CVD POLYRIBBON

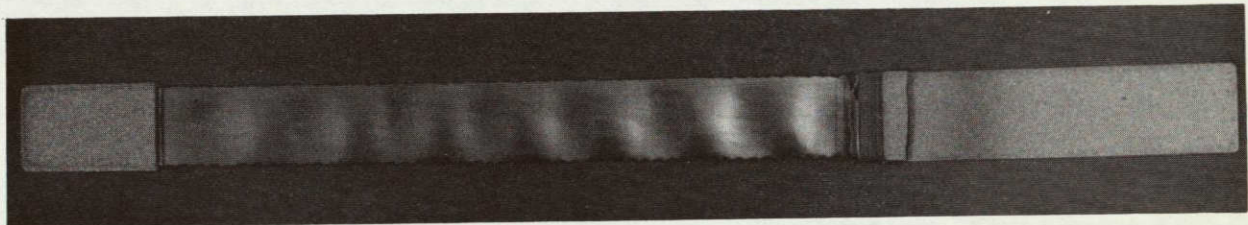


FIGURE 18: DOPED CVD POLYRIBBON REGROWN BY THE RTR PROCESS

ORIGINAL PAGE IS
OF POOR QUALITY

4.1 EVALUATION RESULTS

Several groups of solar cells have been evaluated during this report period. Tables I and II summarize results from two lots.

TABLE I

LOT # R121

GROWTH PARAMETERS: Starting Material - Cz, (100), [100], 5 Ω -cm P type
 Translation Mode - Lock
 Laser Power - ~360W
 Growth Velocity - 1"/min
 Laser Irradiation - Both sides
 Furnace Profile - A4, A5

	RIBBON CELLS 41 GOOD, 5 REJECT		RIBBON CONTROLS 10 CELLS		CONTROLS 6	
	MAX	AVG	MAX	AVG	MAX	AVG
V _{OC}	.505	.485	.573	.553	.574	.573
J _{SC}	27.9	24.9	34	31.8	35.5	34.1
η	9.4	7.5	13.8	12.3	14.4	13.9
F.F.	.67	.62	.71	.70	.715	.71

TABLE II

LOT # R122

GROWTH PARAMETERS: Starting Material - Cz (100), [100], 5 Ω -cm P type
 Translation Mode - Ratio - 2" uptake/1" feed
 Laser Power - ~380W
 Laser Irradiation - North Side Only
 Furnace Profile - A5

	RIBBON CELLS 20 CELLS		CONTROLS 7	
	MAX	AVG	MAX	AVG
V _{OC}	.496	.464	.558	.548
J _{SC}	29.1	27	36.1	35.1
η	9.5	7.7	14	13.3
F.F.	.66	.615	.695	.689

4.2 DISCUSSION OF SOLAR CELL EVALUATIONS

The ribbon controls and the pure controls demonstrate high efficiencies and little variation. This points out that the processing sequence utilized was quite good, although improvements in fill factor might be expected.

The ribbon cells, however, exhibit disappointingly low efficiencies -- this is in consideration of the rather good visual appearance of the cells. Much of the relatively poor performance of these groups can be accounted for, though. It has been found that the present metallization process being used, while evidently normally acceptable for single crystal samples, is degrading V_{OC} (and probably the fill factor too) on ribbons. V_{OC} measurements were made on lot R112 before and after the metallization step, and an average $\Delta V_{OC} = -40\text{mV}$ was observed. This is a significant loss and cannot be accounted for by metal coverage. Assuming an improved average V_{OC} for these cells to .504 from .464, and an improved fill factor to .7 from .65, the average efficiency would have been 9.52%. Experimentally these effects have also been observed on single crystal samples when improper metallization procedures were used. It is possible that because of the more numerous defects and grain boundaries, the RTR ribbons are more susceptible for this problem.

The present metallization process utilizes a palladium surface activation with a subsequent nickel plating, then a solder dip. The degradation is associated with the palladium activation step which incorporates a sintering process. It is felt that possibly a lower sintering temperature may be appropriate. For this reason the most recent batch (lot #124) of ribbon solar cells was split into two groups, one for high and one for low temperature metallization. Each group was comprised of wide (2.5cm) and narrow (1.25cm) samples. Unfortunately, it was subsequently found that both groups had been exposed to a high temperature

sintering cycle. Average efficiency for the narrow ribbon cells is 7.6%. The wider ribbon cells averaged 6.5%, with about half of the wide ribbon cells (including control cells) being casualties due to poor photoresist adherence.

It should be noted, however, that in this case many of the control cells were also severely degraded -- consequently some other processing problems may have occurred to these samples.

Experiments are planned to test alternative metallization schemes which hopefully will not degrade the solar cell characteristics. Low temperature ($T < 200^{\circ}\text{C}$) annealing cycles are being tried on test wafers, and will be used on the next lot of ribbon cells. In addition, evaporated titanium-silver or aluminum contacts will be tried.

5.0 MATERIAL EVALUATION

In order to study the electrical activity of planar defects in RTR silicon, an array of 1mm diameter diodes was fabricated on RTR sample 294. The short circuit current (I_{SC}) under AM1 illumination was measured for each diode, and was used as a figure of merit in evaluating the diode quality. Control diodes fabricated on single crystal Czochralski silicon generated I_{SC} ~0.26mA under AM1 illumination. After taking an optical micrograph of each diode, SEM micrographs were taken using the AC Electron Beam Induced Current (EBIC) mode. Figures 19a, 20a, 21a, and 22a are EBIC micrographs of selected diodes, while Figures 19b, 20b, 21b, and 22b are optical micrographs of the corresponding diodes. Unfortunately, the quality of the optical micrographs is poor.

Figure 19a, b, show diode 7-3. This diode is a relatively poor performer, with I_{SC} ~0.20mA. The strongest features in the EBIC micrograph are the three grain boundaries which intersect the numerous parallel twins in the

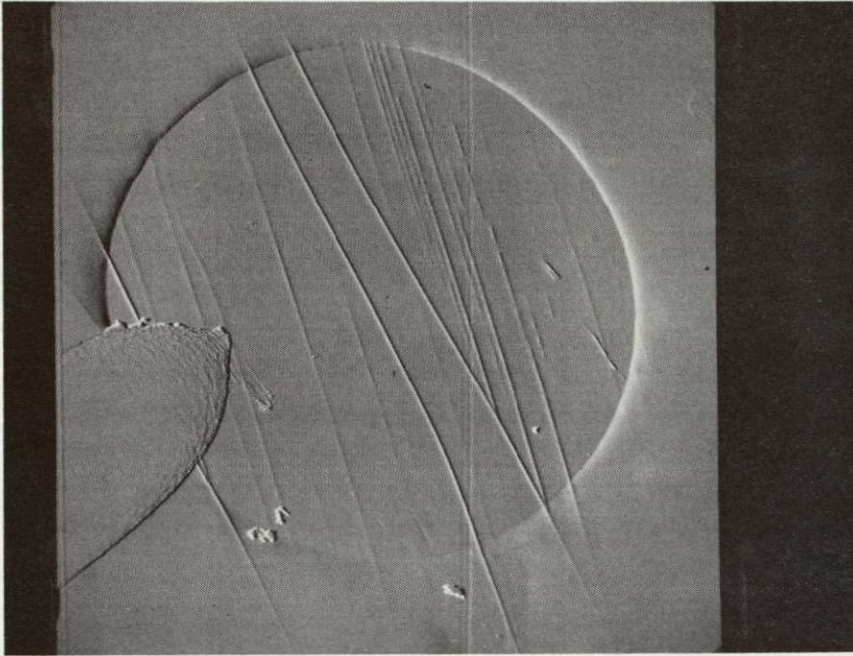


FIG. 19 -a
EBIC Mode Photo
of
Diode
7 - 3

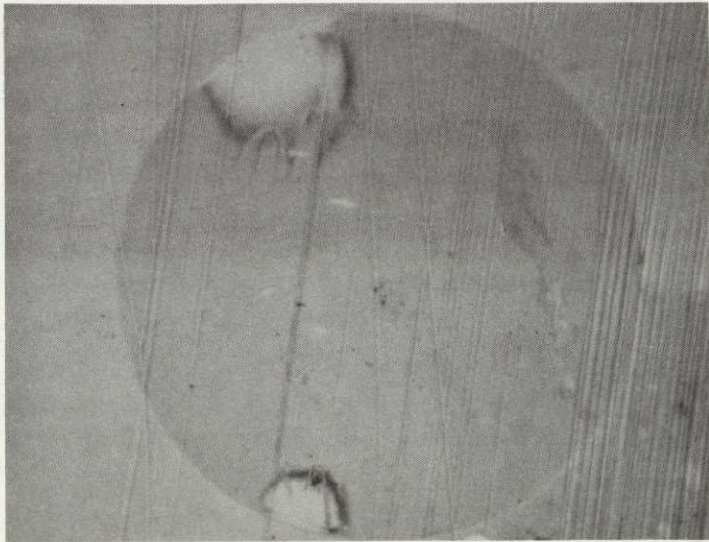


FIG 19 -b
Optical Micrograph
of
Diode
7-3

**ORIGINAL PAGE IS
OF POOR QUALITY**

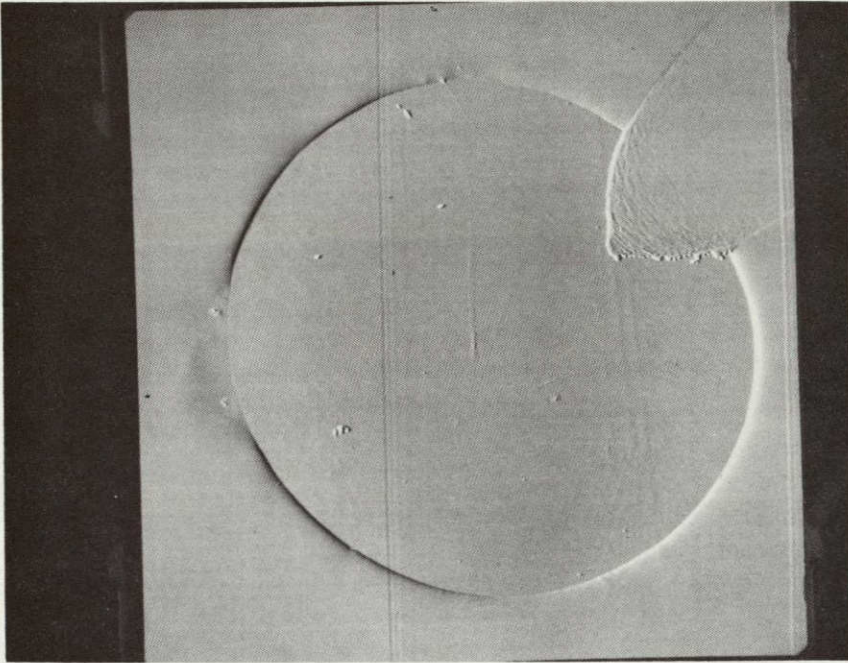


Fig. 20-a
EBIC Mode Photo
of
Diode
5 - 6



Fig. 20 -b
Optical Micrograph
of
5 - 6

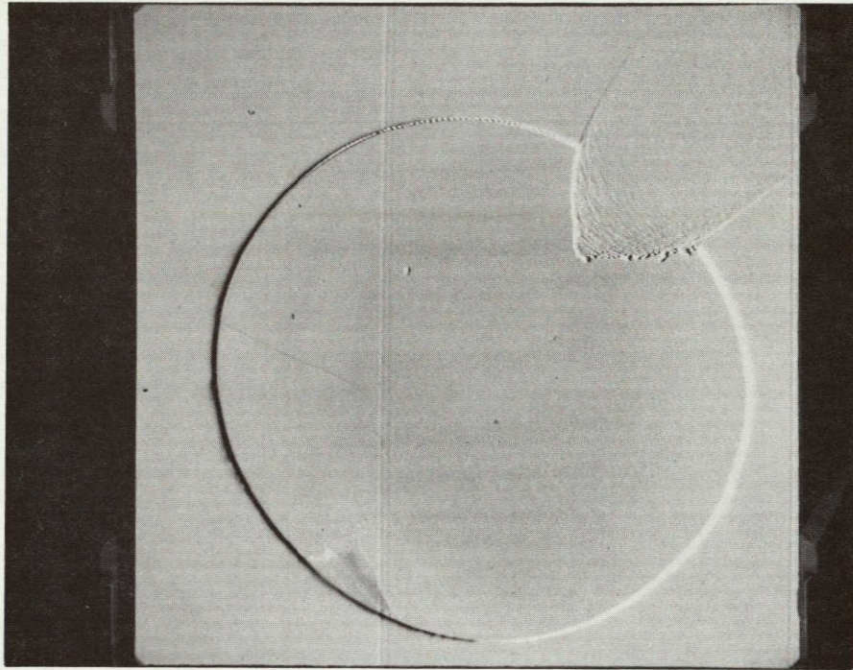


Fig. 21 -a
EBIC Mode Photo
of
Diode
11-2

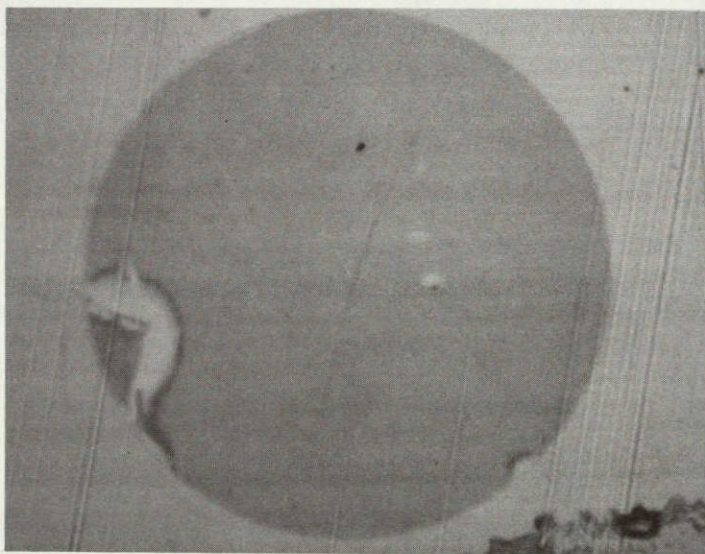


Fig. 21 -b
Optical Micrograph
of
Diode
11-2

**ORIGINAL PAGE IS
OF POOR QUALITY**

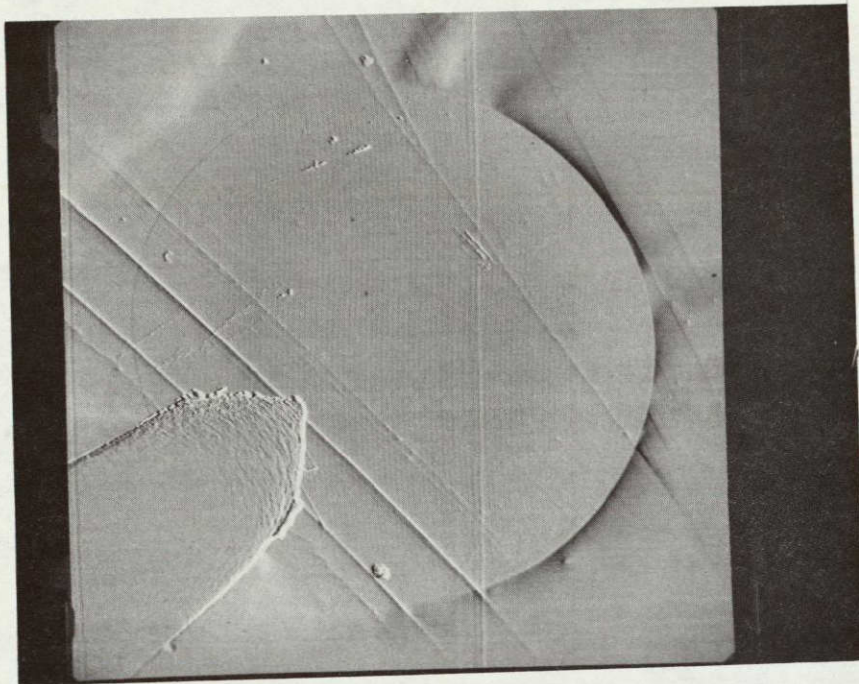


Fig. 22-a
EBIC Mode Photo
of
Diode
5-5



Fig. 22 -b
Optical Micrograph
of
Diode
5-5

sample. Roughly half the parallel boundaries seen in Figure 19 are revealed as electrically active defects in 19a, although they are not as strongly active as the "crossing" boundaries. Several inclusions, which cannot be seen in 19b, are shown as strongly active in 19a. However, they do not cover a significant fraction of the total diode area.

Figures 20a, b show diode 5-6. Its $I_{SC} = 0.26\text{mA}$, matches the short circuit current generated in the control diodes. The faint double line running vertically through the diode is only a synchronous interference (it appears somewhere in most of our EBIC micrographs). The parallel twin boundaries which can be seen faintly in 20b do not appear in 20a. Thus diode 5-6 is a simple case: it performs well and is relatively defect-free in both the optical and the EBIC micrographs.

Figures 21a, b show diode 11-2. This diode is a poor performer, $I_{SC} \sim 0.19\text{mA}$, although both the EBIC and the optical micrographs are relatively free of grain boundaries, twins or stacking faults. Diode 11-2 is thus a counter example to diode 5-6, since it shows that other factors, e.g., a high dislocation density, or a distributed impurity, are reducing the generated current.

However, we can also find a counter example to diode 7-3. Figures 22a, b, are micrographs of diode 5-5. This diode generated an $I_{SC} \sim 0.25\text{mA}$, almost matching the $I_{SC} \sim 0.26\text{mA}$ of diode 5-6. Figure 22a shows ~ 5 reasonably well-defined active planar defects, plus a number of barely visible lines. Note that the dense parallel twin bundles seen in Figure 22b are not electrically active. It is also apparent that one cannot predict from 22b which would be the most active boundaries in 22a.

Since only one RTR sample has been examined, these EBIC results are preliminary. Several tentative conclusions can be drawn, however. Parallel

ORIGINAL PAGE IS
OF POOR QUALITY

twin boundaries are often not innocuous, as shown most clearly in Figure 22. Intersecting grain boundaries are strongly active, and significantly reduce cell performance. Diode 11-2, however, shows that other "distributed" factors, such as a high dislocation density or a distributed impurity, can be responsible for reducing cell performance.

6.0 DEVICE AND PROCESSING STUDIES

6.1 DISLOCATION LENGTH AND DISLOCATION DENSITY MAPPING ON RIBBON SOLAR CELLS

A single RTR ribbon which had been processed into solar cells, except for the last metallization step, was studied in detail. Figure 23 illustrates the analyzed ribbon. Seven solar cell regions measuring $2.1 \times .85\text{cm}$, or 1.79cm^2 each, were available. Device 1 was a control cell -- i.e., a cell residing on ribbon which was not regrown. It did, however, experience some elevated temperatures -- as high as $1200 - 1300^\circ\text{C}$. This is because this portion of the ribbon was in the linear profile furnace prior to growth initiation. Samples #2 and #7 both are partly on control regions and partly on regrown regions. Typically, the worst performance occurs in these regions due to the special (high) stresses in these regions and the fact that these regions are held at high temperatures for a longer period of time than central, steady state regions.

Open-circuit-photovoltage (OCPV) measurements of diffusion length were performed at numerous points on each cell in order to map regions of long and short diffusion lengths. All measurements were performed with a light spot diameter of $\sim 2\text{mm}$. After mapping the OCPV diffusion lengths, the entire ribbon was first stripped of AR coating and then silicon etched to remove both the

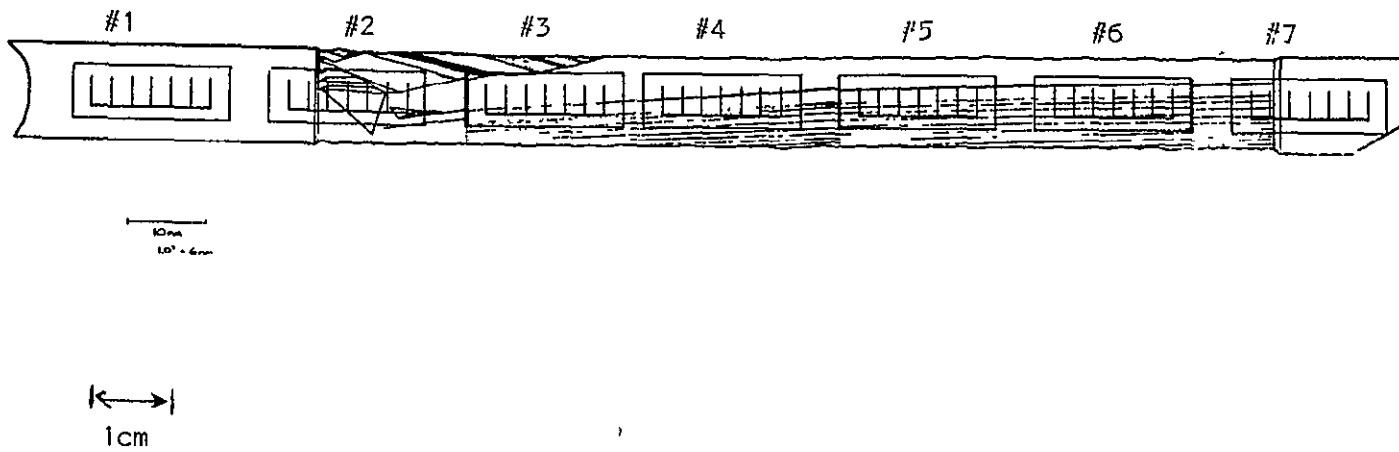


FIGURE 23: RIBBON SOLAR CELLS UTILIZED FOR OCPV/SPV/DISLOCATION DENSITY CORRELATIONS

front n+p, and back p+p junctions. SPV measurements were then made at the same spatial locations where the solar cell OCPV measurements were made. This was to verify that the two techniques indeed measure the substrate diffusion length and that no anomalous readings occur due to the presence of the junctions.

Results of these measurements are shown in Figures 24 through 27. Two values are indicated where both OCPV and SPV diffusion lengths were made. From these data we conclude the following:

- 1) Processed RTR ribbon solar cells are now exhibiting very high diffusion lengths, comparable to starting single crystal values. Diffusion lengths of $178\mu\text{m}$ have been measured on ribbon cells.
- 2) The agreement of the OCPV and SPV diffusion lengths shows that substrate diffusion lengths are indeed quite high compared to unprocessed substrates (typically $6 - 15\mu\text{m}$).
- 3) The average diffusion lengths are high also, but local regions of short diffusion length still exist.
- 4) Regions near initial and final melt exhibit anomalous behaviour in that the control sides have very low diffusion lengths but the adjacent regrown regions are much better. This is in spite of higher dislocation densities in the regrown region. This again points to purely thermal/impurity effects as bad actors.

In performing these measurements, some were made near or over grain boundaries, but most were measured in areas containing twins but no large angle grain boundaries. Measurements over large angle grain boundaries were widely scattered -- $25 - 170\mu\text{m}$.

After completion of the OCPV and SPV measurements for diffusion length, the ribbon was then Wright etched to reveal dislocations. Dislocation density counts were made where possible -- some grain orientations were not conducive

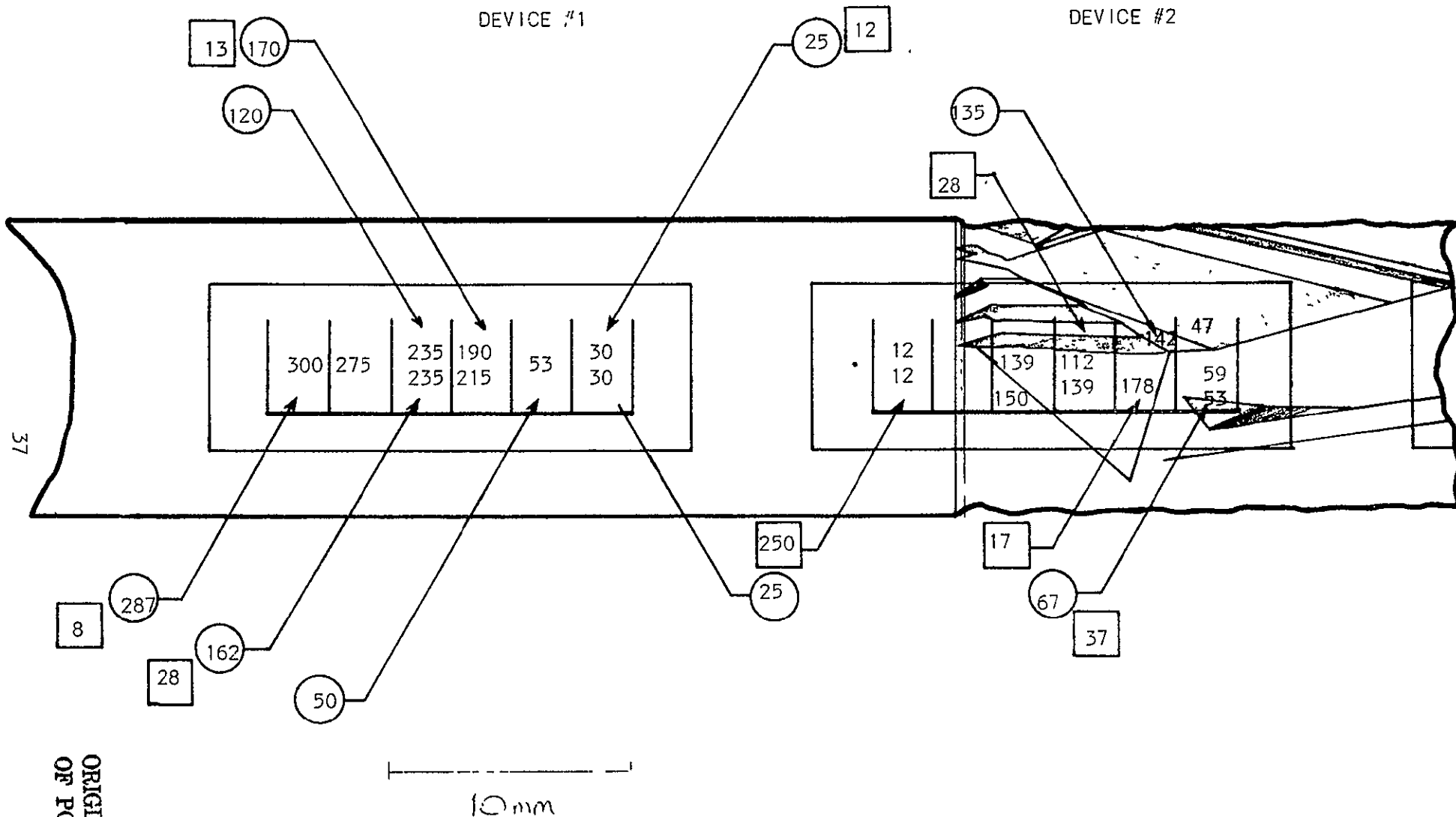


FIGURE 24 OCPV DIFFUSION LENGTHS (NUMBERS ON FIGURE), SPV DIFFUSION LENGTHS (O) AND DISLOCATION DENSITIES (□) MEASURED ON RIBRON SOLAR CELLS. DISLOCATION DENSITIES ARE TIMES 10^4cm^{-2} .

ORIGINAL PAGE IS
OF POOR QUALITY

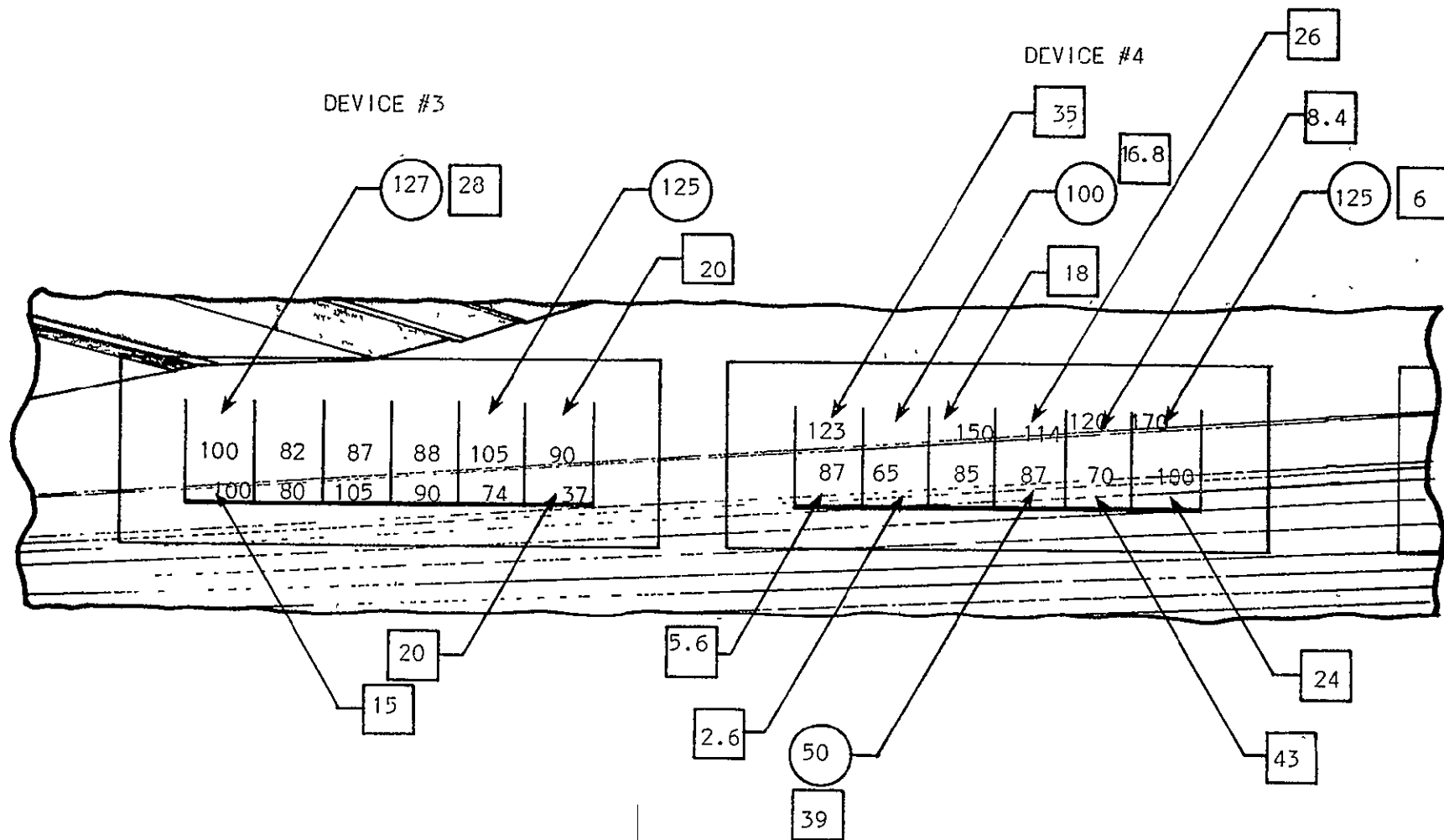


FIGURE 25: OCPV DIFFUSION LENGTHS (NUMBERS ON FIGURE), SPV DIFFUSION LENGTHS (O) AND DISLOCATION DENSITIES (□) MEASURED ON RIBBON SOLAR CELLS. DISLOCATION DENSITIES ARE TIMES 10^4 cm^{-2} .

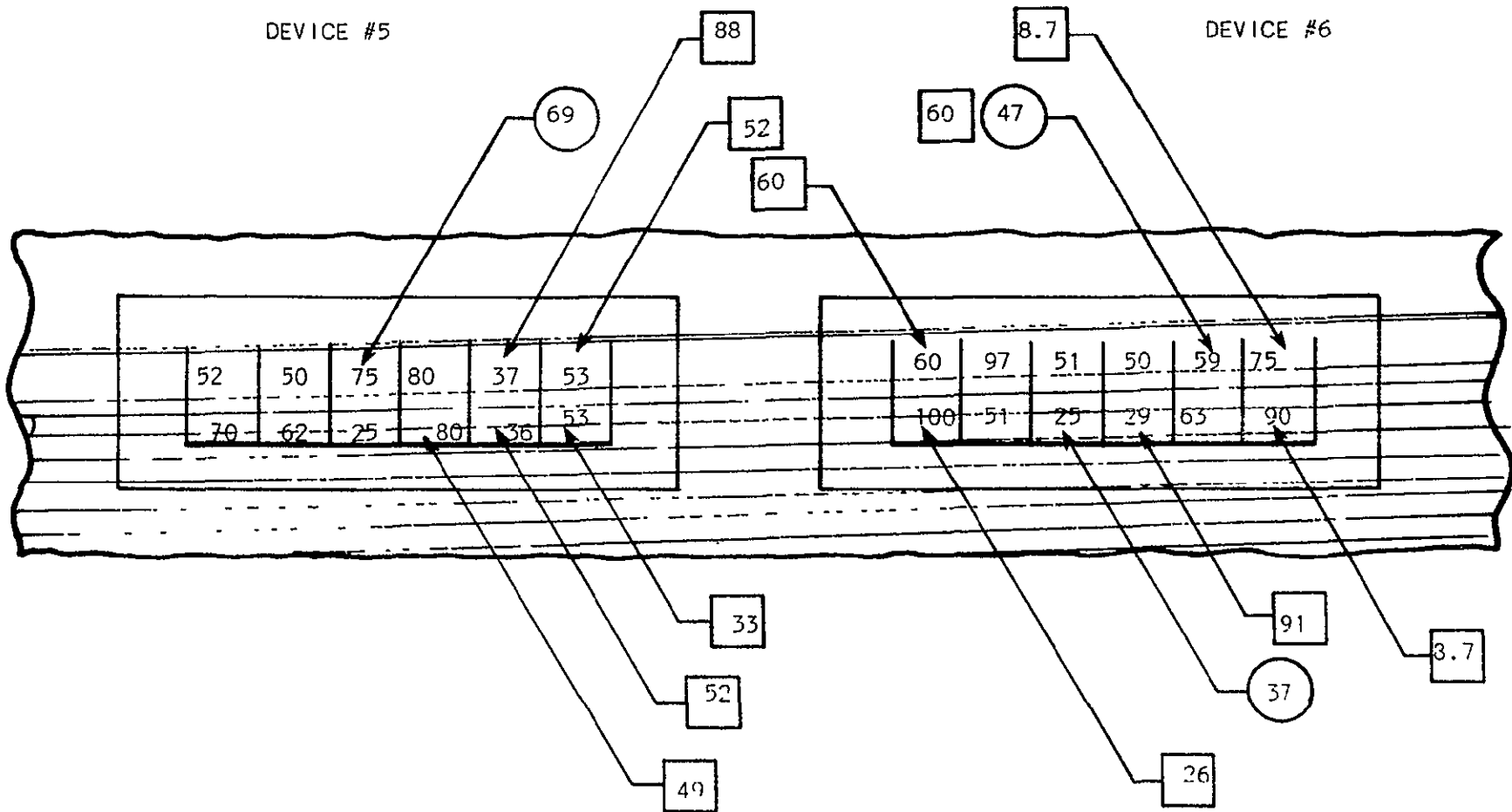


FIGURE 26 OCPV DIFFUSION LENGTHS (NUMBERS ON FIGURE), SPV DIFFUSION LENGTHS (O) AND DISLOCATION DENSITIES (□) MEASURED ON RIBBON SOLAR CELLS. DISLOCATION DENSITIES ARE TIMES 10^{10} cm^{-2} .

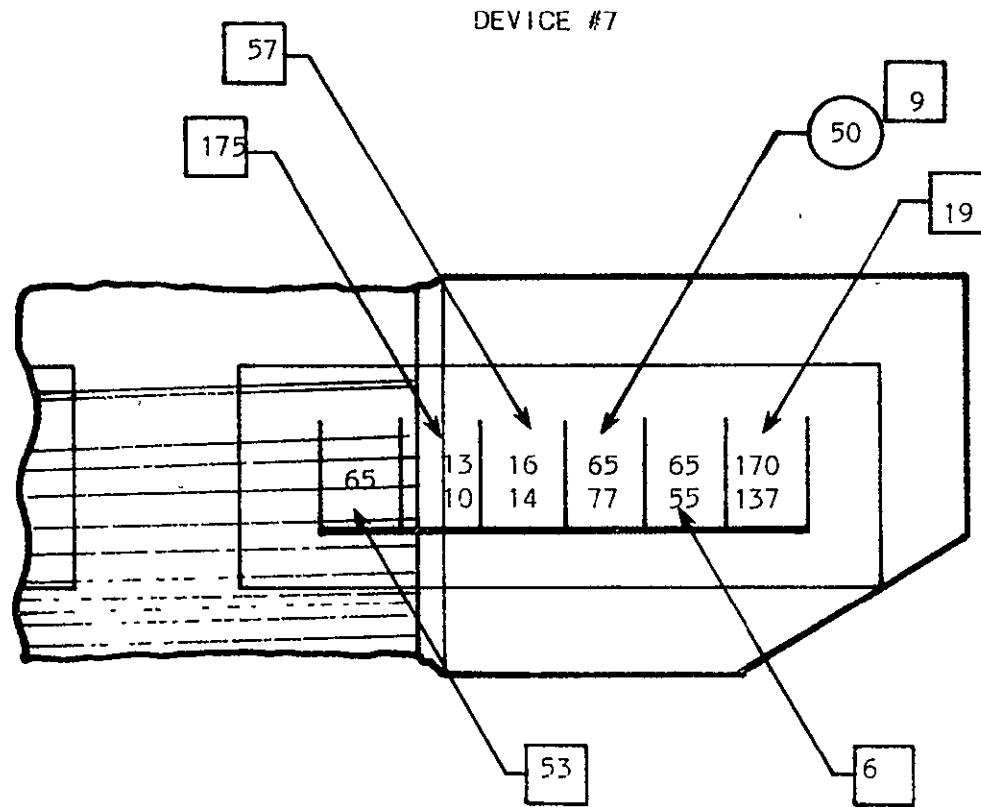


FIGURE 27. OCPV DIFFUSION LENGTHS (NUMBERS ON FIGURE), SPV DIFFUSION LENGTHS (□) AND DISLOCATION DENSITIES (■) MEASURED ON RIBBON SOLAR CELLS. DISLOCATION DENSITIES ARE TIMES 10^4 cm^{-2} .

to dislocation counting. Figure 28 exhibits the correlation obtained between measured diffusion lengths and dislocation densities. Note the good correlation obtained for all points not over grain boundaries. Regions including grain boundaries do not fall within the general trend. But note that even these points can give respectable diffusion lengths. From Figure 28 it may be seen that, away from grain boundaries, diffusion lengths commensurate with efficient solar cell operation can be obtained with $>10^5$ dislocations/cm².

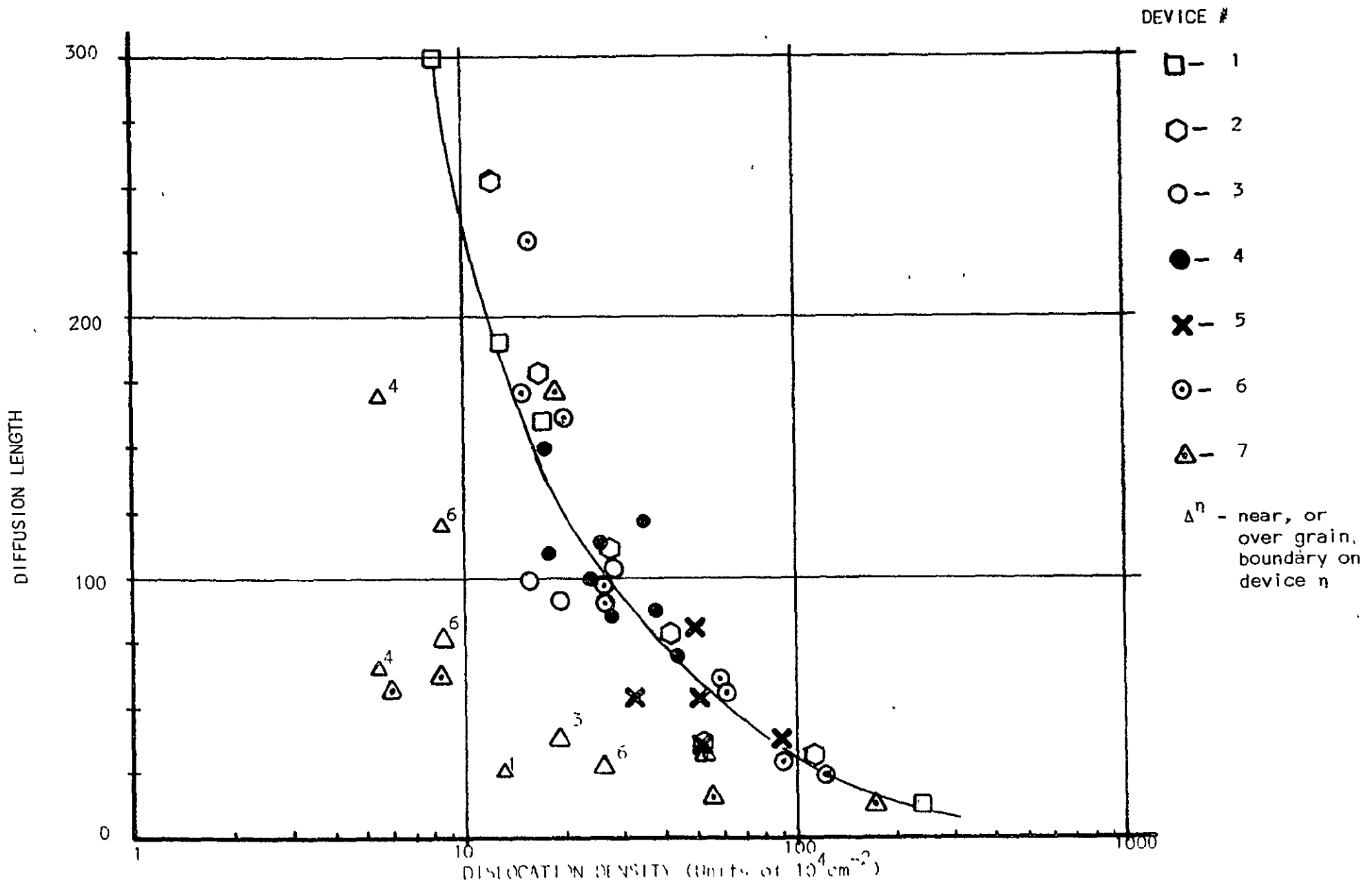
Figure 29 indicates measured dislocation densities near the initial melt region. This is similar to previously reported dislocation density distributions near a melt interface and serves to emphasize the improvement obtained as steady-state growth is achieved.

6.2 DISCUSSION

These results are very encouraging when it is emphasized that as-grown diffusion lengths are only 6 - 15 μ m while processed substrates are dramatically increased. Obviously a "gettering" step is involved. Contrary to this observation is the fact that previous attempts at pure gettering experiments have not resulted in diffusion length enhancement. This indicates that the "right" gettering cycle has not been achieved but that it occurs during our process sequence.

In our process sequence, several high temperature cycles are involved: A boron back surface p⁺ diffusion, a phosphorous diffusion for the front junction, oxidations, and a Si₃N₄ deposition. Previously reported experiments have shown that virtually any high temperature processes attempted heretofore -- gettering, oxidation, annealing, etc. -- all have either degraded lifetime or at best retained initial lifetimes.

FIGURE 28. DIFFUSION LENGTH -- DISLOCATION DENSITY CORRELATIONS



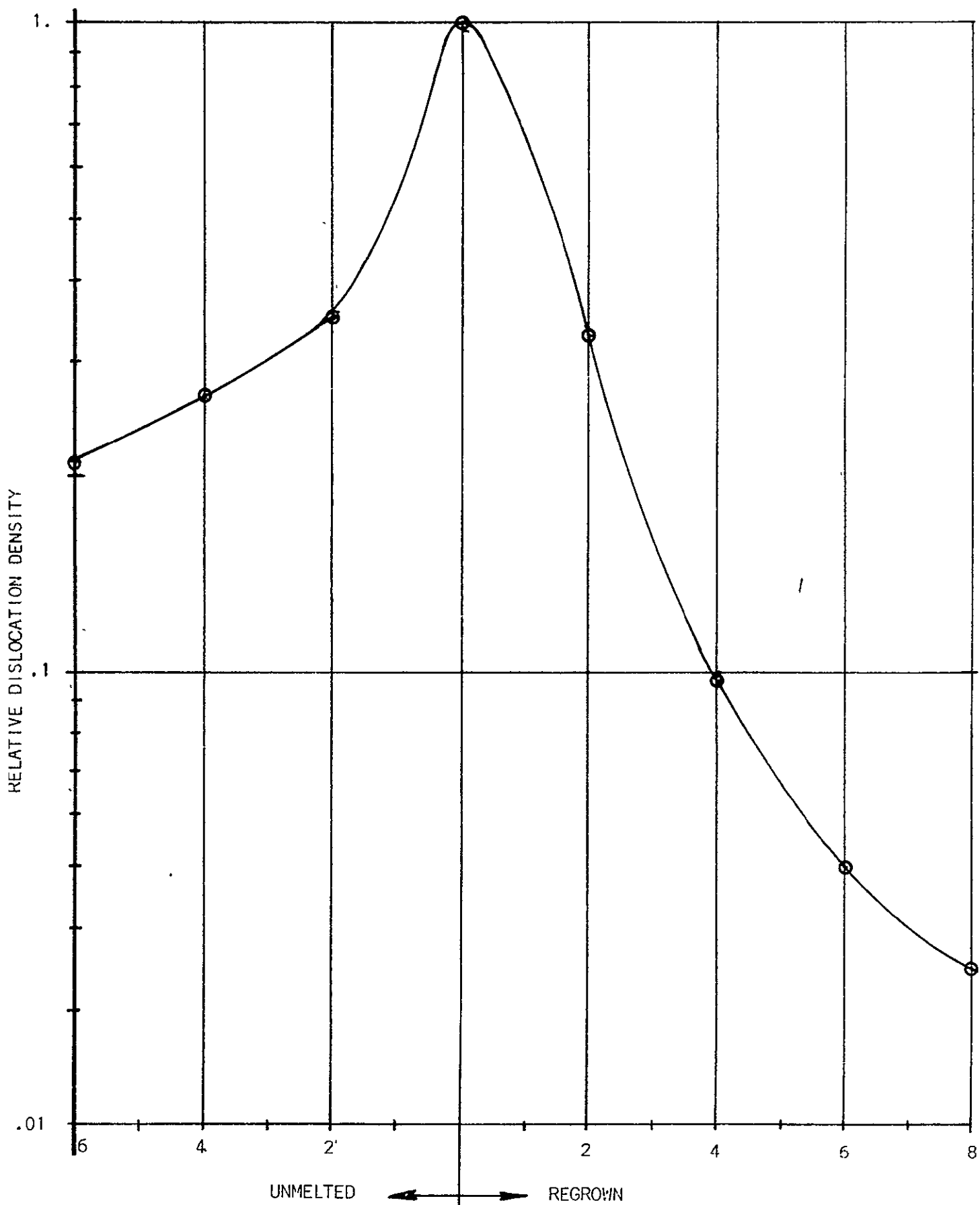


FIGURE 29: POSITION RELATIVE TO FINAL MELT INTERFACE (mm)

6.3 GETTERING STUDIES

In order to ascertain at what step(s) the lifetime is being improved on ribbon samples, SPV measurements have been made after the various high temperature processing steps. Evaluation of diffusion lengths on samples after the back surface P+ diffusion have indicated no enhancement after this step. But samples undergoing the phosphorous diffusion and AR treatment have shown substantial improvement: A typical ribbon underwent the phosphorous diffusion and AR coating procedures typical of standard processing. The diffusion lengths before and after each step were compared. Average diffusion lengths for the as-grown sample were 7 μ m. After the phosphorous diffusion for the formation of the n-on-p junction, average diffusion lengths were about 20 μ m. Subsequently, an AR treatment involving growth of a layer of Si₃N₄, was performed. The AR layer was then removed and diffusion lengths again measured. Resulting average diffusion lengths were then about 47 μ m.

Consequently, a definite "gettering" sequence has been established. An increased level of study will now concentrate on optimizing this procedure and further elucidating the exact mechanisms involved. In particular, it may be the specific atmospheres in the high temperature processing which further enhance the diffusion length, or it may be a stress-induced effect due to the nitride layer in conjunction with the n+ layer. Alternatively, it may simply be the annealing cycle represented by the temperatures and times of the AR sequence. Phosphorous gettering has been widely used in the semiconductor industry, but previous attempts using "standard" phosphorous gettering have been unsuccessful. We hope to find out why this sequence works.

7.0 MEASUREMENT TECHNOLOGY

**ORIGINAL PAGE IS
OF POOR QUALITY**

7.1 HIGH RESOLUTION DIFFUSION LENGTH MAPPING

For purposes of diffusion length mapping of wafers using the SPV technique, it is necessary to employ small beam sizes. However, we have observed that a small beam size (~1mm) does not result in a straight line on the I vs α^{-1} plot. We have, therefore, studied the effect of beam size (in comparison to diffusion length) on the SPV measurement.

Figure 30 shows typical plots of light intensity, I , (required to keep SPV constant), and the reciprocal absorption coefficient, α^{-1} , with beam size, d , as the parameter. It is seen that (1) reduction in beam size results in a larger value of diffusion length L (I vs α^{-1} still remains a straight line); (2) as the beam size is reduced below a value such that $d/L \approx 10$, the lines begin to curve and in such a case it is not possible to get a unique value for the diffusion length.

Experiments were carried out using Si wafers, both p and n type, with diffusion lengths up to 300 μ m (resistivity range: 0.1 - 10 Ω -cm). Figure 31 shows an experimentally determined plot of L/L_{∞} vs d/L , where L_{∞} is the diffusion length obtained with a large beam size. Such a plot gives a correction for diffusion length when a small beam size is employed in order to get high spatial resolution mapping.

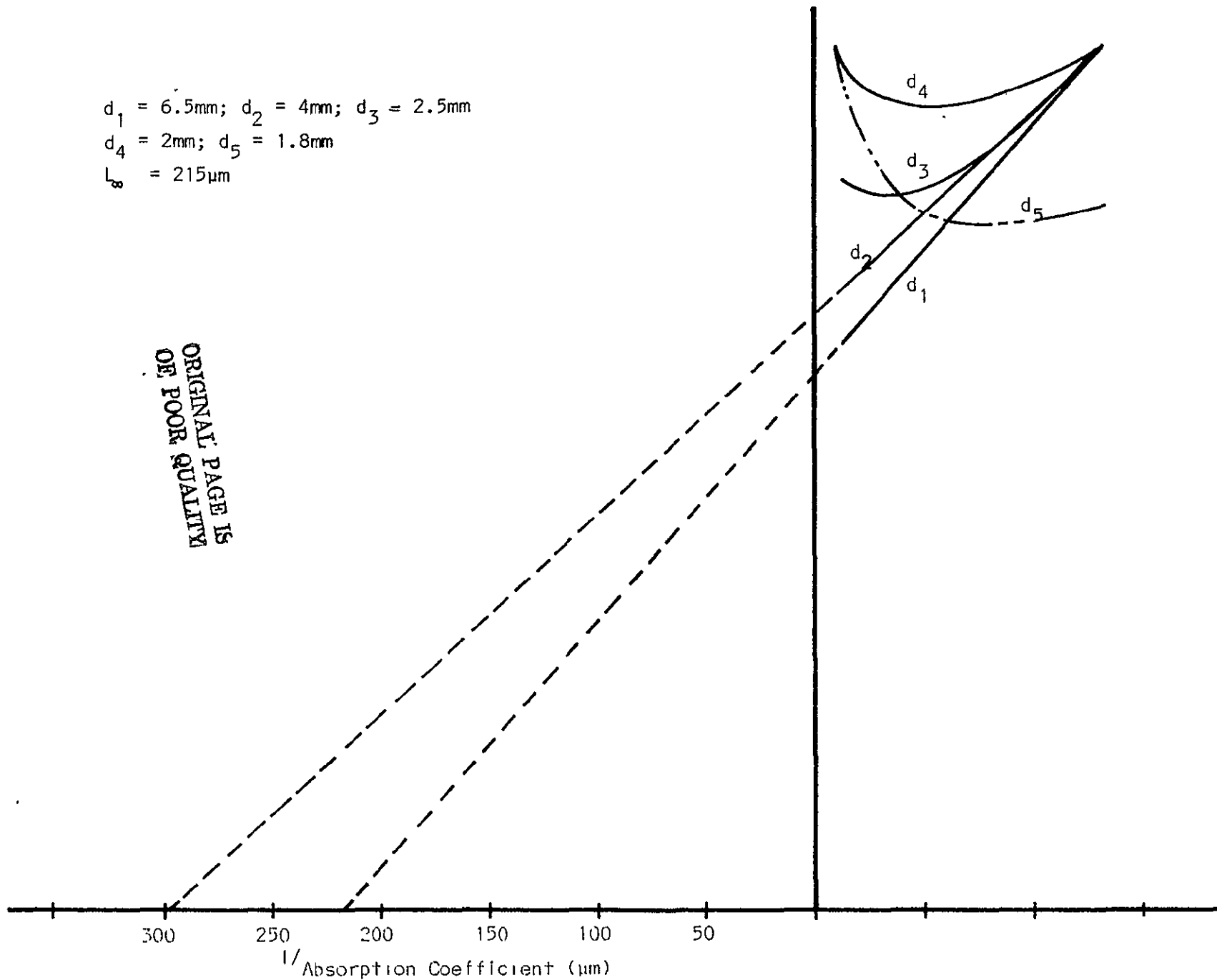
It should be pointed out that wafers with large surface roughness may show deviation from the previous results. E.g, texture etched silicon wafers and solar cells do not follow exactly the same behaviour as shown in Figure 31. This is due to the fact that surface roughness increases the effective beam size due to scattering.

A theoretical study of this effect has also been undertaken.

8.0 ECONOMIC ANALYSIS

**ORIGINAL PAGE IS
OF POOR QUALITY**

$d_1 = 6.5\text{mm}; d_2 = 4\text{mm}; d_3 = 2.5\text{mm}$
 $d_4 = 2\text{mm}; d_5 = 1.8\text{mm}$
 $L_g = 215\mu\text{m}$



ORIGINAL PAGE IS
 OF POOR QUALITY

FIGURE 30 SPV BEHAVIOR AS A FUNCTION OF BEAM SIZE
 FOR A SAMPLE WITH A FIXED DIFFUSION LENGTH.

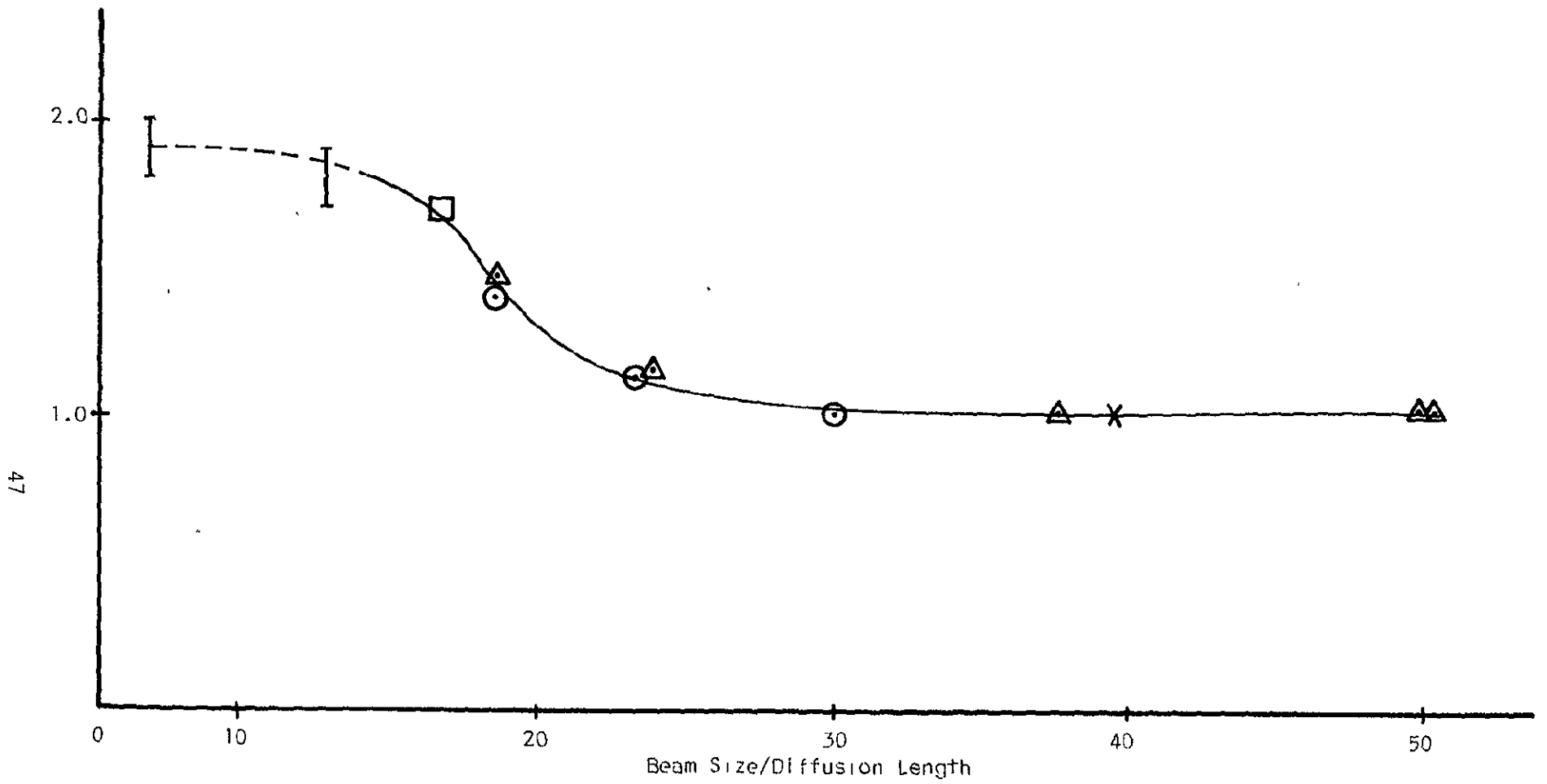


FIGURE 11 MEASURED SPV DIFFUSION LENGTH AS A FUNCTION OF BEAM SIZE/DIFFUSION LENGTH RATIOS.

8.1 EVALUATION OF SAMICS MODEL

Table I is a comparison of the actual prices of a Motorola production operation with both the SAMICS model and the model we have used in our economic analysis. The actual prices have been assigned a value of 100, and the other prices have been scaled accordingly. The "actual" and "Motorola" columns include all the items considered in the SAMICS model except the "start-up" costs. Assuming these costs would increase prices in the range of 5 - 10%, the SAMICS model would produce an overestimate of 10% - 5%. This is excellent agreement for a general equation applied to a specific operation.

When specific categories were compared, however, the agreement is poor. Part of the disagreement is simply due to the assignment of profit: In the SAMICS model, the profit is derived from the capital investment, while we have simply distributed the profit as a percentage of production cost. This factor can account for the difference in the "Labor" and "Utility" categories, and a major fraction of the difference in the "Capital Equipment" category. The SAMICS estimate of the factory component of the cost, however, remains too high.

8.2 POLYCRYSTALLINE FEEDSTOCK

A preliminary economic analysis of two proposed methods of producing the polycrystalline feedstock needed for RTR growth was carried out. The first method uses conventional CVD to deposit a polycrystalline silicon ribbon on a moving substrate (this method has been successfully demonstrated on fixed substrates, using both SiHCl_3 and SiCl_4 as source gases). The economic analysis assumes SiHCl_3 is the source gas, at \$7/Kg silicon -- the present price of trichlorosilane. Figure 32 shows the price of a 100 μm ribbon as a function of growth rate, assuming a 10MW plant.

**ORIGINAL PAGE IS
OF POOR QUALITY**

TABLE I

CATEGORY	ACTUAL PRICE	MOTOROLA MODEL PRICE	SAMICS MODEL PRICE
1. Capital Equip- ment	100	83	161
2. Factory	100	85	334
3. Labor	100	100	77
4. Materials	100	100	100
5. Utility	100	100	80
TOTAL	100	97	115

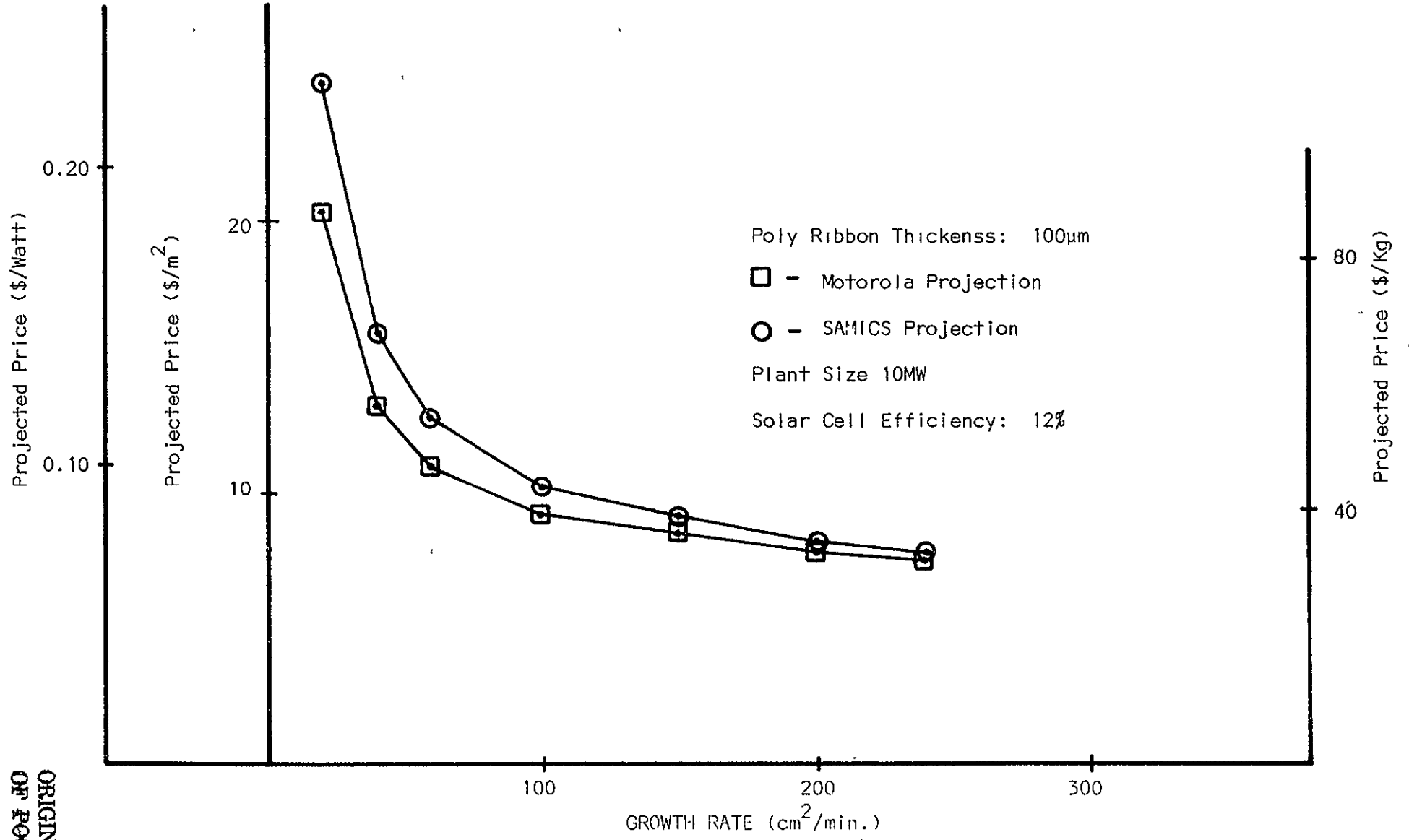


FIGURE 32: CHEMICAL VAPOR DEPOSITION PRICE PROJECTION

The second method for producing the poly feedstock uses a plasma deposition process which is presently under development at Motorola. High deposition rates have been achieved using SiCl_4 , SiHCl_3 or SiH_4 as source gases. The economic analysis for this process assumes SiH_4 as the source process at \$5/Kg-silicon (this is the projected cost of the Union Carbide silane production process). Figure 33 shows the price of a 100 μm ribbon as a function of growth rate, assuming a 500MW plant.

Figures 32 and 33 also show the price of the polyribbon obtained using the SAMICS model. The two methods of obtaining the ribbon price are obviously in good agreement.

The polyribbon feedstock could thus be sold at a price of $\sim \$7.5/\text{M}^2$, \$0.082/watt or $\sim \$36/\text{Kg}$ -silicon in a 10MW plant using conventional CVD or at $\sim \$3.5/\text{M}^2$, \$0.032/watt, or $\sim \$15/\text{Kg}$ -Si in a 500MW plant using plasma deposition.

8.5 RTR CRYSTAL GROWTH

Figure 34 is a projection of the add-on price of the RTR ribbon as a function of growth rate. In this case, the SAMICS price estimate is about 30% higher than our estimate. Figure 35 shows the price of the RTR ribbon including buying the polyribbon at \$0.065/watt (CVD method, produced in a 500MW plant). The SAMICS price estimate is $\sim 20\%$ higher than our estimate. Using the SAMICS price estimate, RTR ribbon could be sold at a price of \$0.19/watt using polyribbon produced by CVD, or $\sim \$0.16/\text{watt}$ using polyribbon produced by plasma deposition.

These prices demonstrate that the LSSA goal of 50¢/watt solar cells could be achieved using RTR ribbon. The RTR process can reach this goal basically because it uses a minimum of raw materials, can reach a high throughput ($>100\text{cm}^2/\text{min.}$) per ribbon, and should not require a high labor cost.

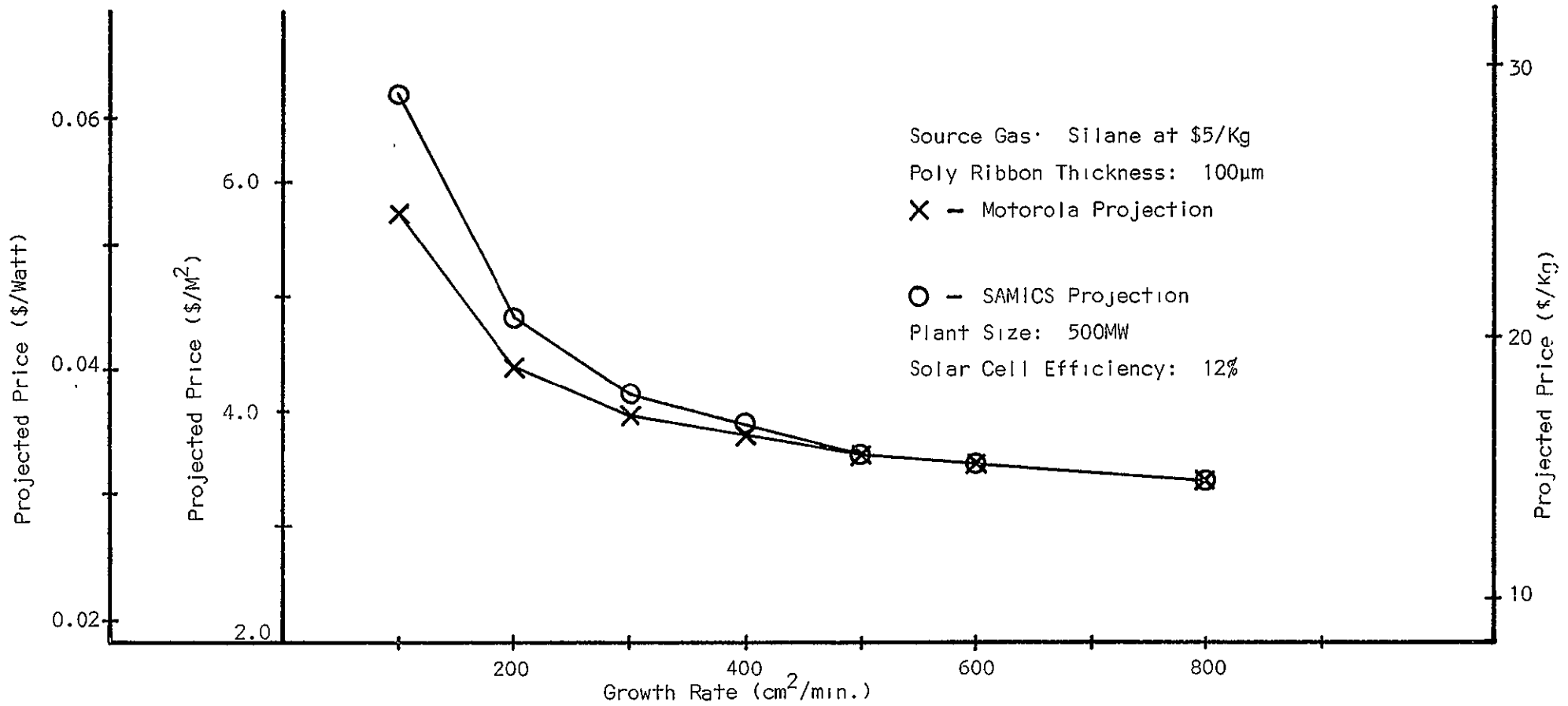


FIGURE 33: PLASMA DEPOSITION PRICE PROJECTION

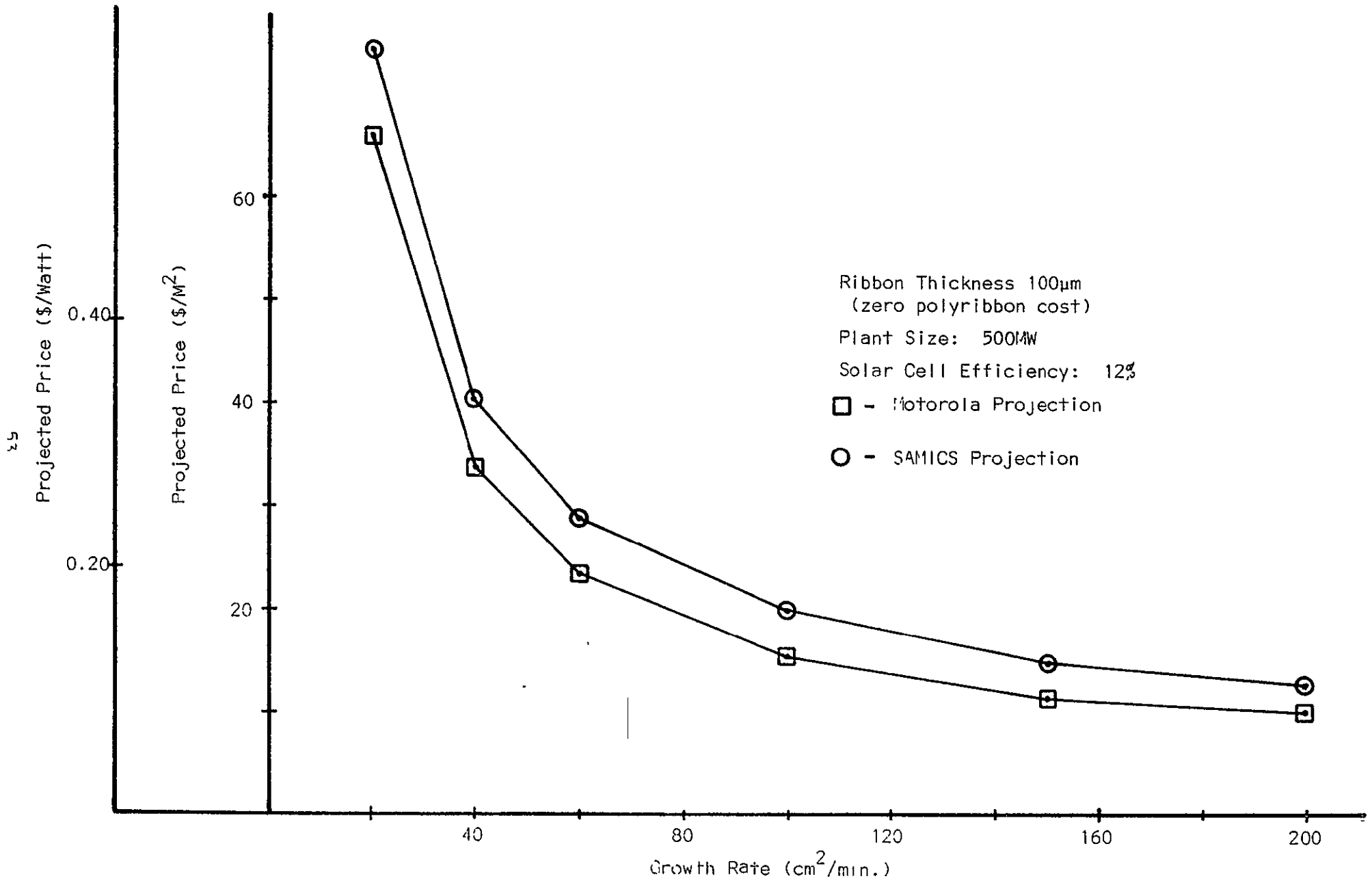


FIGURE 34 . RTR ADD-ON PRICE PROJECTION

54

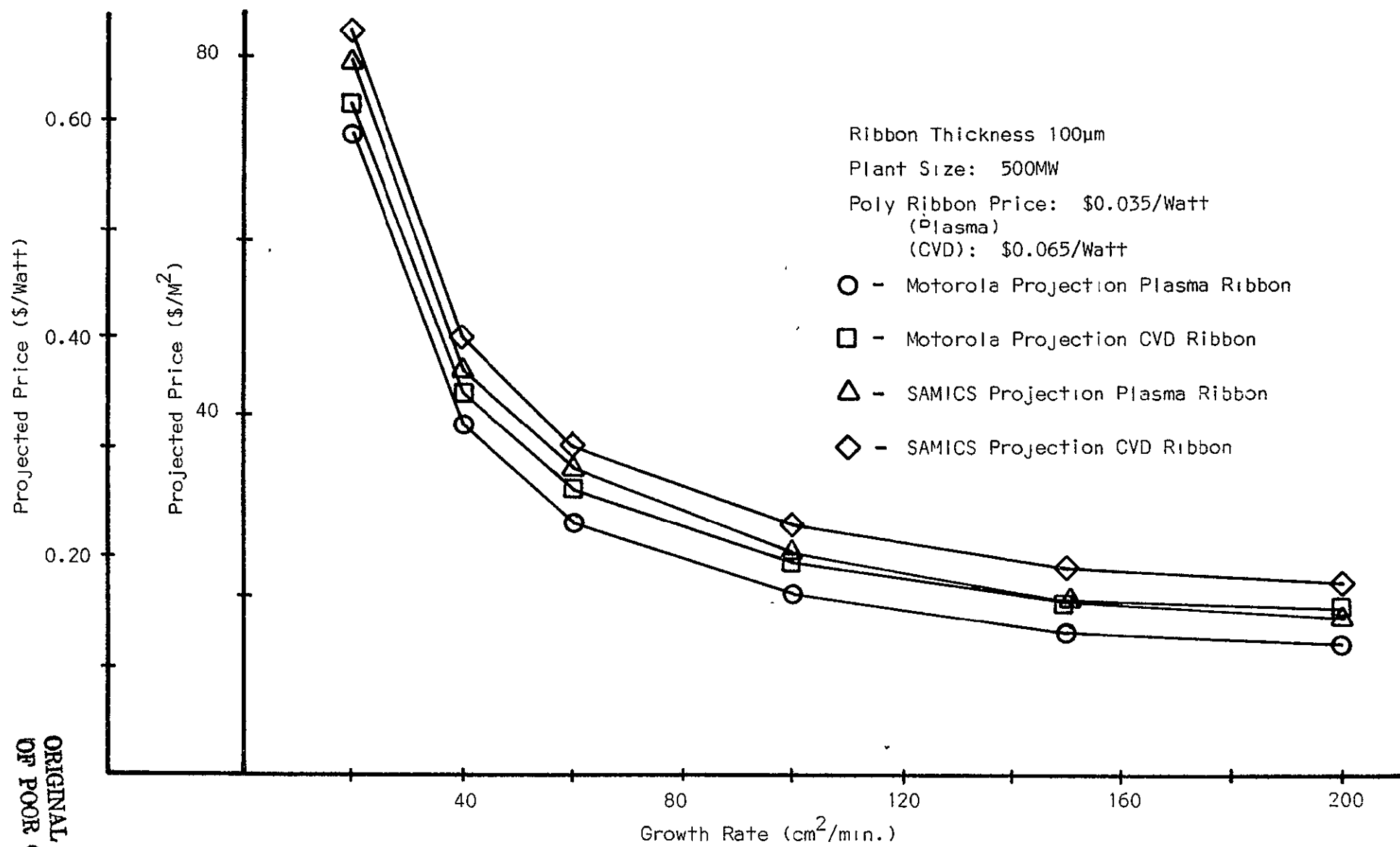


FIGURE 35. RTR PRICE PROJECTION

ORIGINAL PAGE IS
OF POOR QUALITY

9.0 PROBLEMS

Problems experienced this quarter have been numerous due to the relocation of the laser lab and the "Flood" referred in the test. These problems have delayed the program, but no serious problems exist at present which will prevent the accomplishment of our major goals.

10.0 PLANS

Plans this next quarter will be towards completion of major program goals. Emphasis will be placed on demonstration of wide ribbon growth and high efficiency ribbon solar cells. Solar cells fabricated from CVD poly-ribbon will receive special attention.

11.0 NEW TECHNOLOGY

The following New Technology item has been developed on this program:

I. Description - Polygon Scanner System

Innovator - Dr. Richard Gurtler

Progress Reports - Technical Progress Report No. 14
October 1977

Pages - Pages I, 10, 11A, and 11

12.0 PROGRAM PLAN/MILESTONES

Activities associated with the total program are shown in the Program Plan/Milestone charts contained in Appendix I.

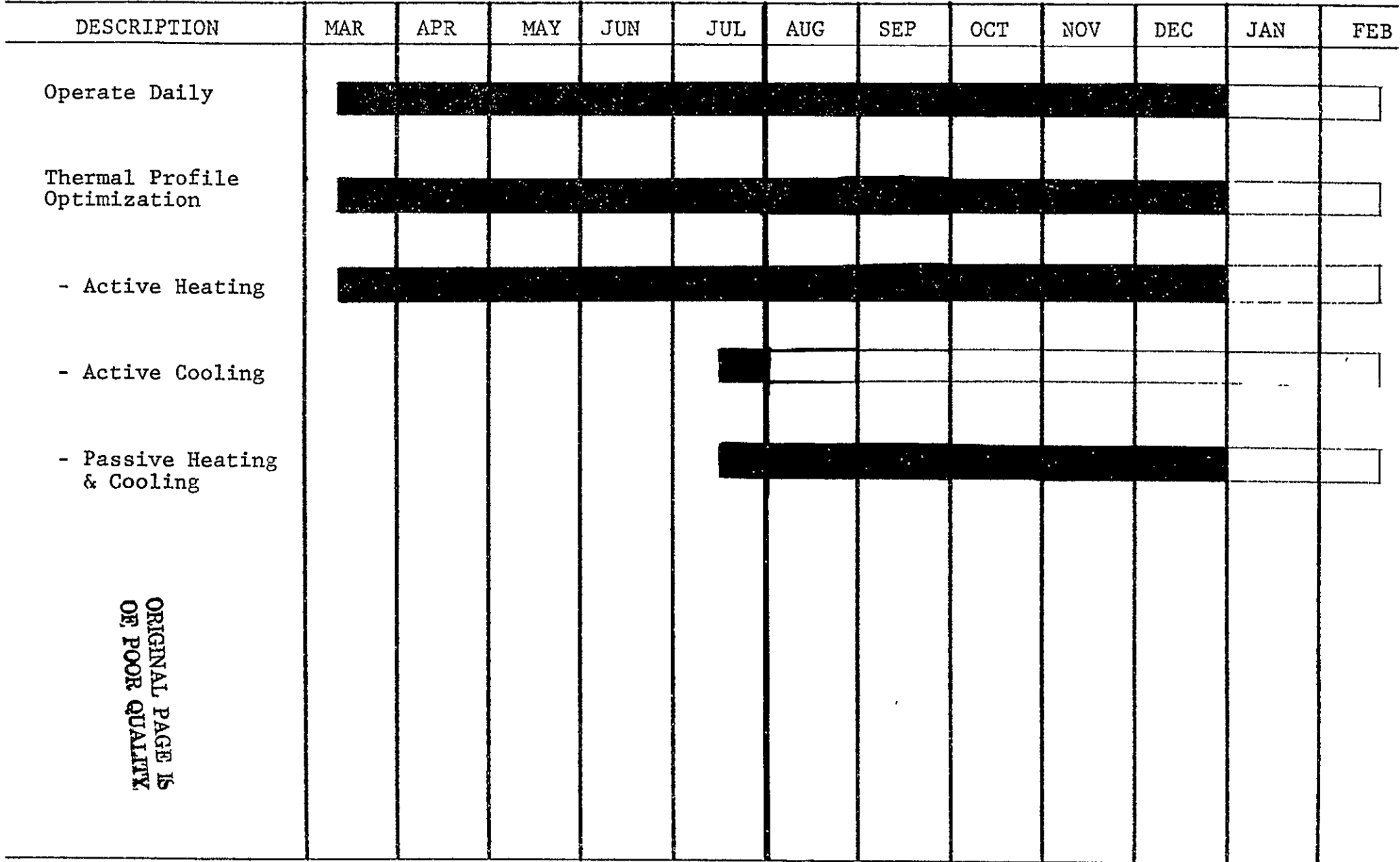
13. ENGINEERING DRAWINGS

Drawings of the improved transport stage and preliminary drawings of components for the RTR apparatus are contained in Appendix II.

WORK BREAKDOWN SCHEDULE NO.1

Model 1 RTR Apparatus

MOTOROLA PROJECT NO. 2319



ORIGINAL PAGE IS
OF POOR QUALITY

FIGURE 1

PROGRAM PLAN/MILESTONE CHART

LEGEND □ SCHEDULED ■ COMPLETED △ DELIVERY SCHEDULE ▲ DELIVERED

WORK BREAKDOWN SCHEDULE NO. 2

Model 2 RTR Apparatus

MOTOROLA PROJECT NO. 2320

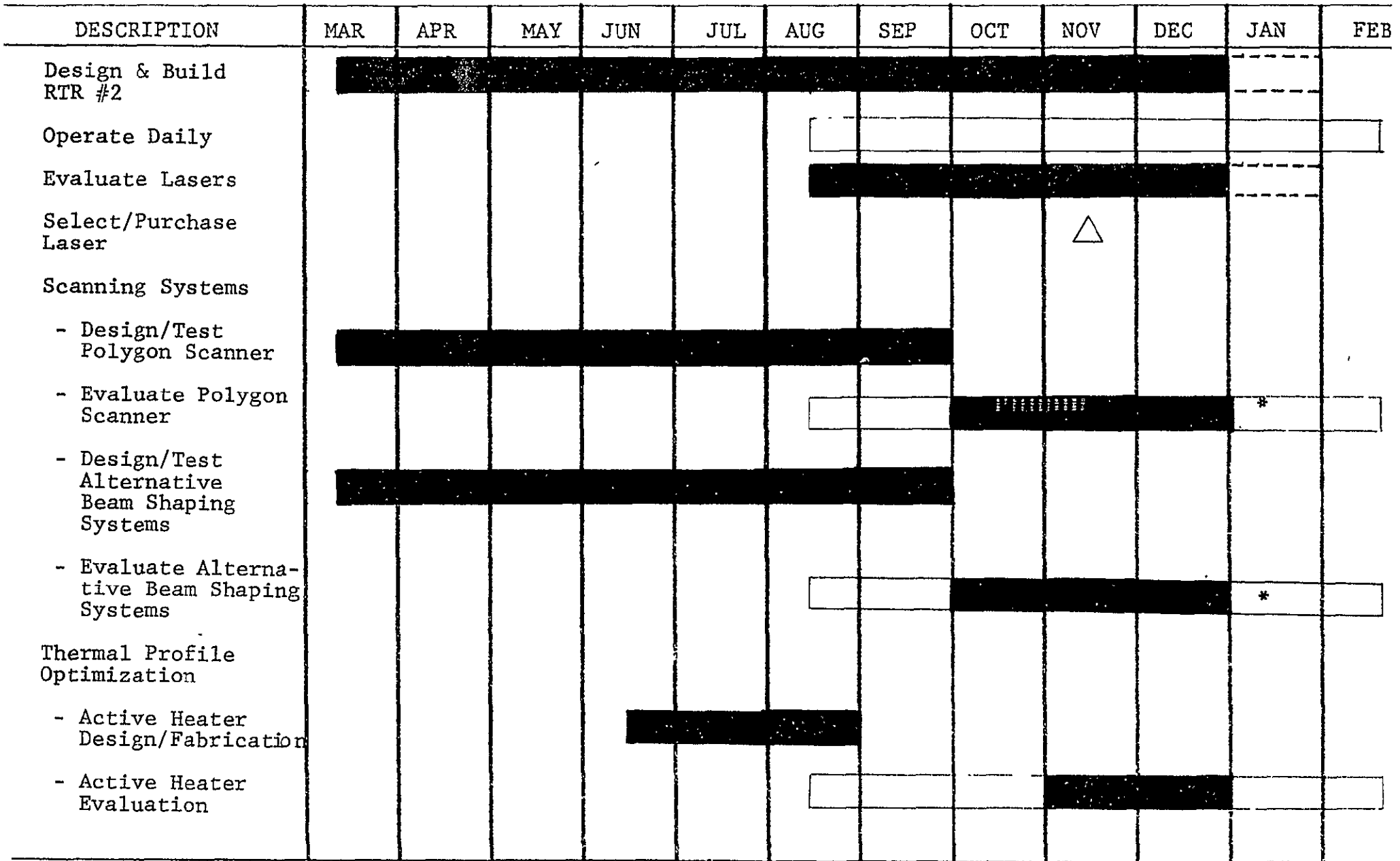


FIGURE 2


PROGRAM PLAN/MILESTONE CHART

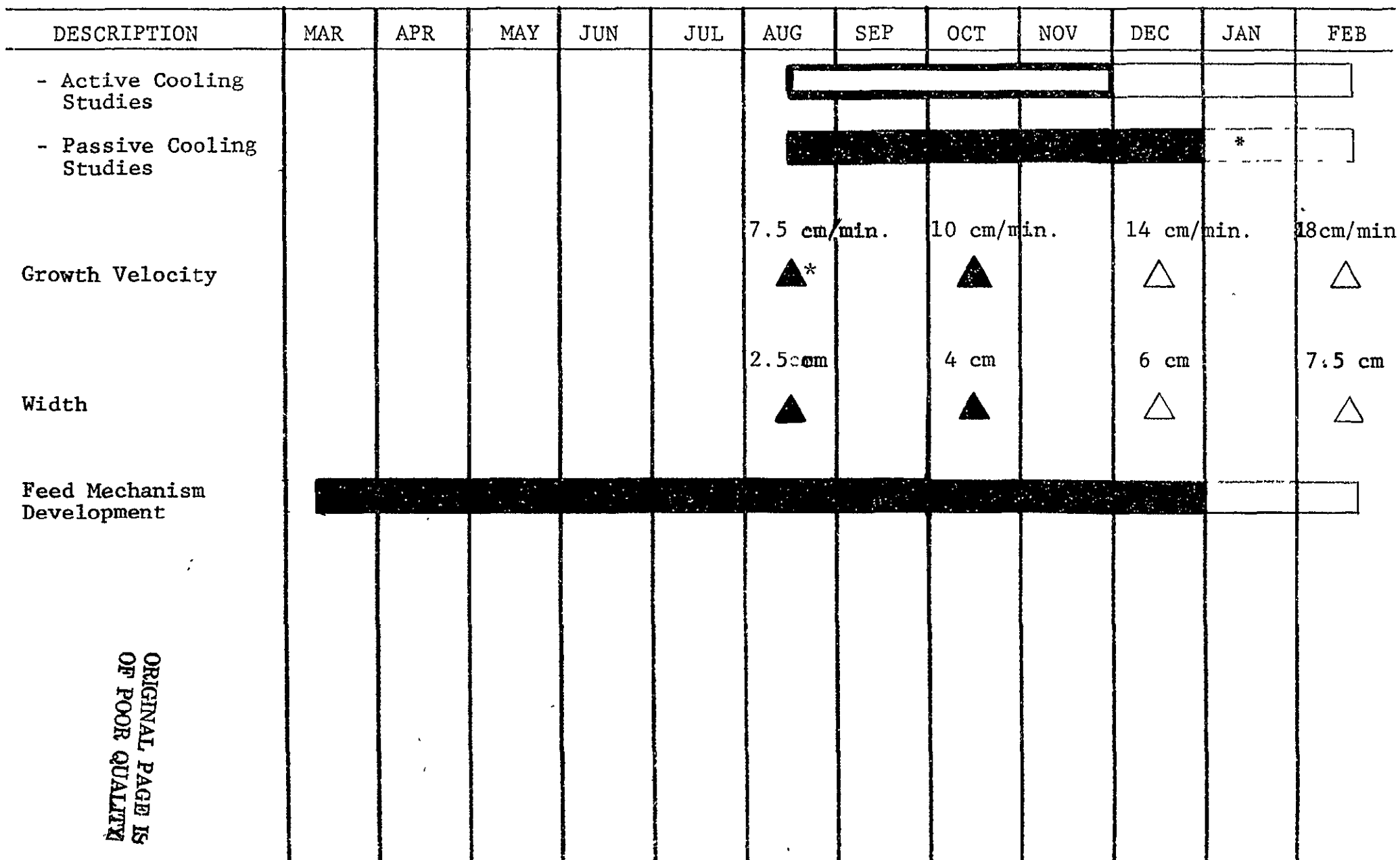
LEGEND 

SCHEDULED 

COMPLETED * Done on RTR #1

 DELIVERY SCHEDULE

 DELIVERED



ORIGINAL PAGE IS
OF POOR QUALITY

FIGURE 2 (Cont.) PROGRAM PLAN/MILESTONE CHART

LEGEND □

SCHEDULED [Hatched Box]

COMPLETED [Solid Black Box]

* Done on RTR #1

△ DELIVERY SCHEDULE

▲ DELIVERED

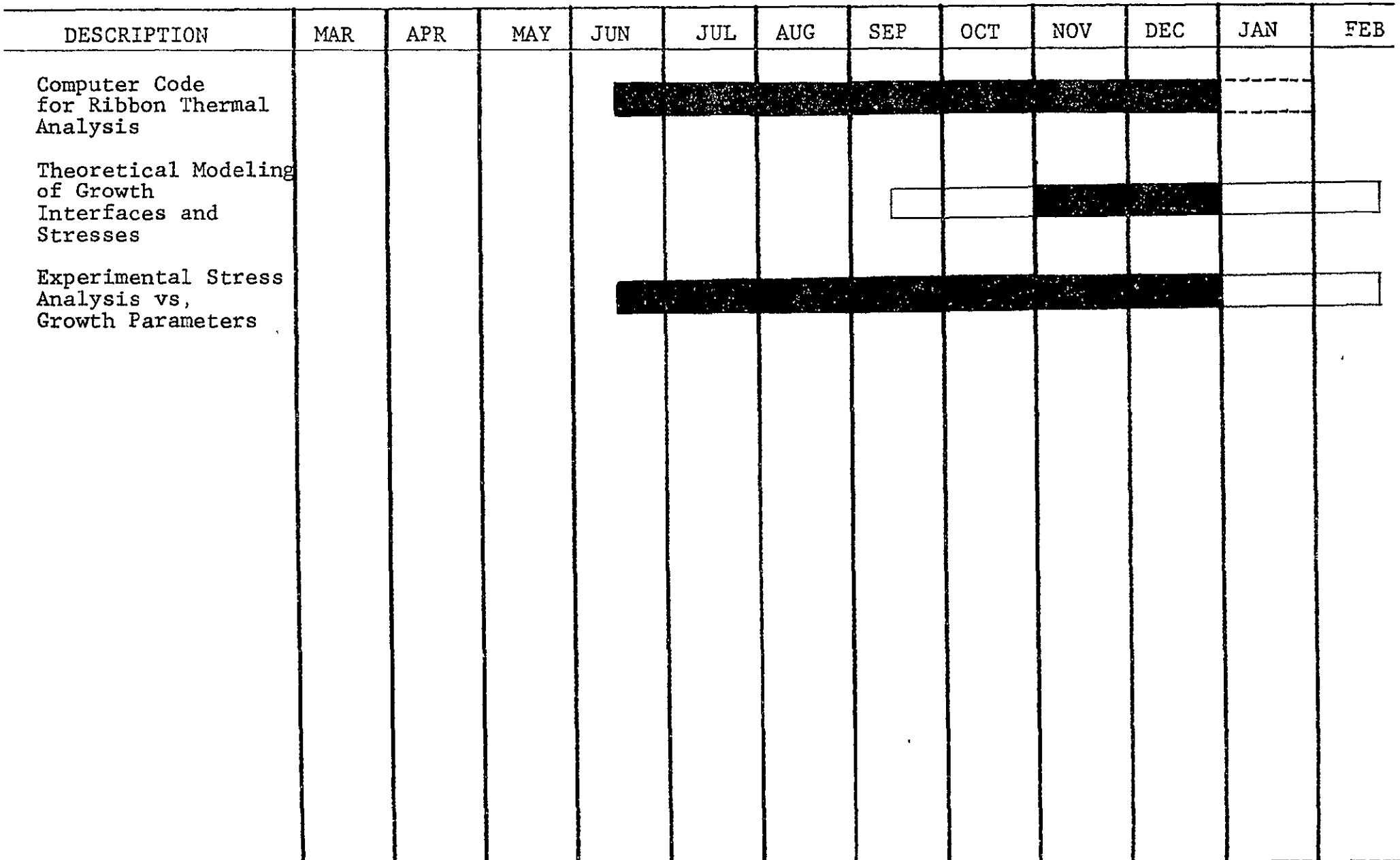




FIGURE 3


PROGRAM PLAN/MILESTONE CHART

LEGEND 

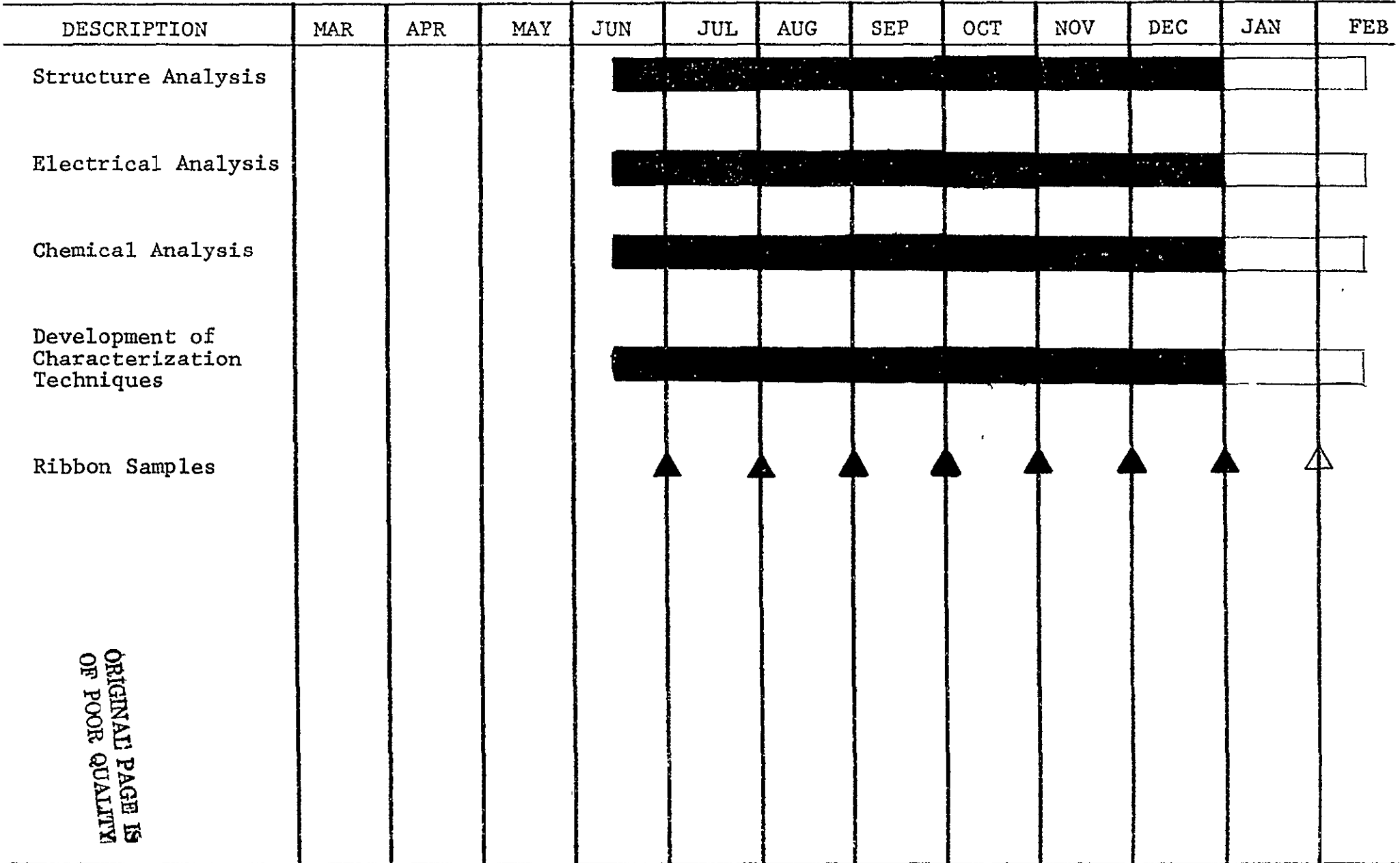
SCHEDULED 

COMPLETED

 DELIVERY SCHEDULE

 DELIVERED

Ribbon Characterization



ORIGINAL PAGE IS
OF POOR QUALITY

FIGURE 4

PROGRAM PLAN/MILESTONE CHART

LEGEND □ SCHEDULED ■ COMPLETED ▲ DELIVERED △ DELIVERY SCHEDULE

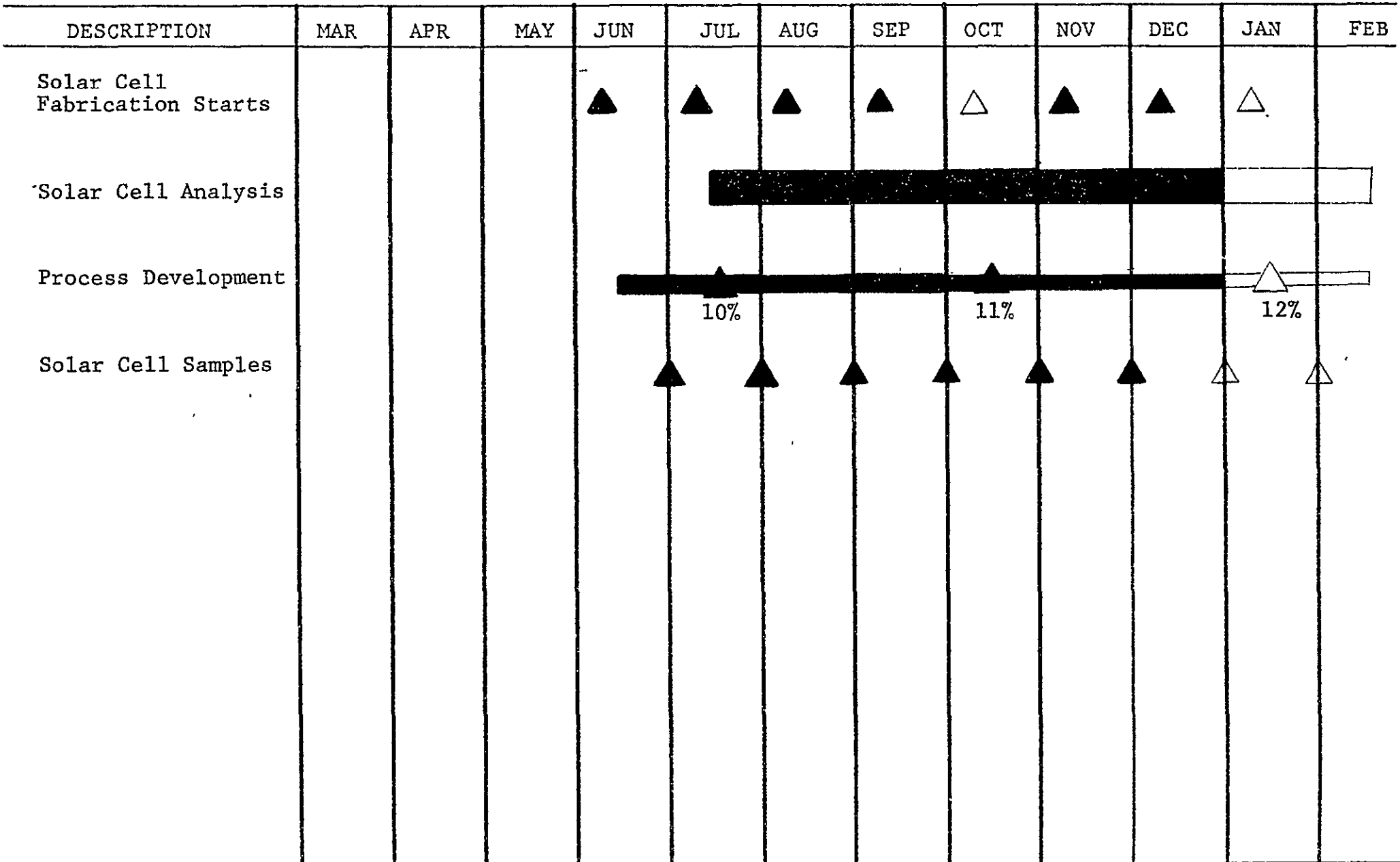


FIGURE 5

PROGRAM PLAN/MILESTONE CHART

LEGEND □

SCHEDULED ■

COMPLETED

△ DELIVERY SCHEDULE

▲ DELIVERED


Economic Analysis


DESCRIPTION	MAR	APR	MAY	JUN	JUL	AUG	SEP	OCT	NOV	DEC	JAN	FEB
Economic Analysis of RTR Growth												

ORIGINAL PAGE IS
OF POOR QUALITY

FIGURE 6


PROGRAM PLAN/MILESTONE CHART

LEGEND 

SCHEDULED 

COMPLETED

 DELIVERY SCHEDULE

 DELIVERED

WORK BREAKDOWN SCHEDULE NO. 7

Program Management and Documentation

MOTOROLA PROJECT NO. 2325

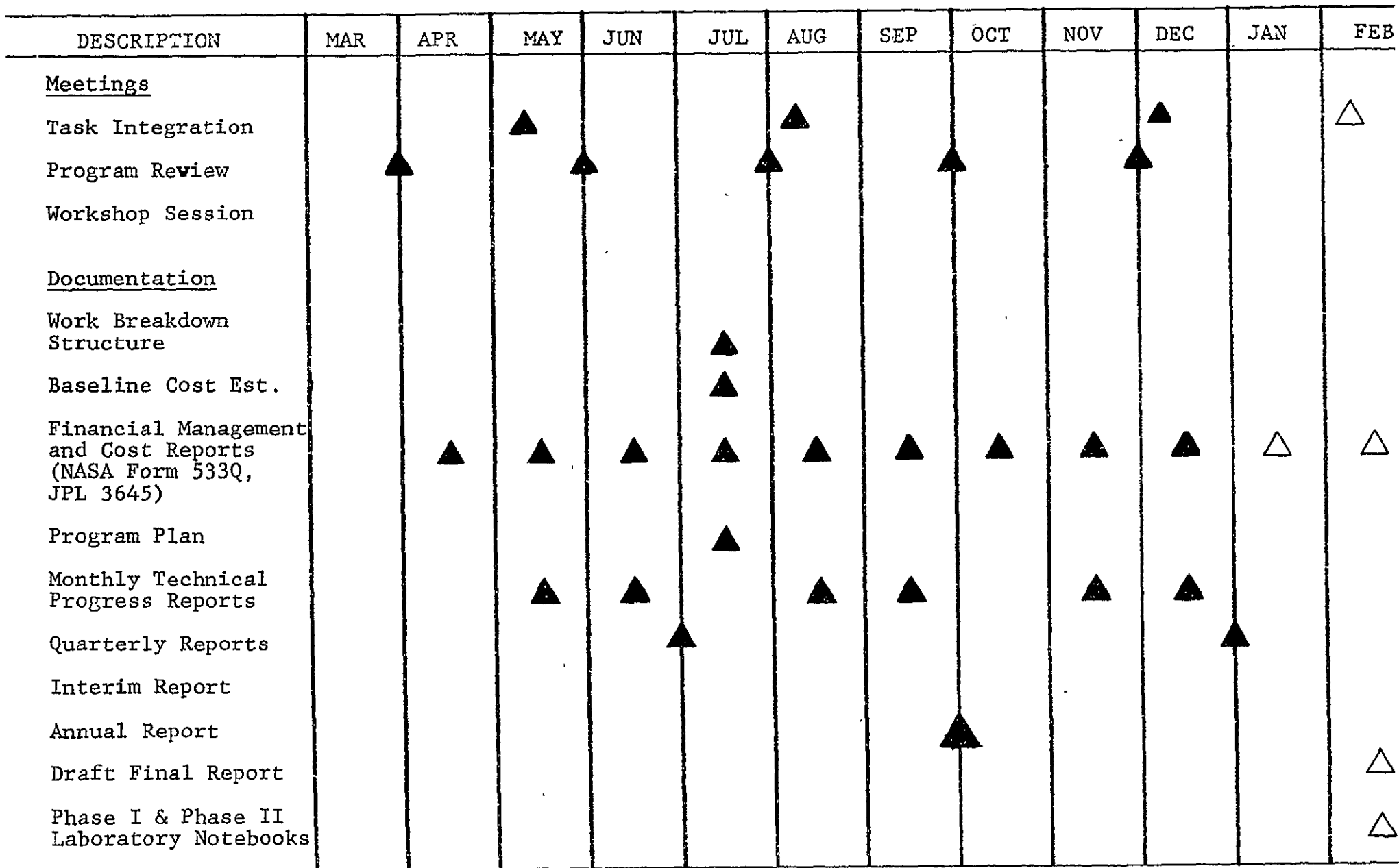


FIGURE 7

PROGRAM PLAN/MILESTONE CHART

LEGEND □

SCHEDULED ■

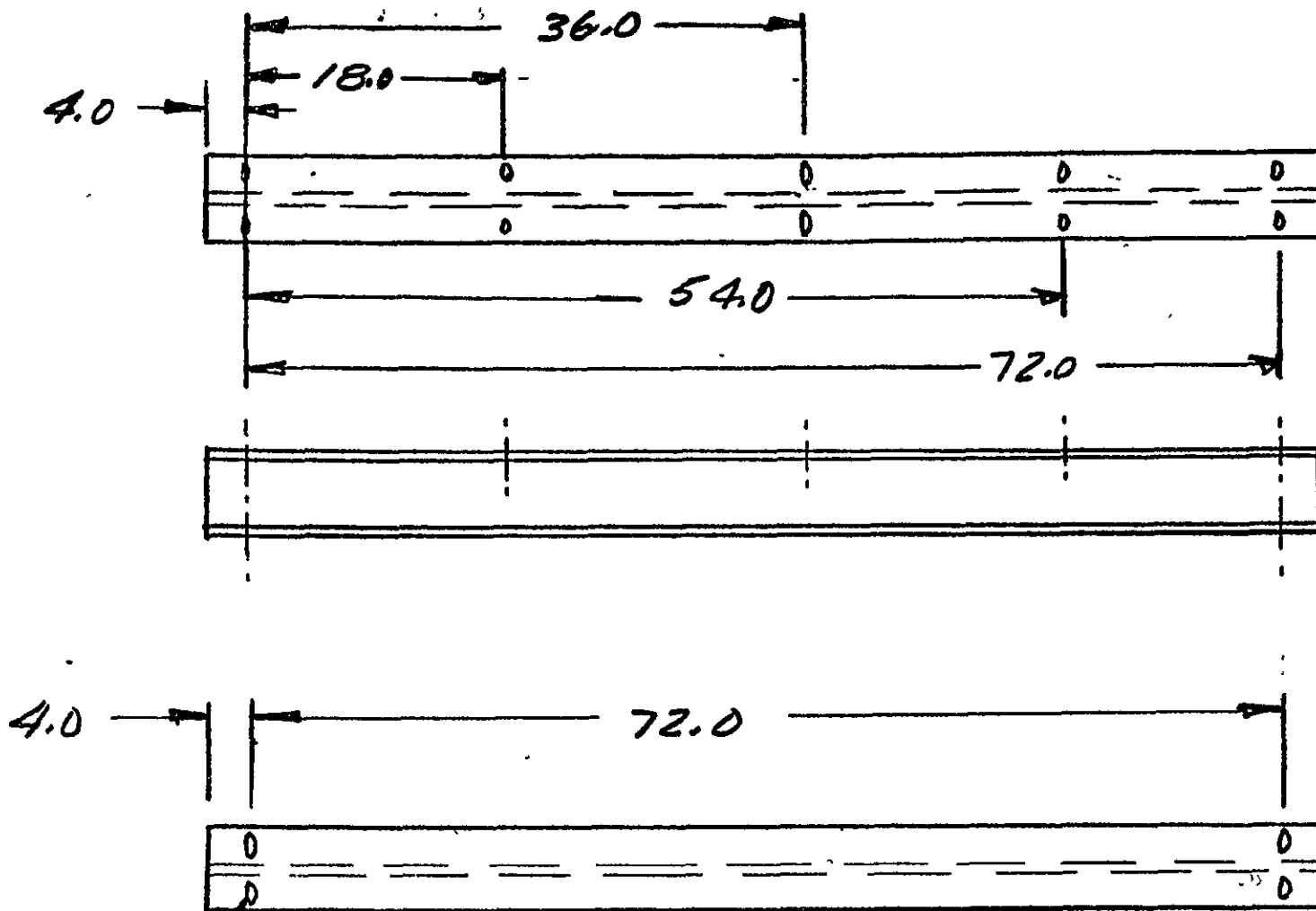
COMPLETED

△ DELIVERY SCHEDULE

▲ DELIVERED

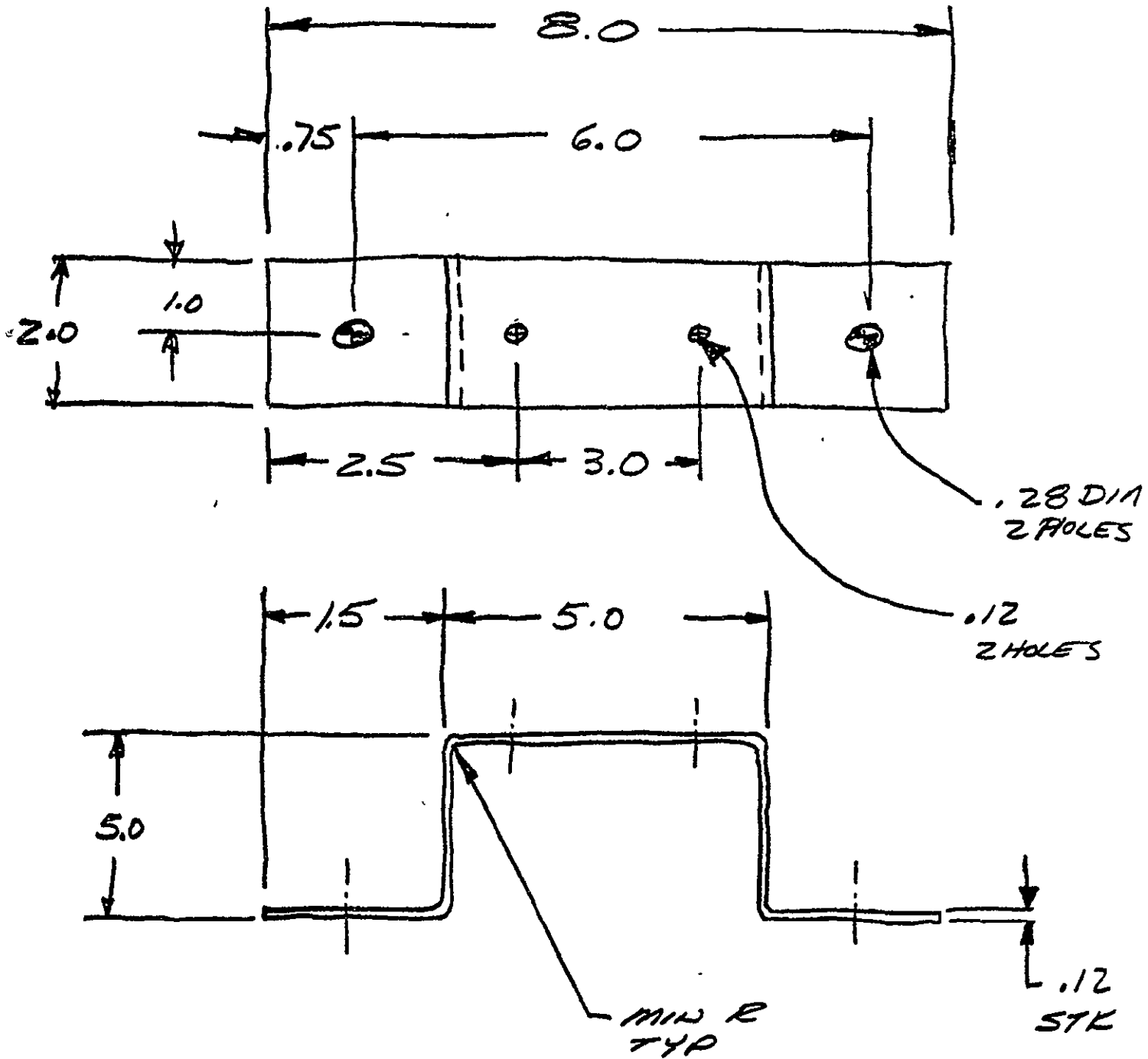
APPENDIX II

Engineering Drawings



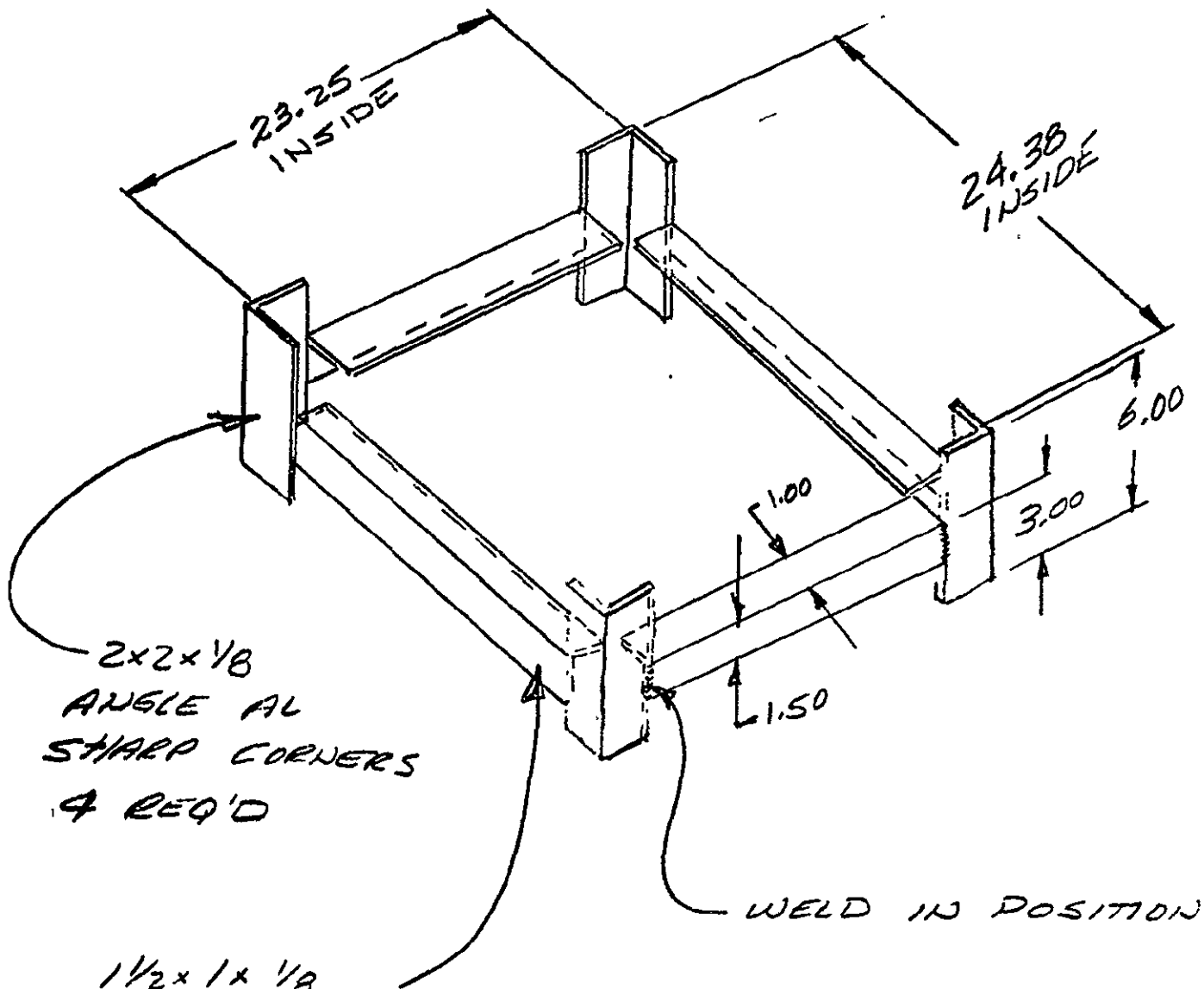
SEE SHEET #2
FOR SLOT DIMENSIONS
14 PLACES

"H" BEAM
SHEET #1



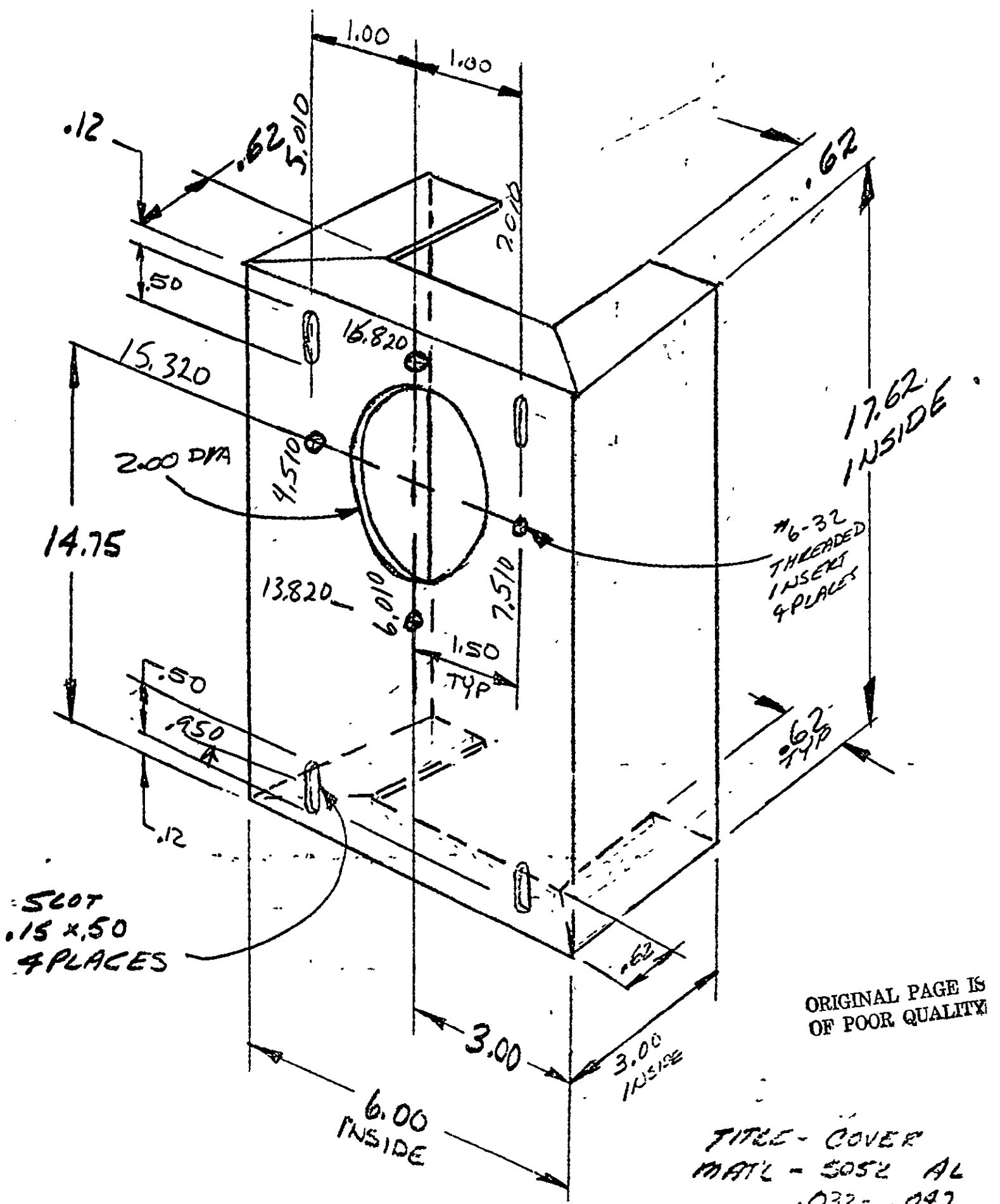
ORIGINAL PAGE IS
OF POOR QUALITY

BRACKET
 MAT'L - 5052
 REQ'D - 2
 SK 102077-1
 GLENIS BUDAY



ALL WELDED
CONSTRUCTION

GLENN BUDAY
EX 5360
DATE 9-6-77



17.62
INSIDE

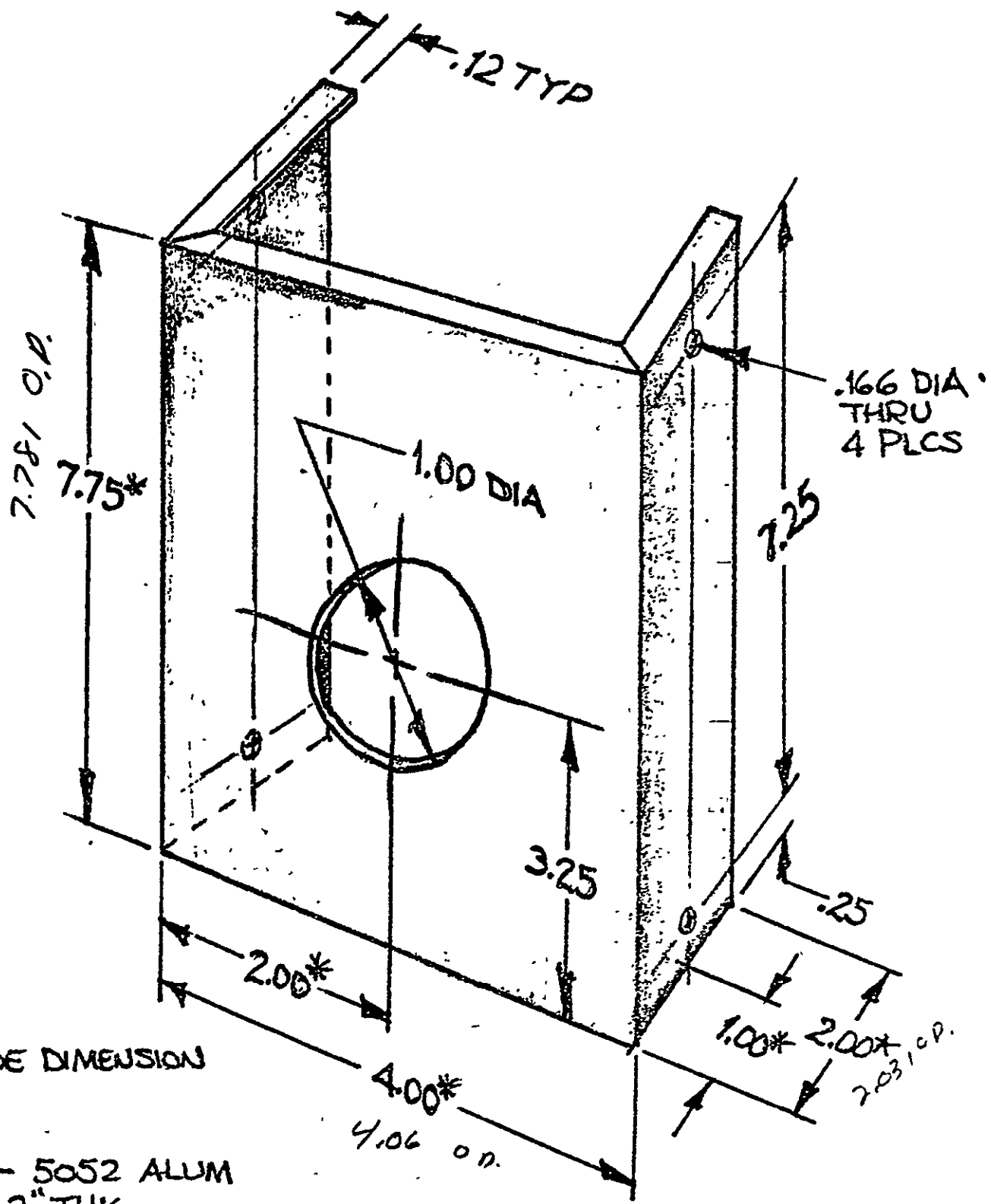
#6-32
THREADED
INSERTS
4 PLACES

SCOT
.15 x .50
4 PLACES

ORIGINAL PAGE IS
OF POOR QUALITY

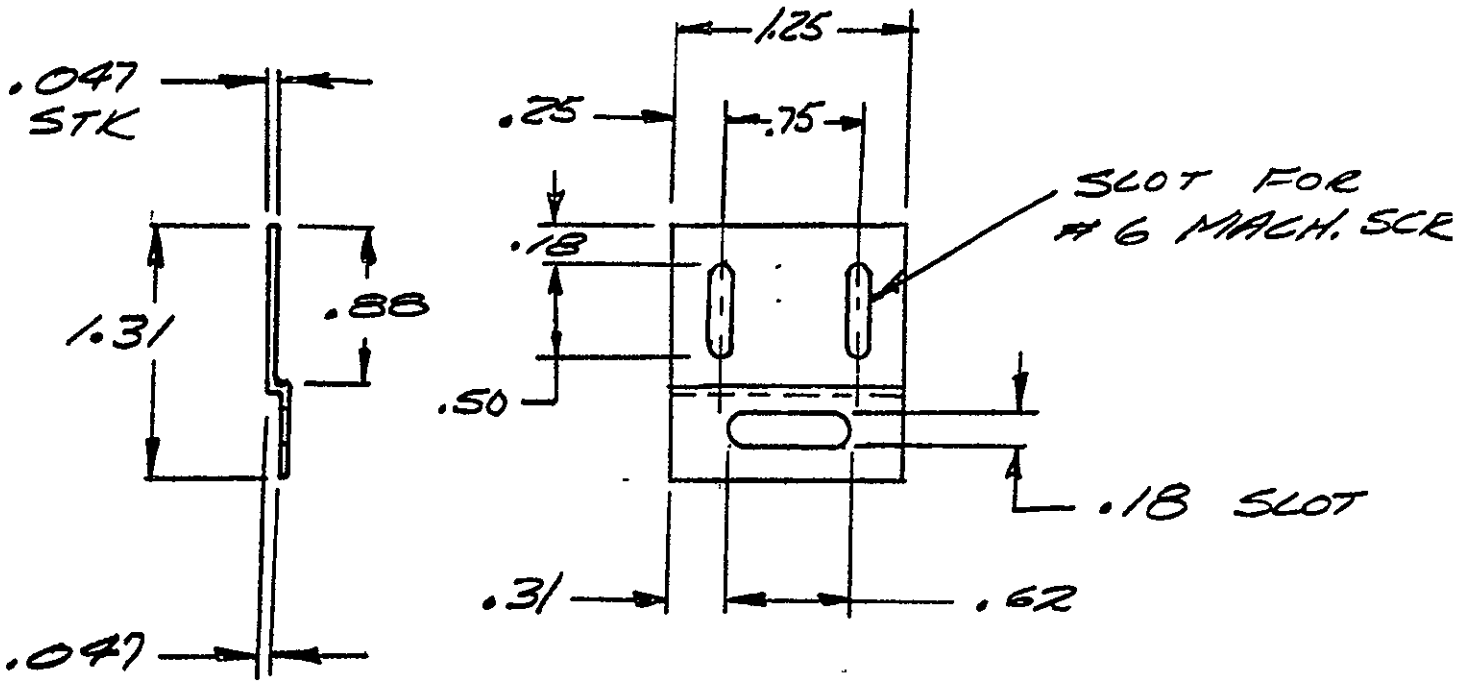
TITLE - COVER
MATERIAL - 5052 AL
.037 - .047
THICK

SK1018771 FILED R. DAY



*- INSIDE DIMENSION

MAT'L - 5052 ALUM
 $.032 \text{ THK}$



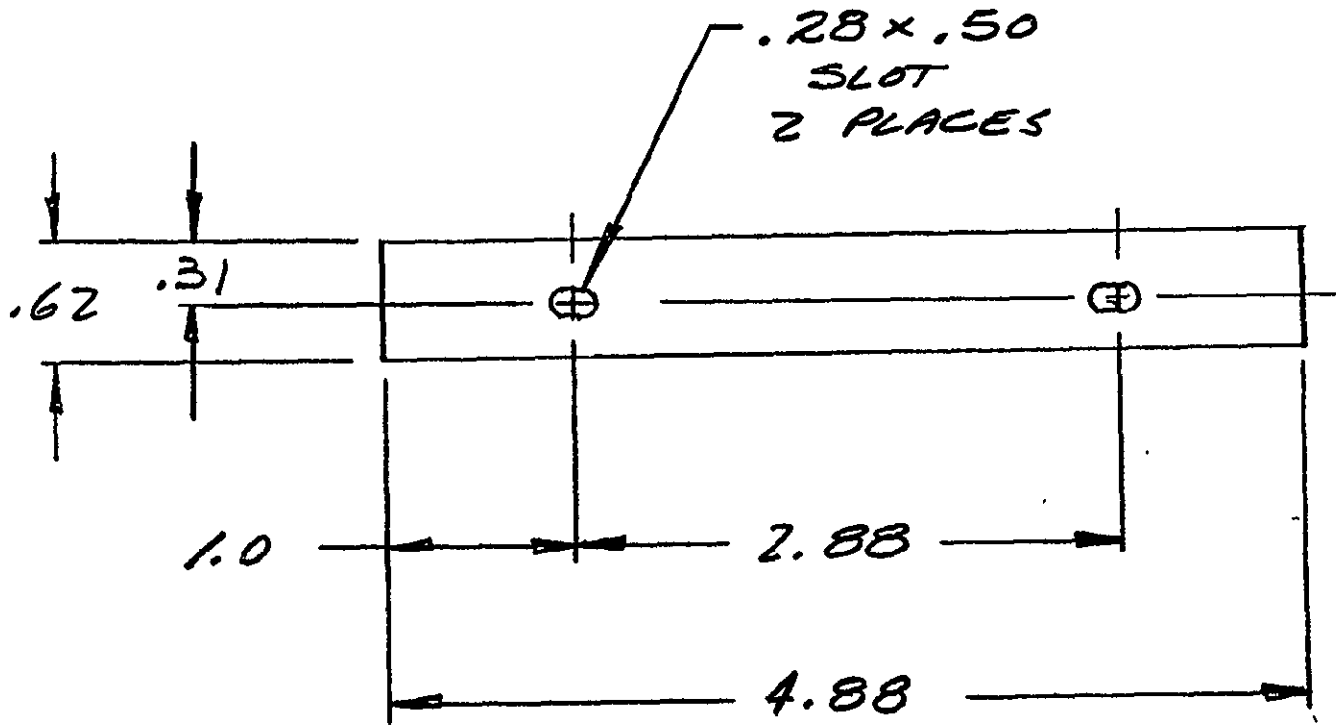
ORIGINAL PAGE IS
 OF POOR QUALITY

MAT'L - STAINLESS

GLEN BUDAY

SK-101077

REQ'D 38

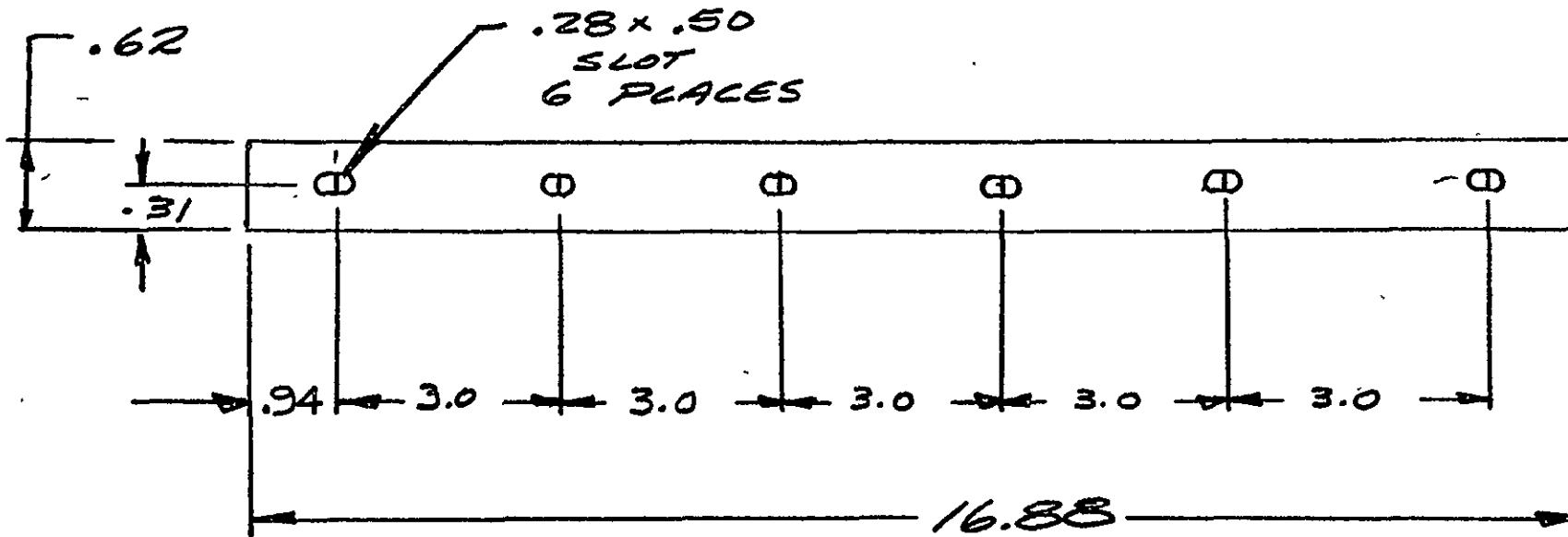


NOTE: SAND SURFACE

MAT'L - AL
 $\frac{1}{8}$ THICK

SK11677-4

G. BUDAY
 4 REQ'D



ORIGINAL PAGE IS
OF POOR QUALITY

NOTE: SAND
SURFACE

MAT'L - 1/8 THICK
AL

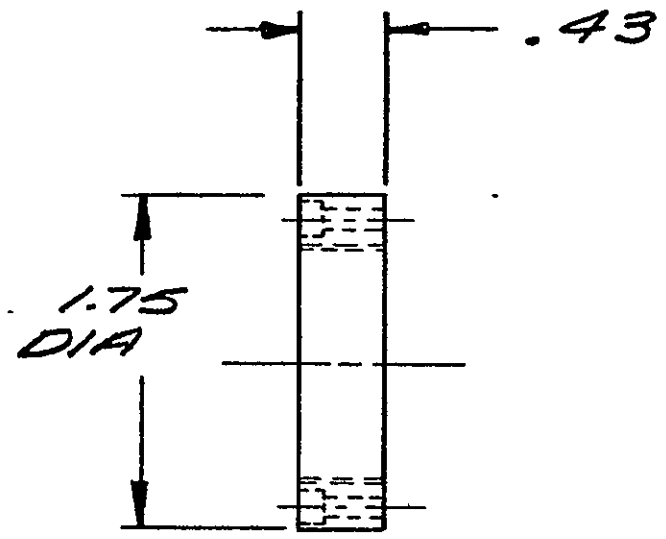
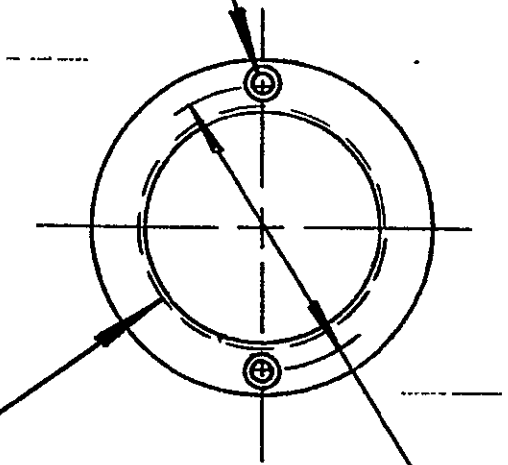
G. BUDAY

SK 111677-3

4 REQ'D

ORIGINAL PAGE IS
OF POOR QUALITY

DRILL & C'BORE
FOR #4 S.H.C.S
2 PLACES

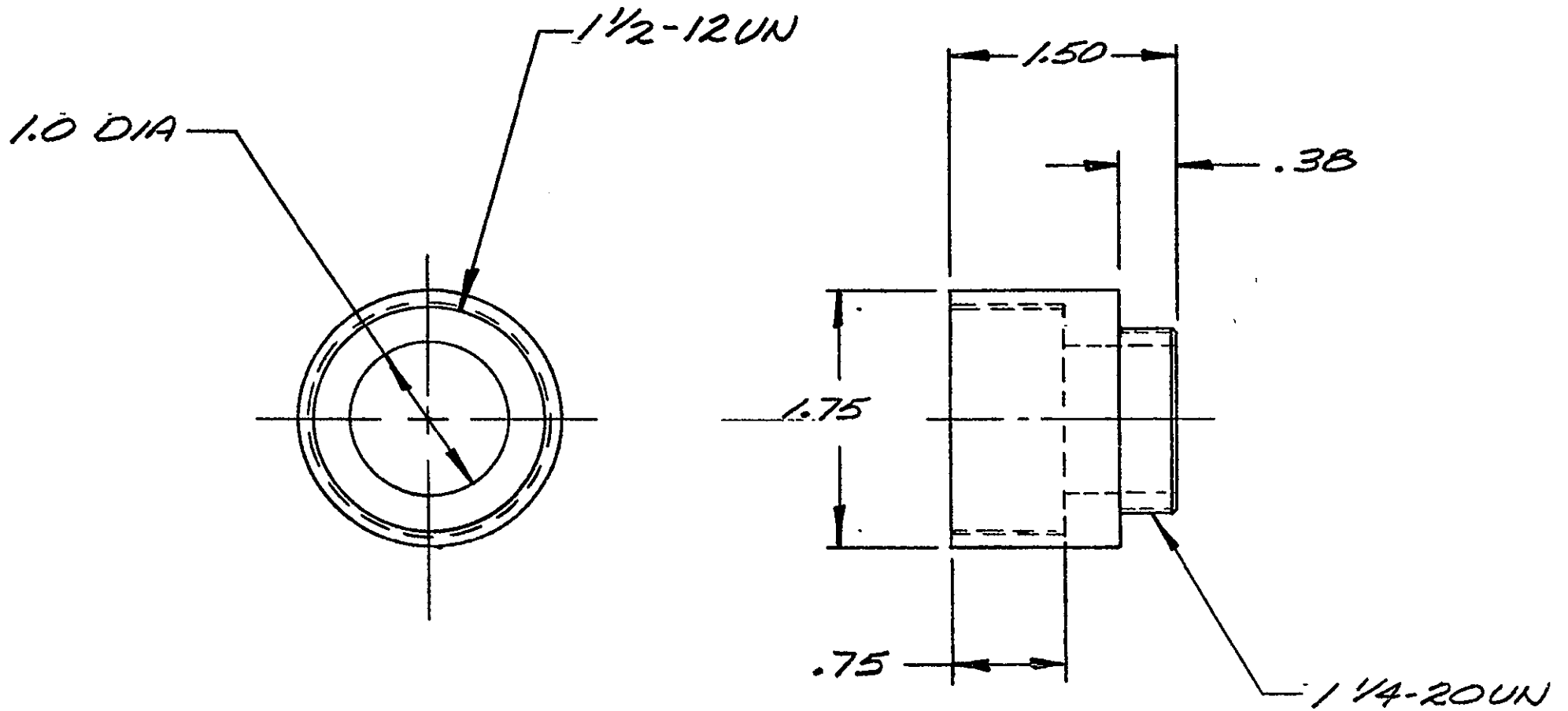


1.50 B.C.

1/4-20 UN
TO MATE WITH
DETAIL R-0272-77-50

MAT'L - AL
G. BUDAY
11-2-77

FLOW METER
ADAPTER
R-0272-77-51

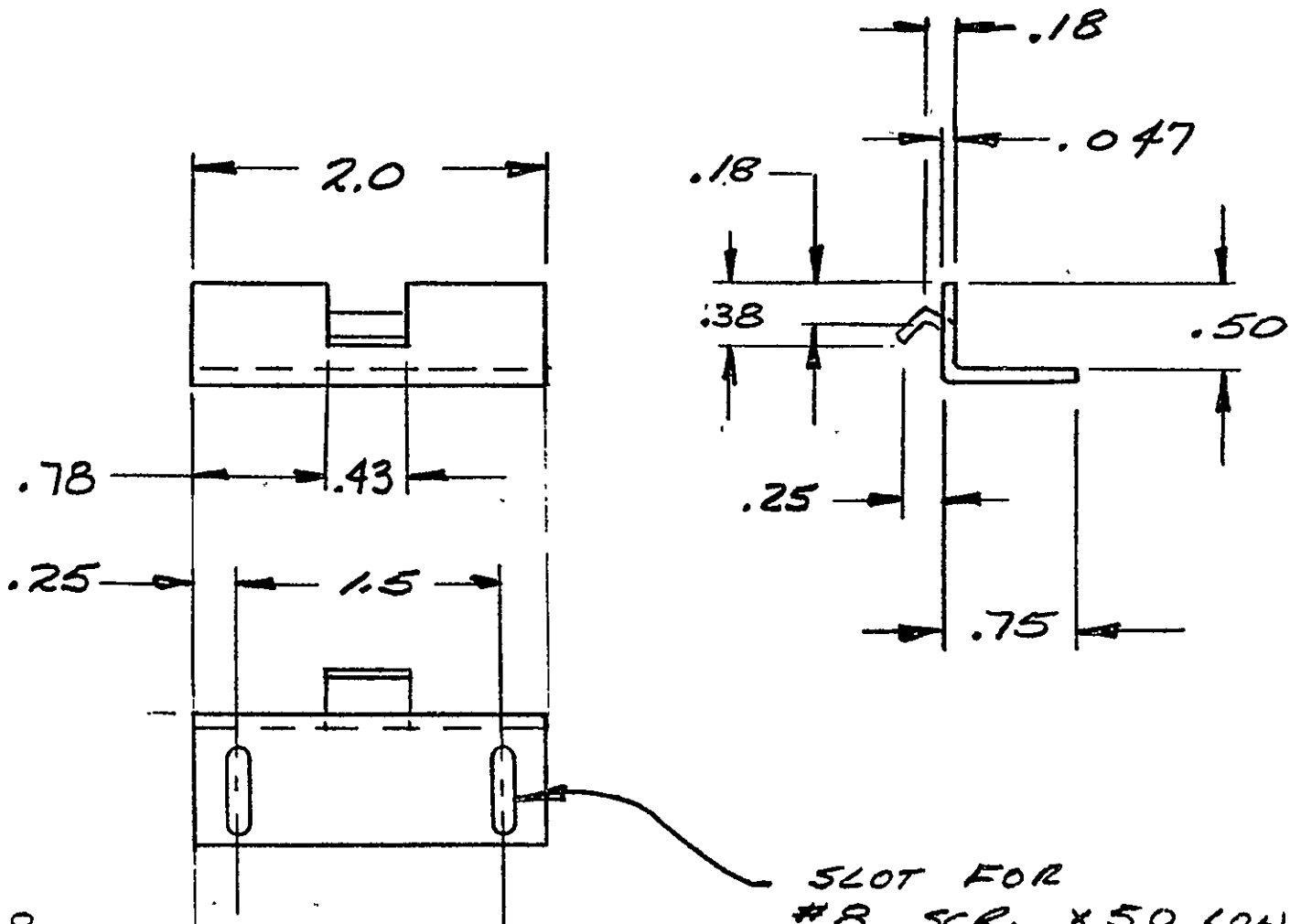


MAT'L - AL.

G. BUDAY
11-2-77.

BEAM-SPLITTER
ADAPTER

R-0272-77-50

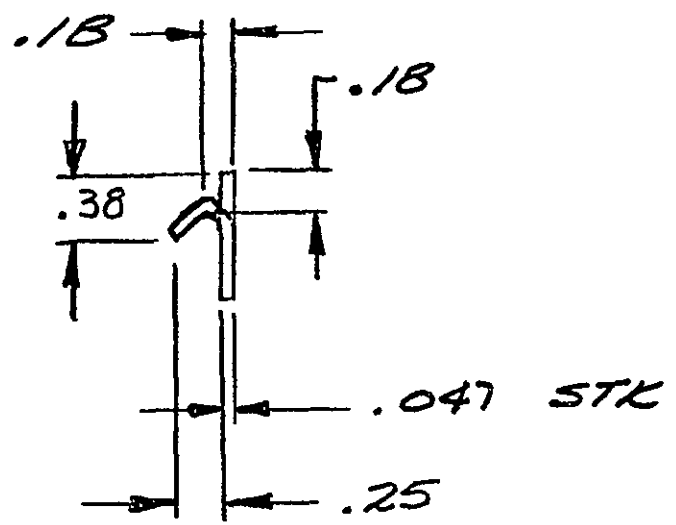
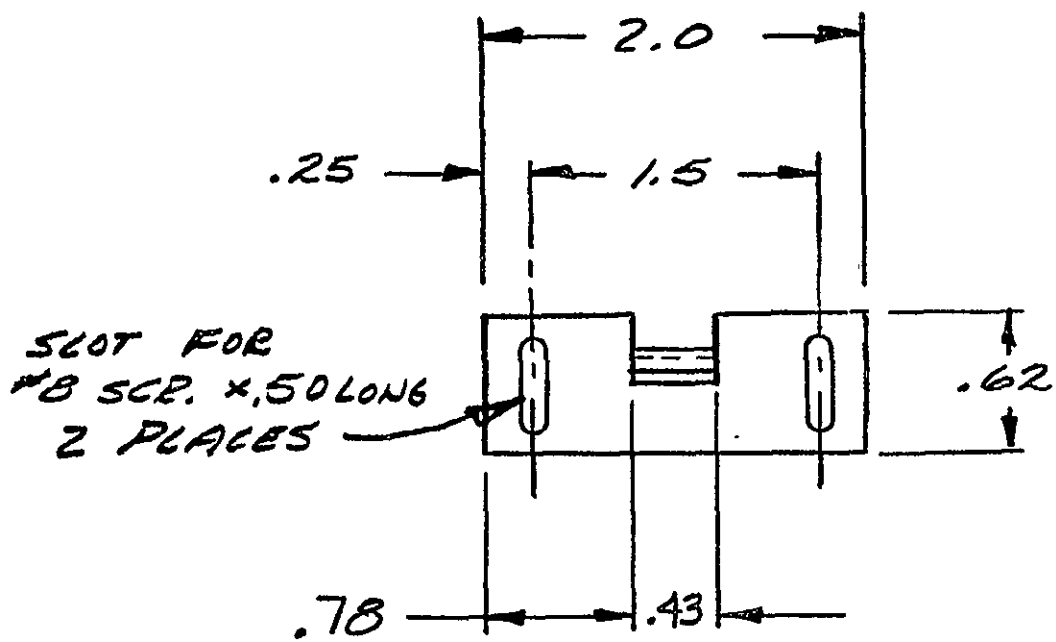


SLOT FOR
#8 SCR. x.50 LONG
2 PLACES

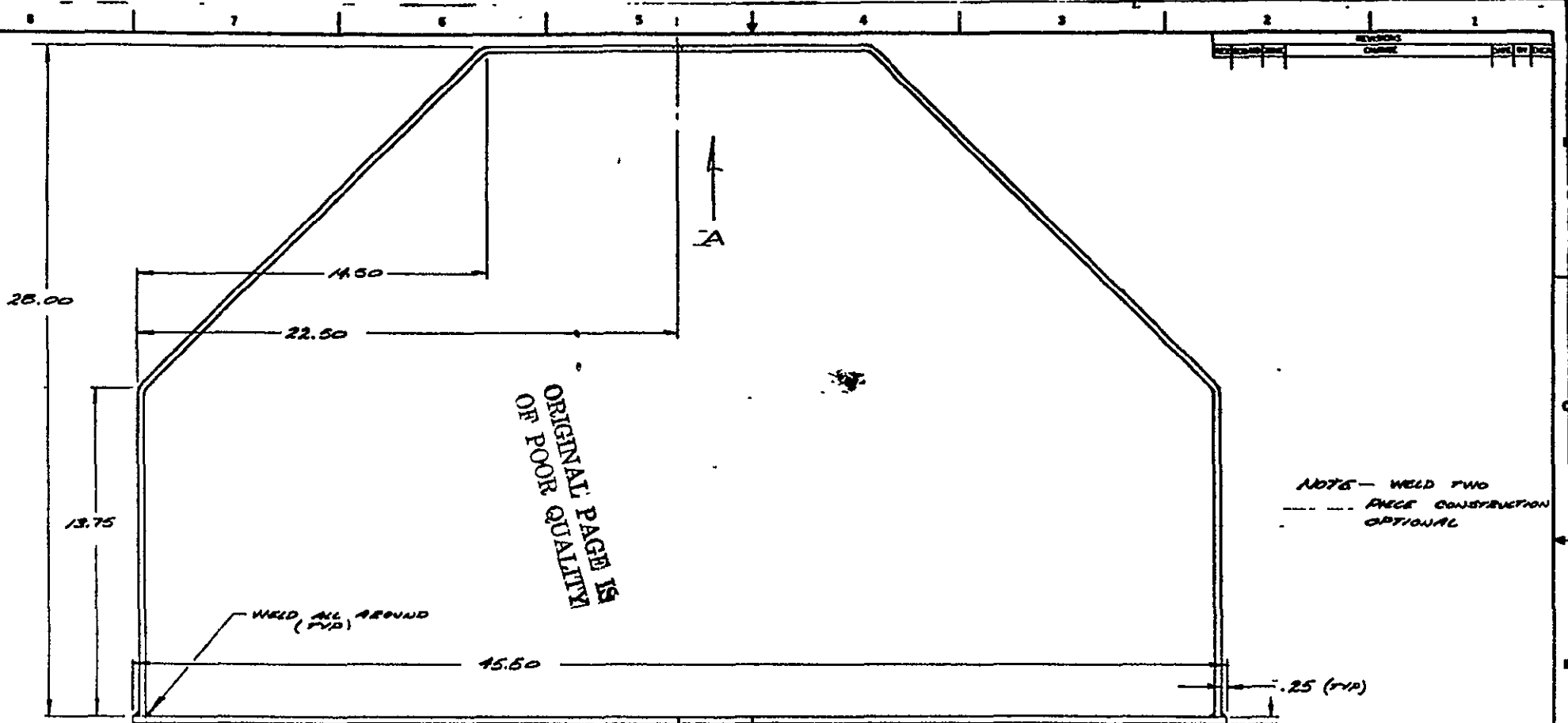
MAT'L - STN STL
.047 THICK

SK 102677-2

ORIGINAL PAGE IS
OF POOR QUALITY

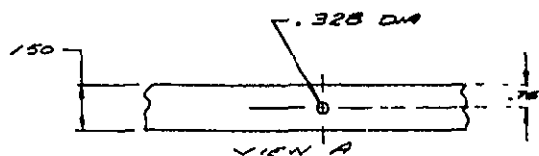
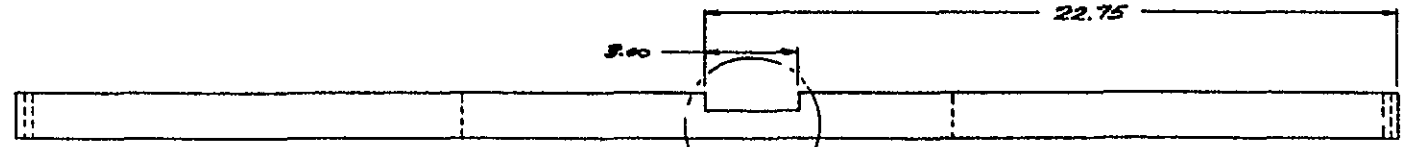


MATL - STN STL
 .047 THICK
 SK 102677-1



ORIGINAL PAGE IS
OF POOR QUALITY

NOTE - WELD TWO
--- PACE CONSTRUCTION
OPTIONAL

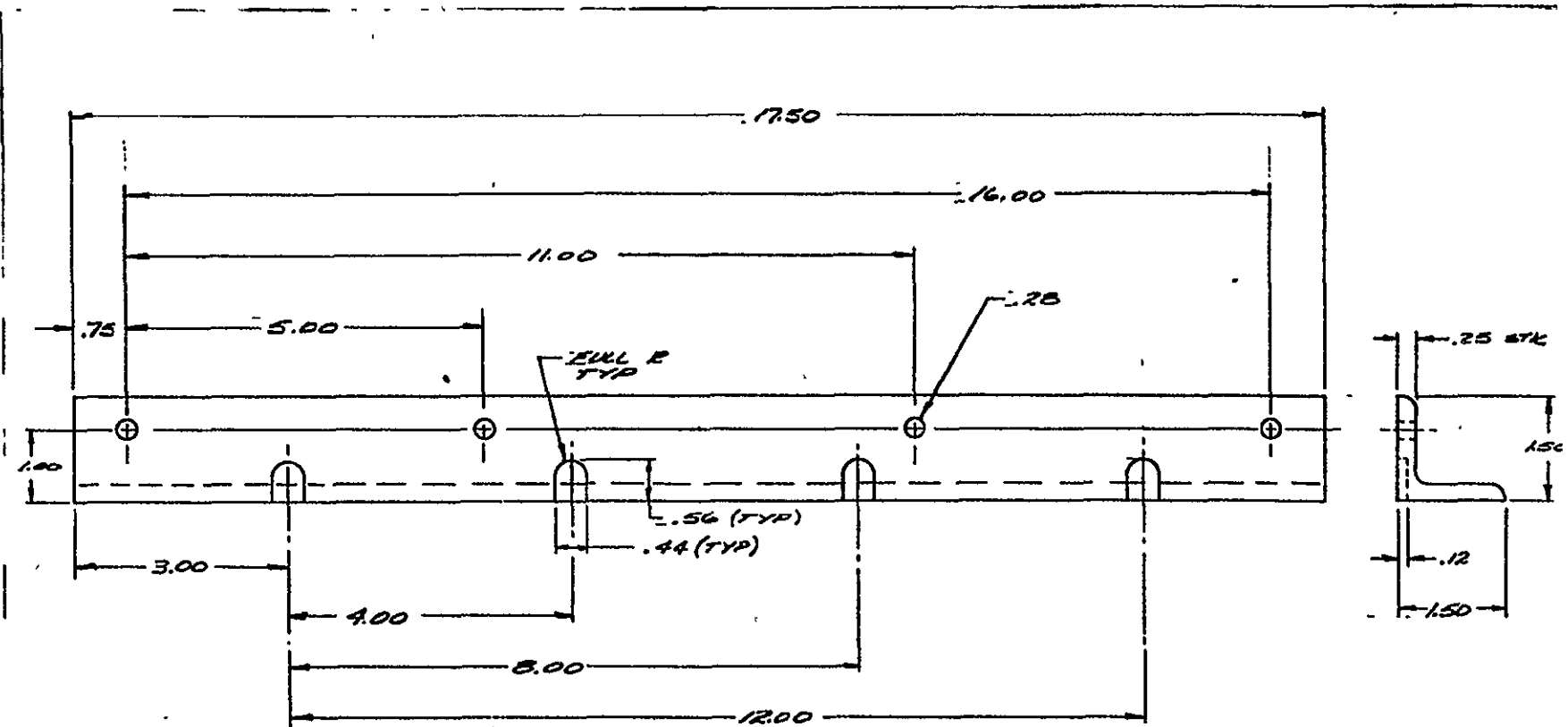


DRIVING IS
SK11177-1A

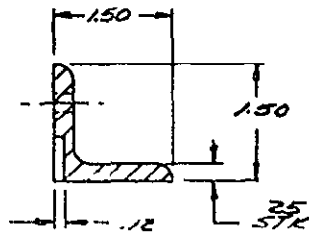
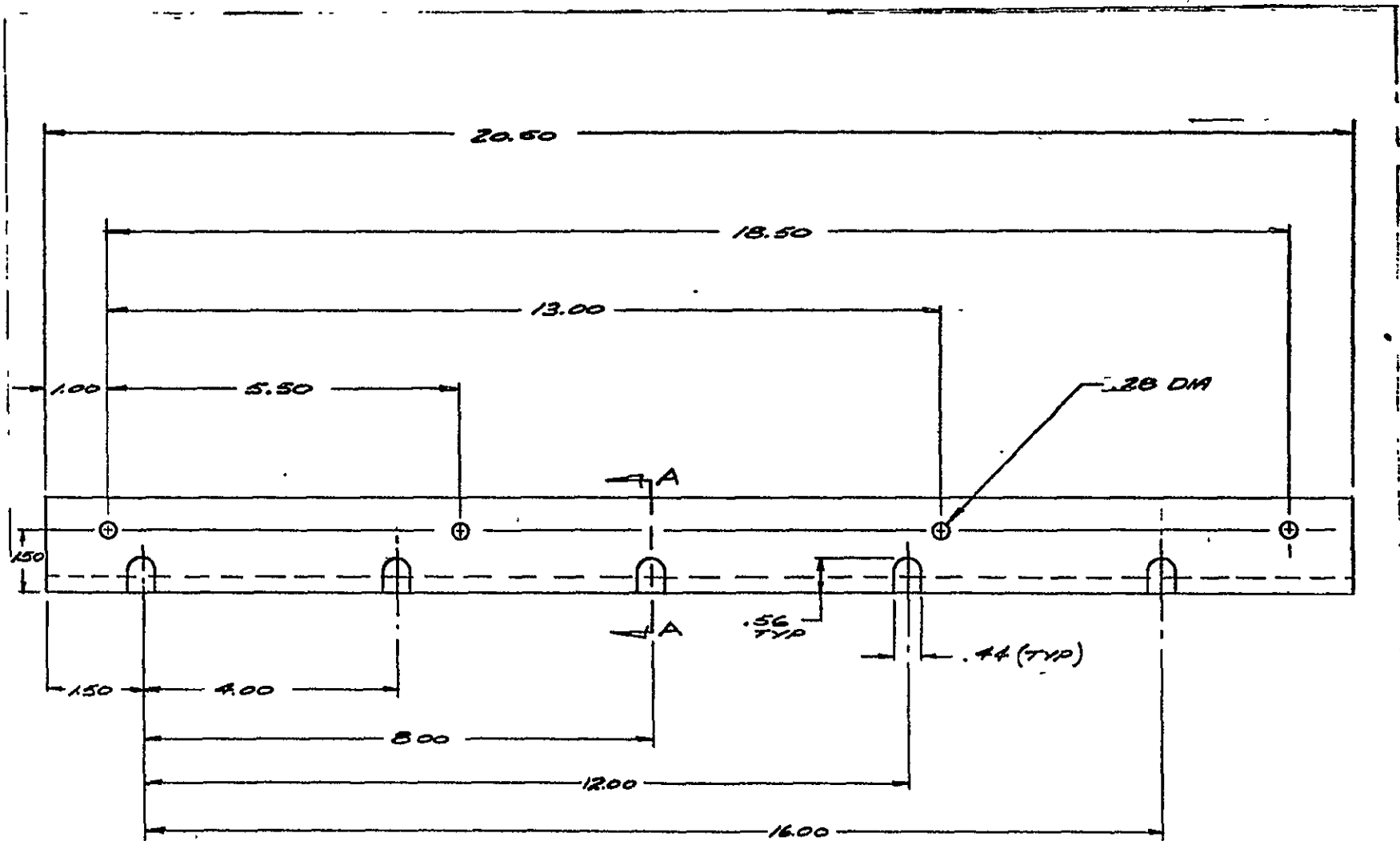
NOT TO BE ON OPPOSITE SIDE
AS SHOWN FOR ALTERNATE PART

UNLESS OTHERWISE SPECIFIED, TOLERANCES DIMENSIONS IN INCHES USE MILLIMETERS 25/100 IN ANGULAR M/F MADE ALL MACHINES SURFACES	MATERIAL ALUM 25 THICK	① ANOTOMOLA INC. Silicon Semiconductor Division
FEATURE CONTROL SYMBOLS PER ASME Y14.5	HEAT TREAT APPLIED FRESH	TITLE SAFETY BEZEL
DATE 15 BUDAY	DATE 11/77	DRAWING NO SK11177-1
DESIGNED BY	CHECKED BY	DATE
APPROVED BY	DATE	DATE

REQ'D - 1 EA

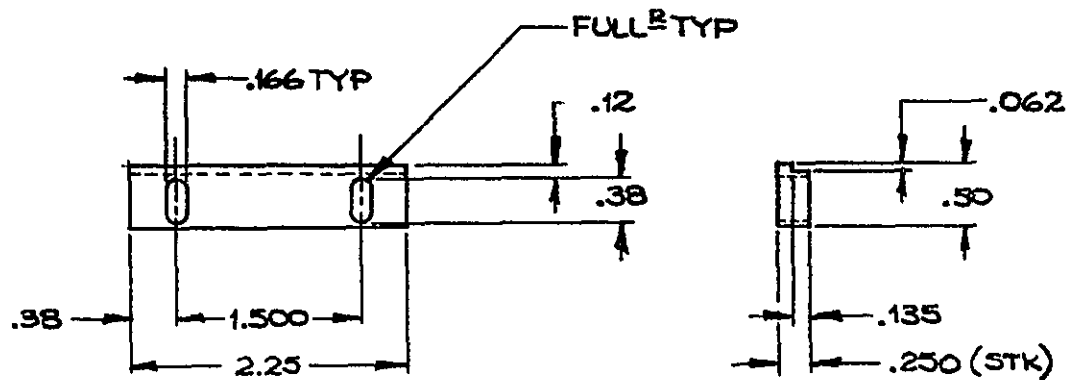


MATL - AL. ANGLE 1 1/2 x 1 1/2
 G. BUDAY 11-15-77
 2 REQ'D
 SK 111577-1



MATL - AL. ANGLE 1/2x1/2
 G. BUDAY 11-16-77
 SK 111677-1
 2 REQ'D

REVISIONS				
REV.	ECO NO.	CHANGE	DATE	ENGR.

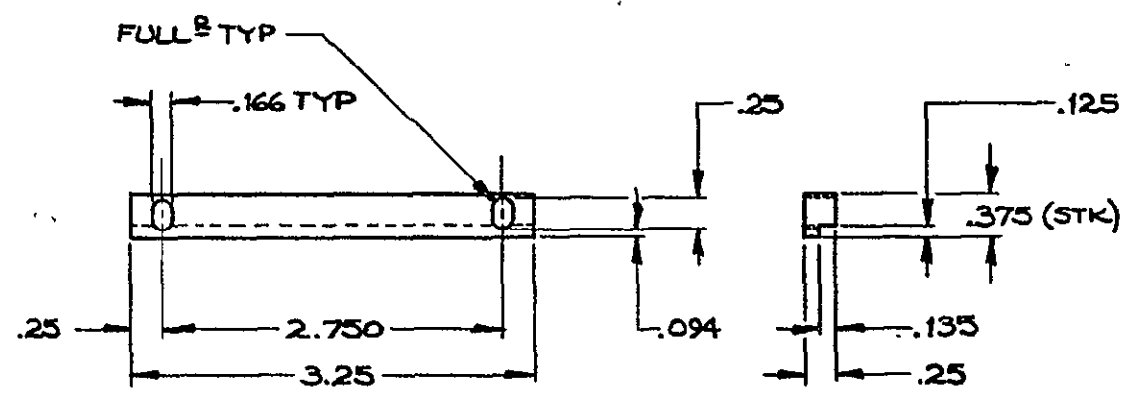


ORIGINAL PAGE IS
OF POOR
QUALITY

ANY SPECIFICATIONS, DRAWINGS OR REPAIRS OR DATA FURNISHED TO BUYER OR SELLER SHALL BE MOTOROLA'S PROPERTY AND SHALL BE KEPT CONFIDENTIAL. SHALL BE USED FOR THE PURPOSE OF CARRYING WITH MOTOROLA'S REQUESTS FOR QUOTATION OR WITH MOTOROLA PURCHASE ORDERS AND SHALL BE RETURNED TO MOTOROLA REQUEST PATENT RIGHTS EMBODIED IN DISCLOSED IDEAS, PATTERNS, DRAWINGS, DEVICES, INFORMATION AND EQUIPMENT SUPPLIED BY MOTOROLA PURSUANT TO THIS REQUEST FOR QUOTATION OR PURCHASE ORDER AND EXCLUSIVE RIGHTS FOR THE USE IN REPRODUCTION THEREOF ARE RESERVED BY MOTOROLA.

UNLESS OTHERWISE SPECIFIED, TOLERANCES INCHES XX ± .02 XXX ± .005 MILLIMETERS .X ± XX ± ANGULAR ± 125 ✓ RMS ALL MACHINED SURFACES FEATURE CONTROL SYMBOLS PER ANSI Y14.5 BREAK ALL SHARP EDGES AND CORNERS, REMOVE BURRS UNDERLINED DIM NOT TO SCALE THIRD ANGLE ORTHOGRAPHIC PROJECTION IS USED	MATERIAL 6061-T6 ALUM		MOTOROLA INC. <i>Discrete Semiconductor Division</i>	
	HEAT TREAT APPLIED FINISH DRAWN BY F.J. MOSNA DATE 10-26-77 CHECKED BY DATE ENGR APPROVAL DATE		TITLE BLOCK RETAINER, SHORT (HeNe LASER ASSY)	
NEXT ASSEMBLY USED ON APPLICATION	SIZE B	CODE IDENT NO. 04713	DRAWING NO R-0299-77-5	SHEET 1 OF 1

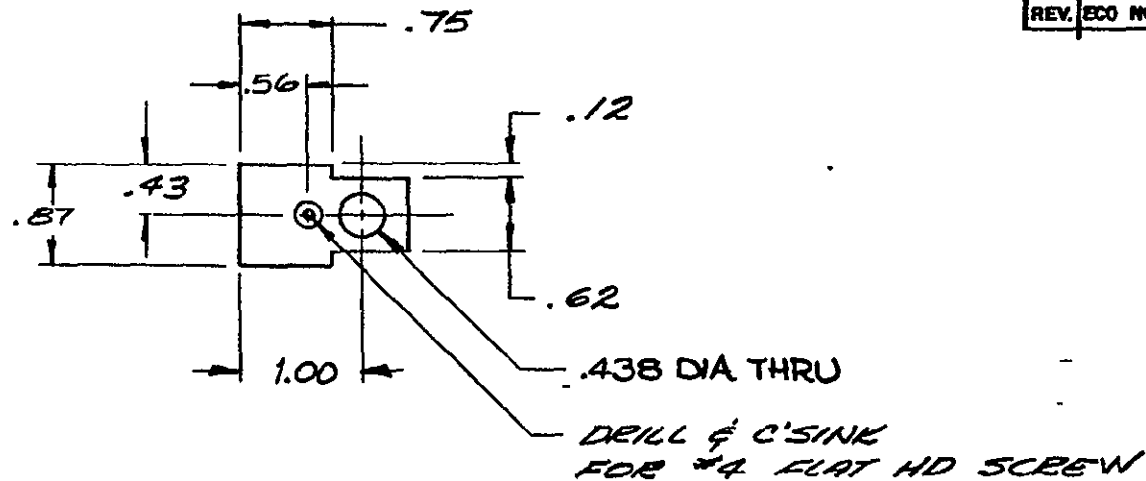
REVISIONS				
REV. ECD NO.	CHANGE	DATE	BY	ENGR.



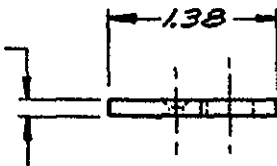
ANY SPECIFICATIONS DRAWINGS OR REPRINTS OR DATA FURNISHED TO BIDDER OR SELLER SHALL REMAIN MOTOROLA'S PROPERTY SHALL BE KEPT CONFIDENTIAL SHALL BE USED FOR THE PURPOSE OF COMPLYING WITH MOTOROLA'S REQUESTS FOR QUOTATION OR WITH MOTOROLA PURCHASE ORDERS AND SHALL BE RETURNED AT MOTOROLA'S REQUEST PATENT RIGHTS EMBODIED IN DESIGNS TOOLS PATTERNS DRAWINGS DEVICES INFORMATION AND EQUIPMENT SUPPLIED BY MOTOROLA PURSUANT TO THIS REQUEST FOR QUOTATION OR PURCHASE ORDER AND EXCLUSIVE RIGHTS FOR THE USE IN REPRODUCTION THEREOF ARE RESERVED BY MOTOROLA

NEXT ASSEMBLY	USED ON	APPLICATION	UNLESS OTHERWISE SPECIFIED, TOLERANCES: INCHES XX ± .02, XXX ± .005 MILLIMETERS X ± .XX ± .XX ± ANGULAR ±		MATERIAL 6061-T6 ALUM	MOTOROLA INC. Discrete Semiconductor Division	TITLE. BLOCK RETAINER, LONG (HeNe LASER ASSY)
			125 RMS ALL MACHINED SURFACES.	HEAT TREAT	DATE		
			FEATURE CONTROL SYMBOLS PER ANSI Y14.5	APPLIED FINISH	DRAWN BY F. J. MOSNA	DATE 10-26-77	SIZE B
			BREAK ALL SHARP EDGES AND CORNERS, REMOVE BURRS		CHECKED BY	DATE	CODE IDENT NO. 04713
			UNDERLINED DIM NOT TO SCALE THIRD ANGLE ORTHOGRAPHIC PROJECTION IS USED		ENGR APPROVAL	DATE	DRAWING NO R-0299-77-4
							SCALE FULL WEIGHT SHEET 1 OF 1

SPD 11837 (6/73)



12 ORIGINAL PAGE IS
OF POOR QUALITY



REVISIONS				
REV.	ECO NO.	CHANGE	DATE	BY ENGR.

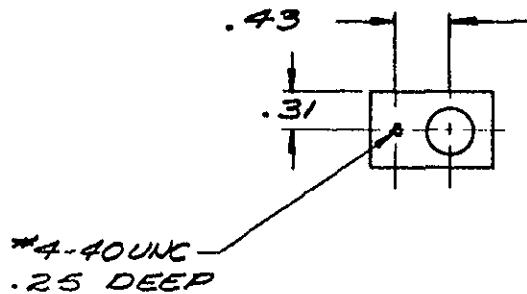
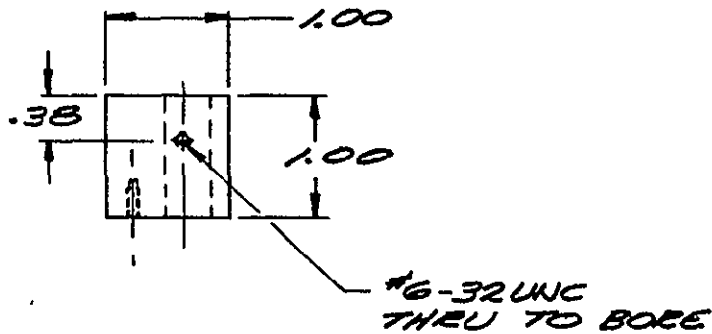
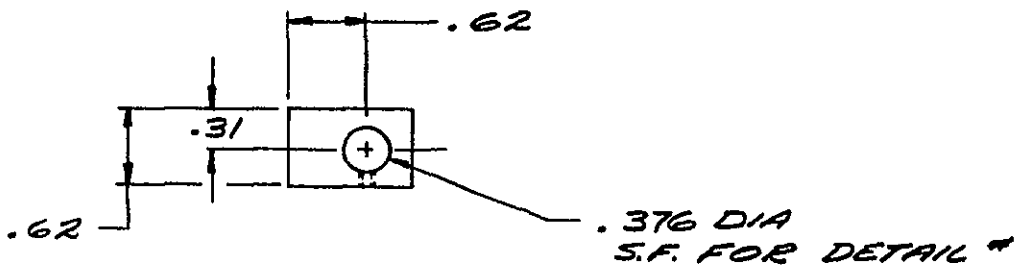
*ANY SPECIFICATIONS, DRAWINGS OR REPRINTS OR DATA FURNISHED TO BUYER OR SELLER SHALL REMAIN MOTOROLA'S PROPERTY. SHALL BE KEPT CONFIDENTIAL. SHALL BE USED FOR THE PURPOSE OF COMPLYING WITH MOTOROLA'S REQUESTS FOR QUOTATION OR WITH MOTOROLA PURCHASE ORDERS AND SHALL BE RETURNED AT MOTOROLA'S REQUEST. PATENT RIGHTS EMPLOYED IN DESIGNS, TOOLS, PATTERNS, DRAWINGS, DEVICES, INFORMATION AND EQUIPMENT SUPPLIED BY MOTOROLA PURSUANT TO THIS REQUEST FOR QUOTATION OR PURCHASE ORDER AND EXCLUSIVE RIGHTS FOR THE USE IN REPRODUCTION THEREOF ARE RESERVED BY MOTOROLA.

NEXT ASSEMBLY	USED ON
APPLICATION	

UNLESS OTHERWISE SPECIFIED, TOLERANCES:
 INCHES .XX ± .02, .XXX ± .005
 MILLIMETERS .X ± .4, .XX ± .4
 ANGULAR ± H
 ✓ RMS ALL MACHINED SURFACES.
 FEATURE CONTROL SYMBOLS PER ANSI Y14.5.
 BREAK ALL SHARP EDGES AND CORNERS, REMOVE BURRS.
 UNDERLINED DIM NOT TO SCALE
 THIRD ANGLE ORTHOGRAPHIC PROJECTION IS USED

MATERIAL TEFLON	
HEAT TREAT —	
APPLIED FINISH —	
DRAWN BY G BUDAY	DATE 10-25-77
CHECKED BY	DATE
ENGR APPROVAL	DATE

MOTOROLA INC. Discrete Semiconductor Division			
TITLE: SLIDE PLATE			
SIZE B	CODE IDENT NO 04713	DRAWING NO E-0299-77-3	
SCALE FULL	WEIGHT	SHEET OF	



REVISIONS				
REV.	ECO NO.	CHANGE	DATE	BY ENGR.

UNLESS OTHERWISE SPECIFIED,
TOLERANCES:

INCHES $XX \pm .02$, $XXX \pm .005$

MILLIMETERS $X \pm H$, $XX \pm H$

ANGULAR $\pm H$

✓ RS RMS ALL MACHINED SURFACES

FEATURE CONTROL SYMBOLS PER ANSI Y14.5.

BREAK ALL SHARP EDGES AND CORNERS, REMOVE BURRS.

UNDERLINED DM NOT TO SCALE
THIRD ANGLE ORTHOGRAPHIC PROJECTION IS USED.

MATERIAL 6061
ALUM

HEAT TREAT H

APPLIED FINISH H

DRAWN BY G. BUDAY DATE 10-25-77

CHECKED BY _____ DATE _____

ENGR APPROVAL _____ DATE _____

M MOTOROLA INC.
Discrete Semiconductor Division

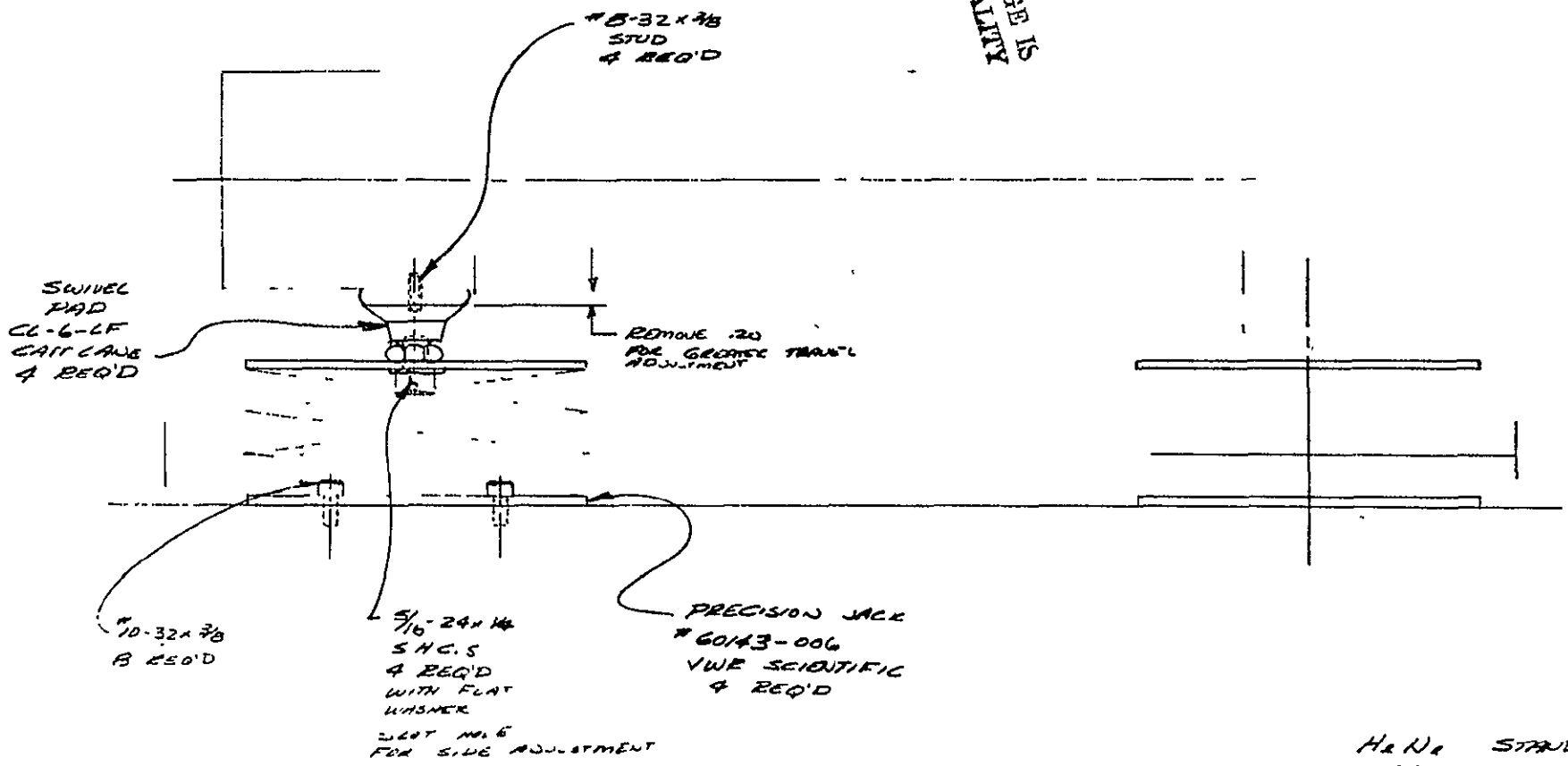
TITLE:
SLIDING BLOCK
FOR H₂ N₂

SIZE	CODE IDENT. NO.	DRAWING NO.
<u>B</u>	<u>04713</u>	<u>R-0299-77-1</u>
SCALE <u>FULL</u>	WEIGHT	SHEET OF

"ANY SPECIFICATIONS, DRAWINGS OR REPRINTS OR DATA FURNISHED TO BIDDER OR BUYER SHALL REMAIN MOTOROLA'S PROPERTY. SHALL BE KEPT CONFIDENTIAL. SHALL BE USED FOR THE PURPOSE OF COMPLYING WITH MOTOROLA'S REQUESTS FOR QUOTATION OR WITH MOTOROLA PURCHASE ORDERS AND SHALL BE RETURNED AT MOTOROLA'S REQUEST. PATENT RIGHTS EMBODIED IN DESIGNS, TOOLS, PATTERNS, DRAWINGS, DEVICES, INFORMATION AND EQUIPMENT SUPPLIED BY MOTOROLA PURSUANT TO THIS REQUEST FOR QUOTATION OR PURCHASE ORDER AND EXCLUSIVE RIGHTS FOR THE USE IN REPRODUCTION THEREOF ARE RESERVED BY MOTOROLA."

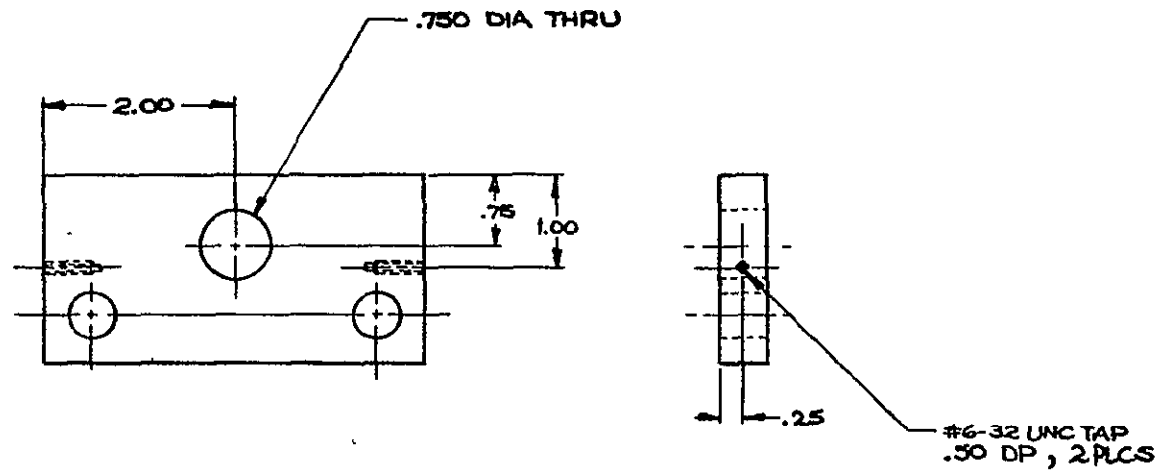
NEXT ASSEMBLY	USED ON
APPLICATION	

ORIGINAL PAGE IS
OF POOR QUALITY



H&N₂ STAND FOR
YAG LASERS
2 SETS
G. BUDAY 11-9-77
SK110977-1

REVISIONS			
REV.	ECO NO.	CHANGE	DATE BY ENGR.



ANY SPECIFICATIONS, DIMENSIONS OR DETAILS ON THIS DRAWING TO BE USED OR REFERRED TO SHALL BE THE PROPERTY OF MOTOROLA INC. NO PARTS OR MATERIALS SHALL BE USED FOR THE PURPOSE OF THIS DRAWING UNLESS SPECIFICALLY REQUESTED AND APPROVED BY MOTOROLA. MOTOROLA ASSUMES NO LIABILITY FOR THE USE OF THIS DRAWING IN ANY MANNER WITHOUT THE WRITTEN PERMISSION OF MOTOROLA. MOTOROLA DISCLAIMS LIABILITY FOR THE USE OF THIS DRAWING IN ANY MANNER WITHOUT THE WRITTEN PERMISSION OF MOTOROLA.

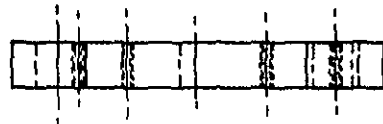
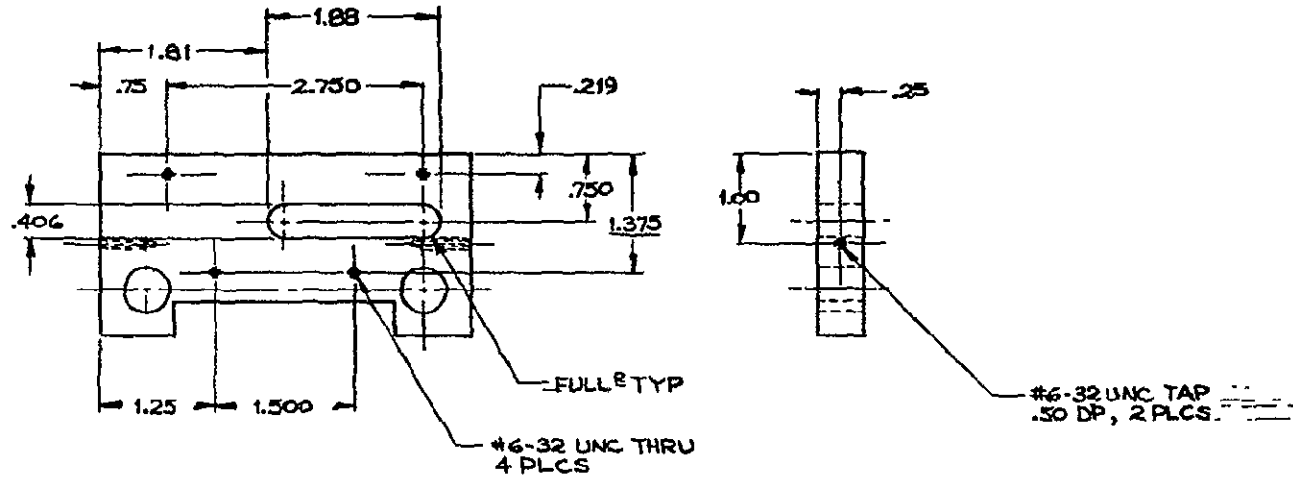
APPLICATION	USED ON

UNLESS OTHERWISE SPECIFIED, TOLERANCES HICHES XX ± .02 XXX ± .005 MILLIMETERS X ± .XX ±		MATERIAL		(AA) MOTOROLA INC. <i>Discrete Semiconductor Division</i>	
ANGULAR ±		HEAT TREAT		TITLE	
<input checked="" type="checkbox"/> RMS ALL MACHINED SURFACES FEATURE CONTROL SYMBOLS PER ANSI Y14.5		APPLIED FINISH		MODIFICATIONS TO PLATE	
BREAK ALL SHARP EDGES AND CORNERS, REMOVE BURRS		DRAWN BY	F. J. MOSWA	DATE	10-28-77
UNDERLINED DIM NOT TO SCALE		CHECKED BY		DATE	
THIRD ANGLE ORTHOGRAPHIC PROJECTION IS USED		ENGR APPROVAL		DATE	
		SIZE	C	CODE IDENT NO	04713
		SCALE	FULL	WEIGHT	
		DRAWING NO	R-0299-77-8		
		SHEET		1 OF 1	

SP. 113-2 (10/77)

C-2

REVISIONS				
REV.	ECO NO.	CHANGE	DATE	BY



THIS DRAWING IS THE PROPERTY OF MOTOROLA INC. IT IS TO BE USED ONLY FOR THE PURPOSES OF THE PROJECT FOR WHICH IT WAS DRAWN. IT IS NOT TO BE REPRODUCED OR TRANSMITTED IN ANY FORM OR BY ANY MEANS, ELECTRONIC OR MECHANICAL, INCLUDING PHOTOCOPYING, RECORDING, OR BY ANY INFORMATION STORAGE AND RETRIEVAL SYSTEM. ANY UNAUTHORIZED REPRODUCTION OR TRANSMISSION OF THIS DRAWING IS PROHIBITED. MOTOROLA INC. 1977

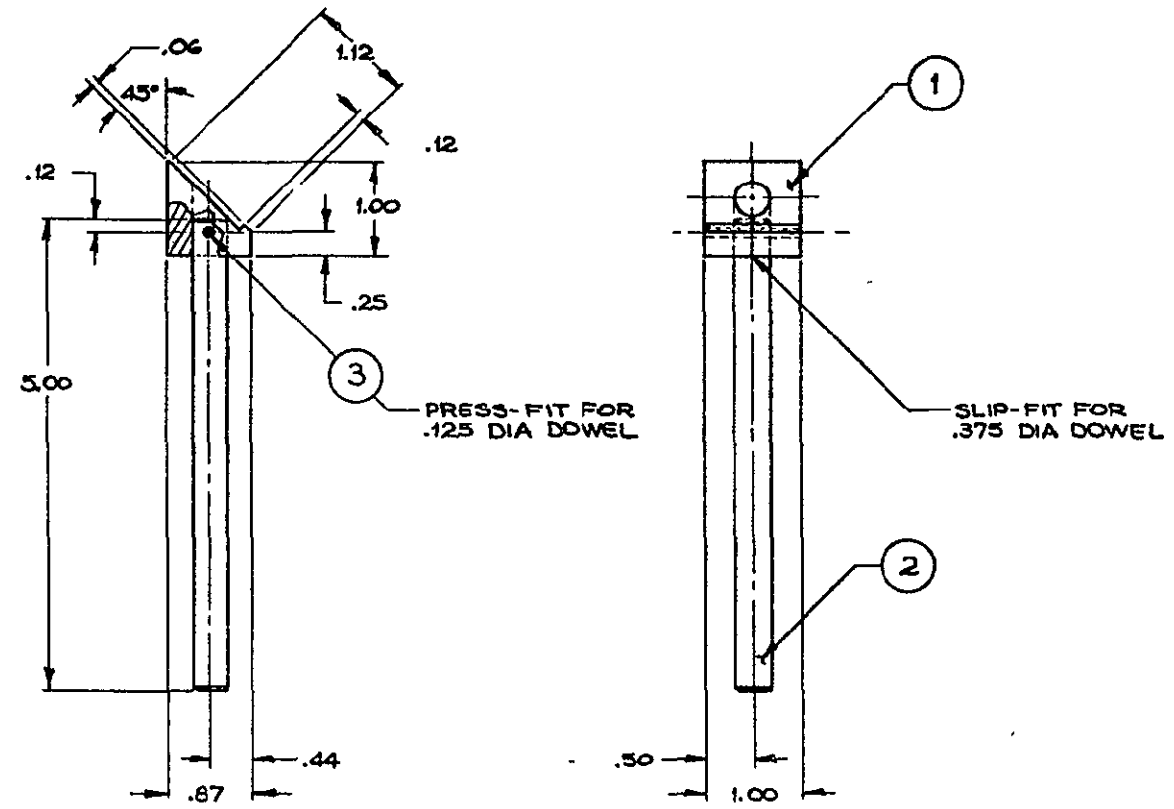
APPLICATION	DATE	BY
NEXT ASSEMBLY	USED ON	

UNLESS OTHERWISE SPECIFIED, TOLERANCES
 INCHES XX ± .02 XXX ± .005
 MILLIMETERS X ± .XX ± .1
 ANGULAR ±
 ✓ RNS ALL MACHINED SURFACES
 FEATURE CONTROL SYMBOLS PER ANSI Y14.5
 BREAK ALL SHARP EDGES AND CORNERS, REMOVE BURRS
 UNDERLINED DIM NOT TO SCALE
 THIRD ANGLE ORTHOGRAPHIC PROJECTION IS USED

MATERIAL	
HEAT TREAT	
APPLIED FINISH	
DRAWN BY	F.J. MOSNA
CHECKED BY	
ENGR APPROVAL	

MOTOROLA INC. Discrete Semiconductor Division		
TITLE		
MODIFICATIONS TO EXISTING PLATE		
SIZE	CODE IDENT NO	DRAWING NO
C	04713	R-0299-77-6
SCALE	FULL	WEIGHT
		SHEET 1 OF 1

REVISIONS				
REV	ECO NO	CHANGE	DATE	BY



PRESS-FIT FOR
.125 DIA DOWEL

SLIP-FIT FOR
.375 DIA DOWEL

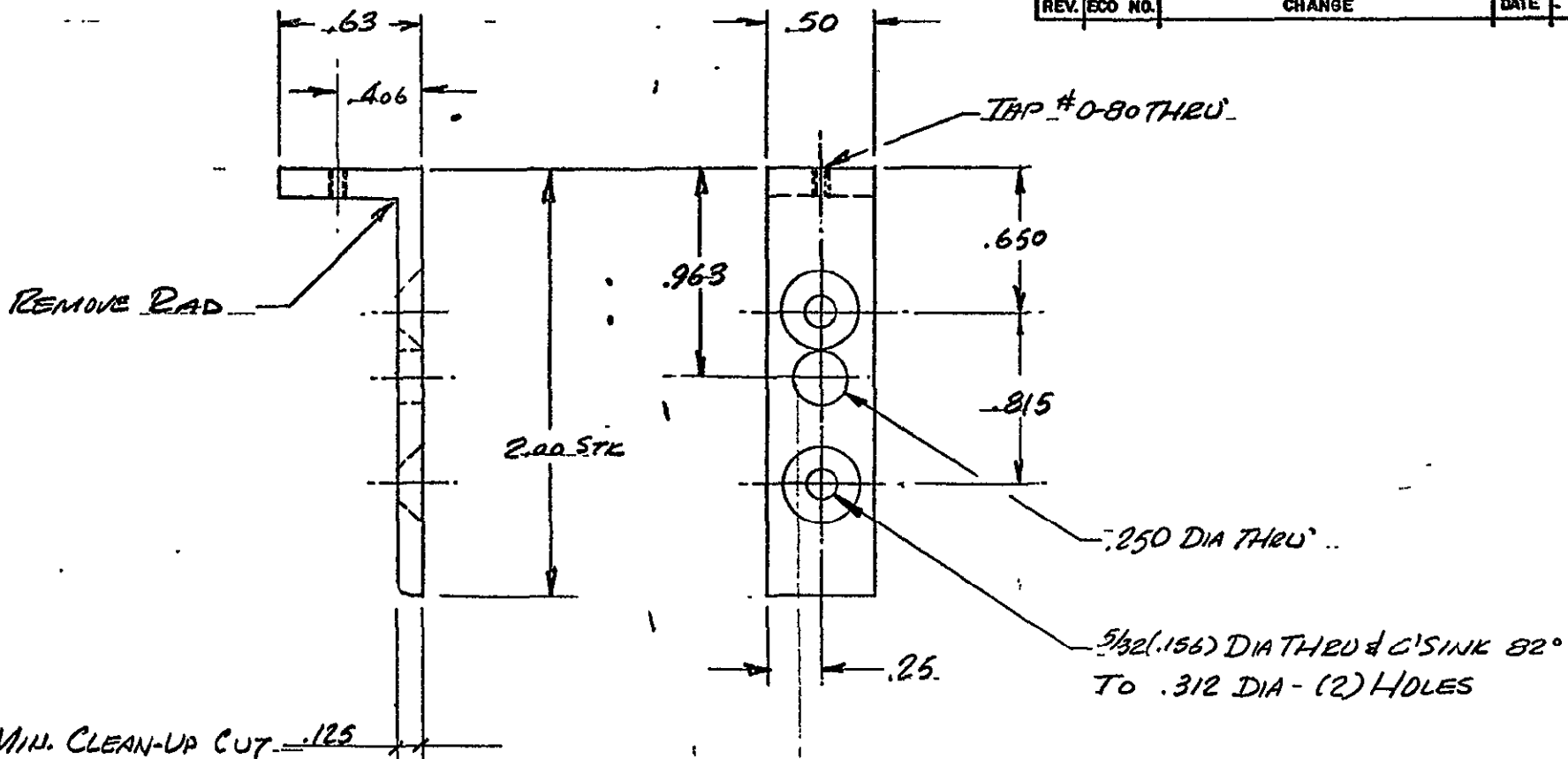
ITEM	REQ'D	DESCRIPTION
3	1	.125 DIA DOWEL 1.0 LG
2	1	.375 DIA X 5.0 LG 6061-T6 ALUM ROD
1	1	1.0 X 1.0 X .87 6061-T6 ALUM

UNLESS OTHERWISE SPECIFIED,
TOLERANCES
INCHES XX ± .02 XXX ± .005
MILLIMETERS X ± .XX ± .XX ±
ANGULAR ±
125 RMS ALL MACHINED
SURFACES
FEATURE CONTROL SYMBOLS
PER ANSI Y14.5
BREAK ALL SHARP EDGES AND
CORNERS, REMOVE BURRS
UNDERLINED DIM NOT TO SCALE
THIRD ANGLE ORTHOGRAPHIC
PROJECTION IS USED

NOTE: SPECIFICATIONS, DIMENSIONS OR WEIGHTS ON THIS DRAWING TO BE USED AS BELIEVED SHALL REMAIN THE PROPERTY OF MOTOROLA INC. NO PART OF THIS DRAWING SHALL BE REPRODUCED OR TRANSMITTED IN ANY FORM OR BY ANY MEANS, ELECTRONIC OR MECHANICAL, INCLUDING PHOTOCOPYING, RECORDING, OR BY ANY INFORMATION STORAGE AND RETRIEVAL SYSTEM, WITHOUT THE WRITTEN PERMISSION OF MOTOROLA INC. THIS DRAWING IS THE PROPERTY OF MOTOROLA INC. AND IS LOANED TO YOU FOR YOUR USE ONLY. IT IS NOT TO BE REPRODUCED OR TRANSMITTED IN ANY FORM OR BY ANY MEANS, ELECTRONIC OR MECHANICAL, INCLUDING PHOTOCOPYING, RECORDING, OR BY ANY INFORMATION STORAGE AND RETRIEVAL SYSTEM, WITHOUT THE WRITTEN PERMISSION OF MOTOROLA INC.	NEXT ASSEMBLY	USED ON	APPLICATION
--	---------------	---------	-------------

MATERIAL	MOTOROLA INC. Discrete Semiconductor Division	
HEAT TREAT	TITLE	
APPLIED FINISH	MIRROR STAND ASSY.	
DRAWN BY F. J. MCSNA	DATE 10 25 77	SIZE CODE IDENT NO
CHECKED BY	DATE	C 04713
ENGR APPROVAL	DATE	DRAWING NO R-0299-77-2
	SCALE FULL	WEIGHT
		SHEET 1 OF 1

REVISIONS				
REV.	ECO NO.	CHANGE	DATE	BY ENGR.



UNLESS OTHERWISE SPECIFIED,
TOLERANCES:
INCHES $.XX \pm .015$ $.XXX \pm .005$
MILLIMETERS $.X \pm .XX \pm$
ANGULAR \rightarrow

$63 \sqrt{}$ RMS ALL MACHINED SURFACES.

FEATURE CONTROL SYMBOLS PER ANSI Y14.5.

BREAK ALL SHARP EDGES AND CORNERS, REMOVE BURRS.

UNDERLINED DIM NOT TO SCALE
THIRD ANGLE ORTHOGRAPHIC PROJECTION IS USED.

MATERIAL $2'' \times 2'' \times 1/8''$
TYPE 304 CRES ANGLE

HEAT TREAT H

APPLIED FINISH H

DRAWN BY DATE

CHECKED BY DATE

ENGR. APPROVAL DATE

MOTOROLA INC.
Discrete Semiconductor Division

TITLE:
STRIP RETAINING ANGLE

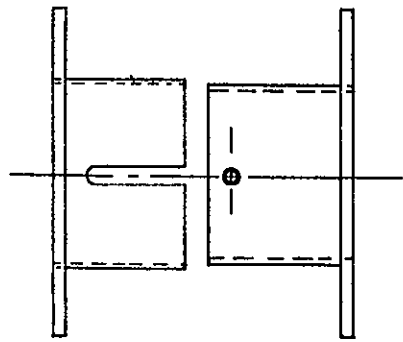
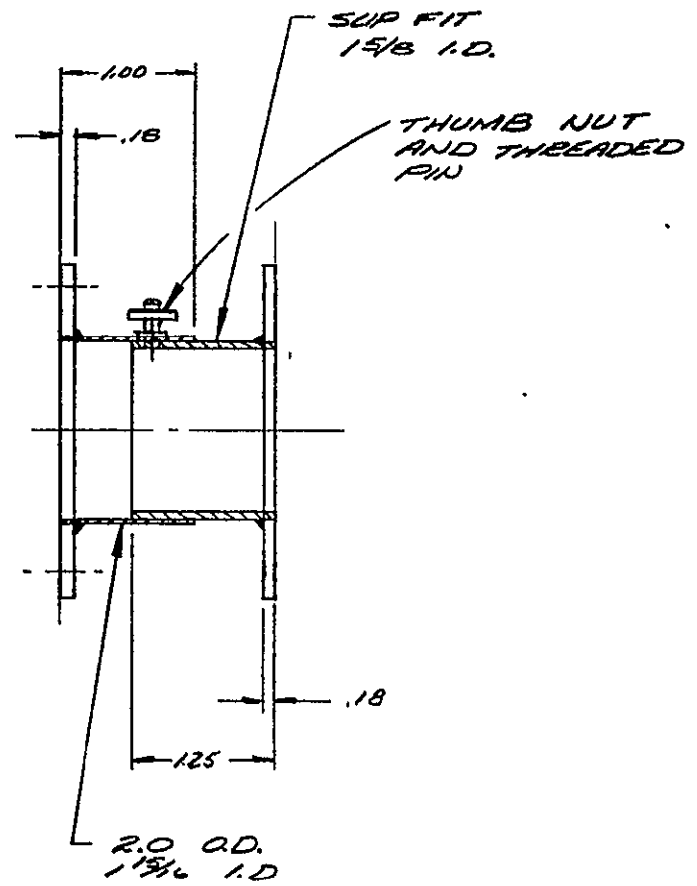
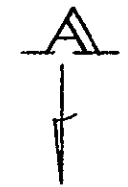
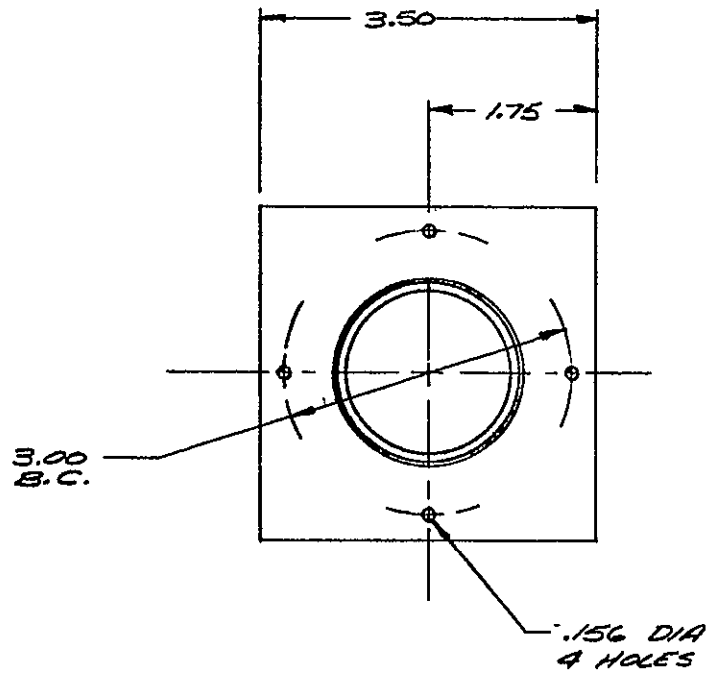
SIZE	CODE IDENT. NO.	DRAWING NO.
B	04713	J5-00-3
SCALE 2:1	WEIGHT <i>wt</i>	SHEET 1 OF 1

SPD TEST (4/75)

"ANY SPECIFICATIONS, DRAWINGS OR REPRINTS, OR DATA FURNISHED TO BUYER OR SELLER SHALL REMAIN MOTOROLA'S PROPERTY, SHALL BE KEPT CONFIDENTIAL, SHALL BE USED FOR THE PURPOSE OF COMPLYING WITH MOTOROLA'S REQUESTS FOR ROTATION OR WITH MOTOROLA PURCHASE ORDERS AND SHALL BE RETURNED AT MOTOROLA'S REQUEST. PATENT RIGHTS EMBODIED IN DESIGNS, TOOLS, PATTERNS, DRAWINGS, DEVICES, INFORMATION AND EQUIPMENT SUPPLIED BY MOTOROLA PURSUANT TO THIS REQUEST FOR ROTATION OR PURCHASE ORDER AND EXCLUSIVE RIGHTS FOR THE USE IN REPRODUCTION THEREOF ARE RESERVED BY MOTOROLA."

NEXT ASSEMBLY	USED ON
APPLICATION	

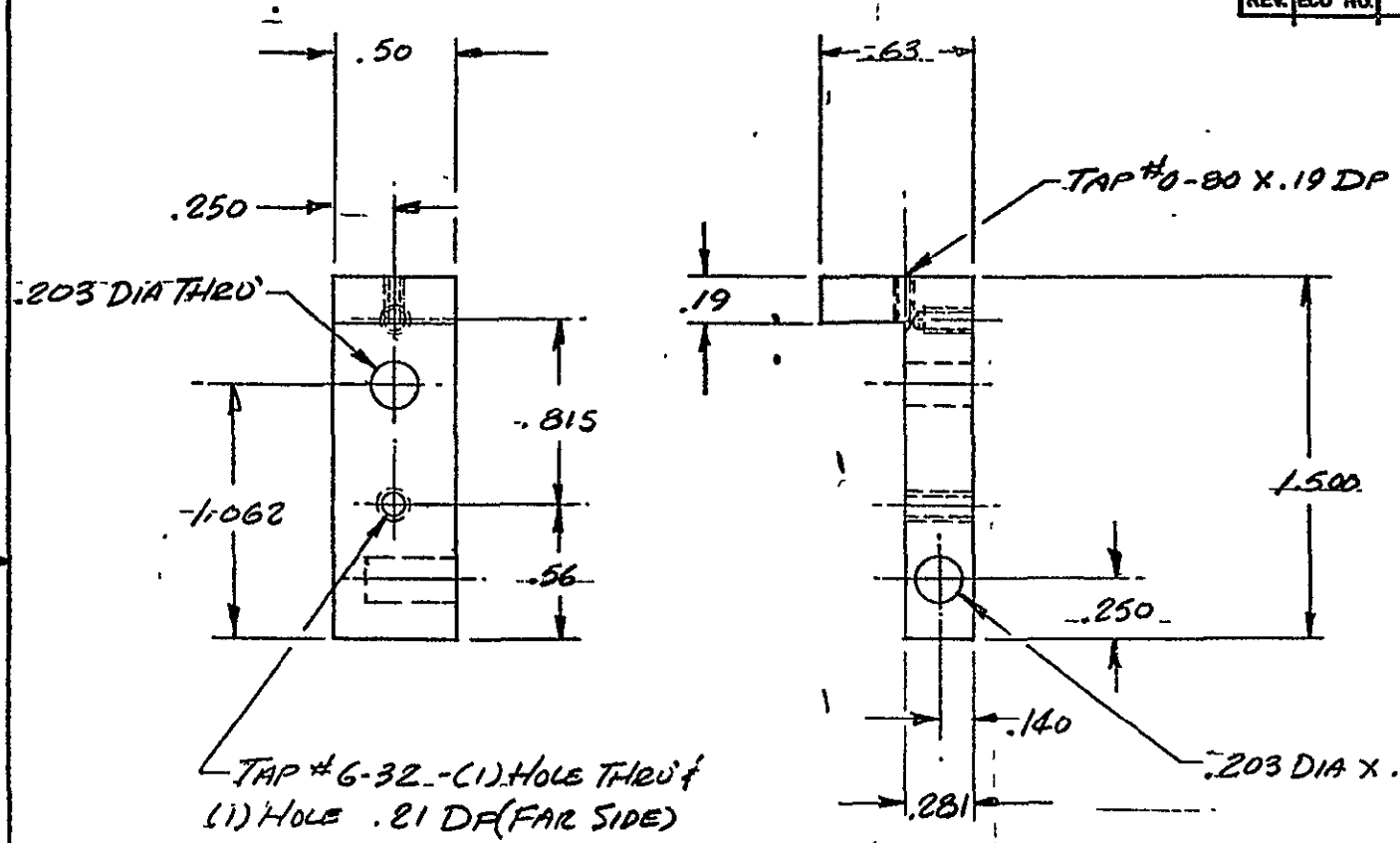




VIEW A
DISASSEMBLED

GLENN BUDAY
TELESCOPE
BEAM ENCLOSURE

REVISIONS				
REV.	ECO NO.	CHANGE	DATE	BY ENGR.



ORIGINAL PAGE IS OF POOR QUALITY

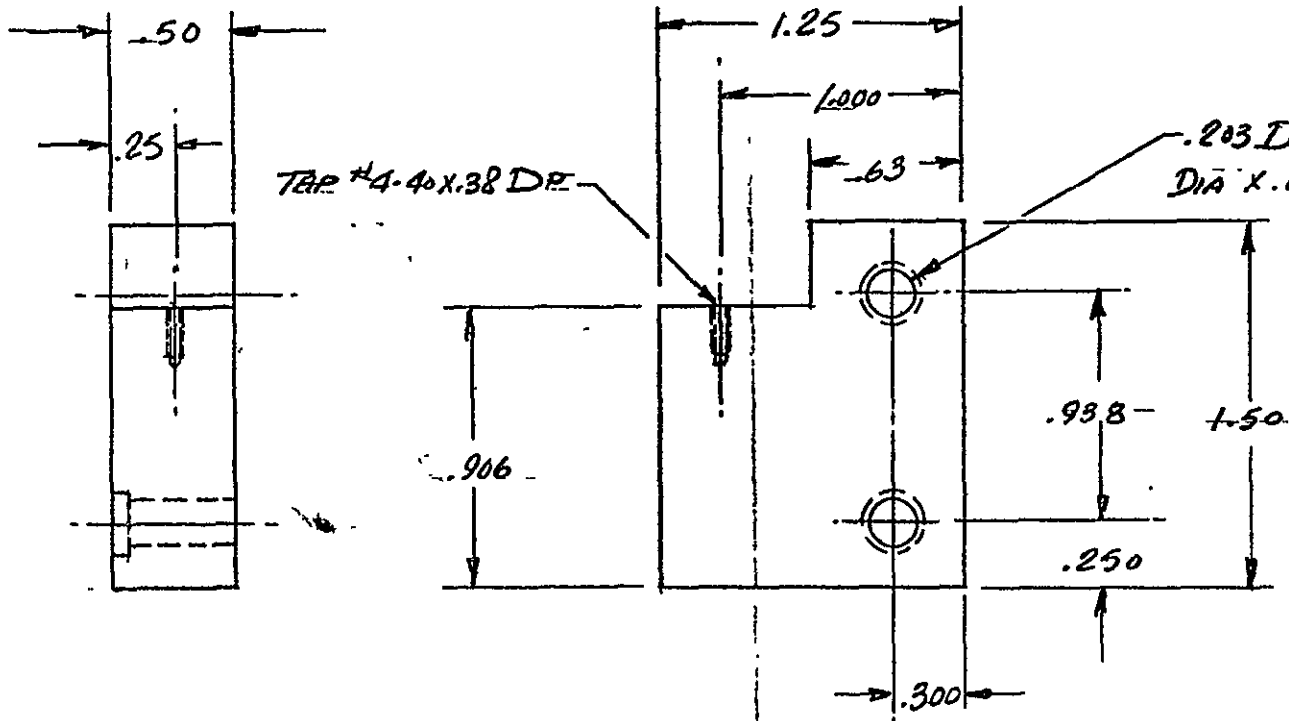
TAP #6-32 - (1) HOLE THRU
(1) HOLE .81 DF (FAR SIDE)

UNLESS OTHERWISE SPECIFIED, TOLERANCES: INCHES $XX \pm 0.15 .XXX \pm 0.05$ MILLIMETERS $.X \pm .XX \pm$ ANGULAR $- \pm$ $63 \sqrt{}$ RMS ALL MACHINED SURFACES. FEATURE CONTROL SYMBOLS PER ANSI Y14.5 BREAK ALL SHARP EDGES AND CORNERS, REMOVE BURRS. UNDERLINED DIM NOT TO SCALE. THIRD ANGLE ORTHOGRAPHIC PROJECTION IS USED.	MATERIAL TYPE 316 CRCS		MOTOROLA INC. Discrete Semiconductor Division	
	HEAT TREAT _____		TITLE: STRIP RETAINER-OUTER	
	APPLIED FINISH _____		DRAWN BY <u>G. SUTHERLAND</u> DATE <u>11-19-77</u>	
	CHECKED BY _____ DATE _____		SIZE B	CODE IDENT. NO. 04713
ENGR. APPROVAL _____ DATE _____		SCALE 2:1	WEIGHT _____	SHEET 1 OF 1

"ANY SPECIFICATIONS, DRAWINGS OR REPRINTS, OR DATA FURNISHED TO BUYER OR SELLER SHALL REMAIN MOTOROLA'S PROPERTY SHALL BE KEPT CONFIDENTIAL, SHALL BE USED FOR THE PURPOSE OF COMPLYING WITH MOTOROLA'S REQUESTS FOR QUOTATION OR WITH MOTOROLA PURCHASE ORDERS AND SHALL BE RETURNED AT MOTOROLA'S REQUEST PATENT RIGHTS EMBODIED IN DESIGNS, TOOLS, PATTERNS, DRAWINGS, DEVICES, INFORMATION AND EQUIPMENT SUPPLIED BY MOTOROLA PURSUANT TO THIS REQUEST FOR QUOTATION OR PURCHASE ORDER AND EXCLUSIVE RIGHTS FOR THE USE IN REPRODUCTION THEREOF ARE RESERVED BY MOTOROLA."



REVISIONS					
REV.	ECO NO.	CHANGE	DATE	BY	ENGR.



UNLESS OTHERWISE SPECIFIED,
 TOLERANCES:
 INCHES XX ± .015 XXX ± .005
 MILLIMETERS .X ± .XX ±
 ANGULAR ±
 ✓ 63 RMS ALL MACHINED SURFACES.
 FEATURE CONTROL SYMBOLS PER ANSI Y14.5.
 BREAK ALL SHARP EDGES AND CORNERS, REMOVE BURRS.
 UNDERLINED DIM NOT TO SCALE.
 THIRD ANGLE ORTHOGRAPHIC PROJECTION IS USED.

MATERIAL
 TYPE 316 CRCS
 HEAT TREAT
 APPLIED FINISH
 DRAWN BY G. Sundeland DATE 11-9-77
 CHECKED BY DATE
 ENGR. APPROVAL DATE

MOTOROLA INC.
 Discrete Semiconductor Division

TITLE:
 HEATER STRIP RETAINER

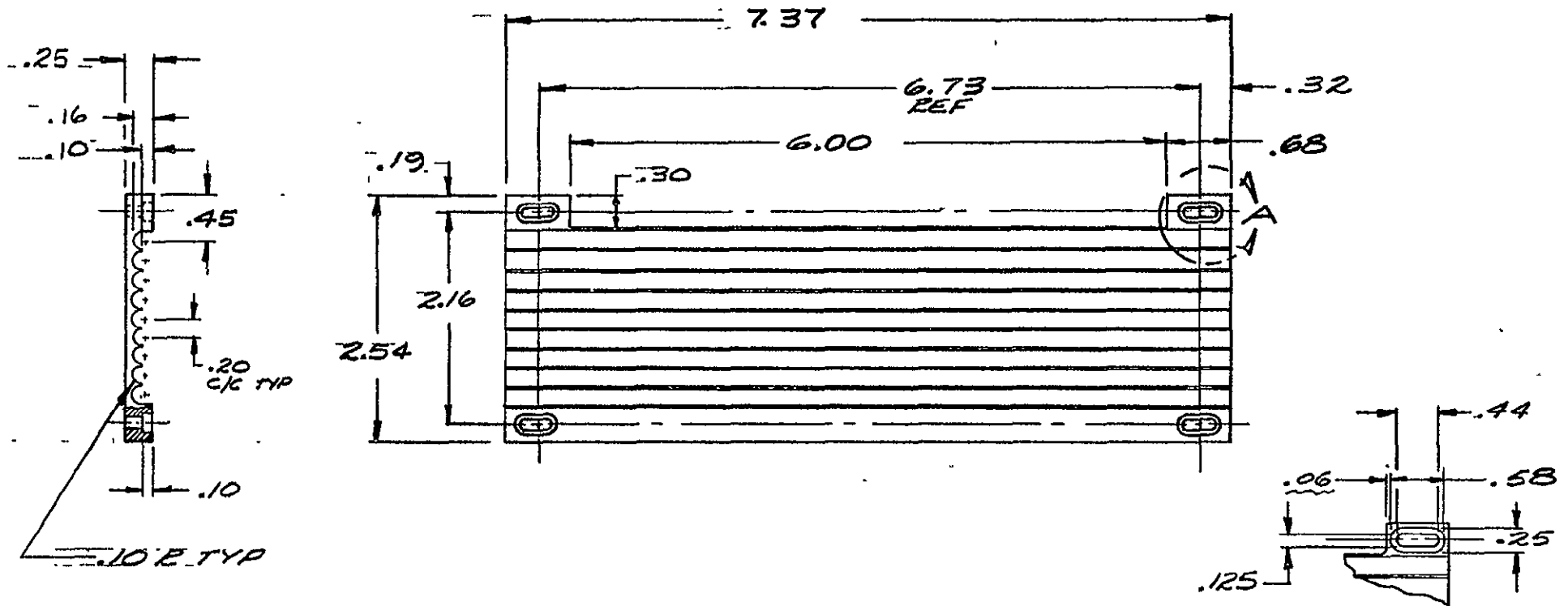
NEXT ASSEMBLY USED ON
 APPLICATION

SIZE B CODE IDENT. NO. 04713 DRAWING NO. 15-00-4
 SCALE 2:1 WEIGHT SHEET 1 OF 1

SPD 1187 (6/76)
 "ANY SPECIFICATIONS, DRAWINGS OR REPRINTS OR DATA FURNISHED TO BUYER OR SELLER SHALL REMAIN MOTOROLA'S PROPERTY, SHALL BE KEPT CONFIDENTIAL, SHALL BE USED FOR THE PURPOSE OF COMPLYING WITH MOTOROLA'S REQUESTS FOR QUOTATION OR WITH MOTOROLA PURCHASE ORDERS AND SHALL BE RETURNED AT MOTOROLA'S REQUEST. PATENT RIGHTS EMBODIED IN DESIGNS, TOOLS, PATTERNS, DRAWINGS, DEVICES, INFORMATION AND EQUIPMENT SUPPLIED BY MOTOROLA PURSUANT TO THIS REQUEST FOR QUOTATION OR PURCHASE ORDER AND EXCLUSIVE RIGHTS FOR THE USE IN REPRODUCTION THEREOF ARE RESERVED BY MOTOROLA."



REVISIONS				
REV.	ECD NO.	CHANGE	DATE	BY ENGR.



VIEW A
4 PLACES

"ANY SPECIFICATIONS, DRAWINGS OR REPAIRS, OR DATA FURNISHED TO BIDDER OR SELLER SHALL REMAIN MOTOROLA'S PROPERTY, SHALL BE KEPT CONFIDENTIAL, SHALL BE USED FOR THE PURPOSE OF COMPLYING WITH MOTOROLA'S REQUESTS FOR QUOTATION OR WITH MOTOROLA PURCHASE ORDERS AND SHALL BE RETURNED AT MOTOROLA'S REQUEST. PATENT RIGHTS EMBODIED IN DESIGNS, TOOLS, PATTERNS, DRAWINGS, DEVICES, INFORMATION AND EQUIPMENT SUPPLIED BY MOTOROLA PURSUANT TO THIS REQUEST FOR QUOTATION OR PURCHASE ORDER AND EXCLUSIVE RIGHTS FOR THE USE IN REPRODUCTION THEREOF ARE RESERVED BY MOTOROLA."

APPLICATION	USED ON	NEXT ASSEMBLY

UNLESS OTHERWISE SPECIFIED, TOLERANCES:
 INCHES .XX ± .02 .XXX ± .005
 MILLIMETERS .X ± .XX ±
 ANGULAR ±
 ✓ RMS ALL MACHINED SURFACES.
 FEATURE CONTROL SYMBOLS PER ANSI Y14.5.
 BREAK ALL SHARP EDGES AND CORNERS, REMOVE BURRS.
 UNDERLINED DIM NOT TO SCALE
 THIRD ANGLE ORTHOGRAPHIC PROJECTION IS USED.

MATERIAL 6061-T6 AL		MOTOROLA INC. Discrete Semiconductor Division	
HEAT TREAT _____		TITLE: HEATER COIL MOUNT	
APPLIED FINISH _____		DRAWING NO. R-0280-11-77	
DRAWN BY GLEN BUDAY	DATE 12-13-77	SIZE B	CODE IDENT NO. 04713
CHECKED BY	DATE	SCALE FULL	WEIGHT
ENGR. APPROVAL	DATE	SHEET	OF

